

**cp-2016-49 Submitted on 24 Apr 2016**

**Sea ice and pollution-modulated changes in Greenland ice core methanesulfonate and bromine**

**O. J. Maselli, N. J. Chellman, M. Grieman, L. Layman, J. R. McConnell, D. Pasteris, R. H. Rhodes, E. Saltzman, and M. Sigl**

**Author's response, Sept 2016**

1. The statements on the MSA and Br temporal trends do not seem to agree with Table S1, which is confusing. For example, though Lines 185-186 reads “Ice core Br levels at each site were stable until ~1830”, Table S1 shows different inflection points for Summit and Tunu, neither of which is 1830. Another example is Lines 283-284, reading “ the decrease in both MSA and bromine at both sites in the early 1800s”. But Table 1 shows different inflection points for MSA and Br, and for Summit and Tunu. Inflection 1 for Summit MSA is 1854 and that for Tunu Br is 1842. I don't think 1854 and 1842 can be called “early 1800s”. Please revise the sentences describing the trends of MSA and Br to avoid these confusions. Also, please display the inflection points and straight regression lines in Fig. 2.

Lines 185- changed to:” Ice core Br levels at each site were stable until ~1820 at Summit and ~1840 at Tunu when they both decreased by ~1 nM, establishing a new baseline that was stable until the mid 1900s.”

Lines 283 changed to :” the decrease in both MSA and bromine at both sites in the early to mid 1800s (Tables S1 and S2). In the 1900s, however, both sites show a divergence between the MSA and Br records”

The 3 step linear regression fit has been added to each data series in fig.2

2. The manuscript argues somewhat convincingly about MSA as a sea ice proxy, with the main argument based on a correlation between MSA and sea ice. But the correlation maps (Figures 6 and 7) are not very convincing. In black bordered regions both positive and negative correlations seem to be observed. But partly because the maps are too small, and colors for negative and positive correlations are hard to distinguish, it is hard to see in some regions if the correlation is positive or negative. I'm also confused by Fig. 6 because different black bordered regions are chosen for 1900-2010 and 1979-2010 without enough explanation. Please revise the correlation maps in Figs. 6 and 7 so that the correlations that the authors argue can be clearly seen, or maybe correlation maps can be removed.

Figures 6 and 7 have been edited so that only the SIC correlation maps from the months that show the best OWIP correlation have been kept. The retained maps have been enlarged. The original figure maps of SIC March-July have been placed in the supplementary. The manuscript focuses on the correlation between the MSA records and the total amount of open water in the ice pack within the black bordered regions which is an indication of the size of the marginal sea ice zone. As the editor notes it is hard to draw direct links between the SIC distribution within the black bordered region and the MSA records because the SIC varies so much within the bordered region that there are areas that show positive correlation and other areas which show negative correlation. The air masses that reach the ice core site take air from the whole black bordered region – in essence

averaging out all the differences in SIC records. The SIC correlation maps are thus presented in order to demonstrate that this typical sea ice measure is not the best link to the MSA record - the OWIP in the pack is better.

The black bordered region of Fig. 6b has been reduced to be the same as 6a. The region was originally expanded because it increased the correlation of the OWIP record, but the increase was only modest and so for clarity the smaller region is used, and the increase in correlation with sample area only mentioned in the figure caption.

3. Please add enrBr(Na) and nsiBr to Figs. 6 and 7 together with OWIP and MSA. This would strengthen the arguments of the manuscript, if enrBr(Na) and nsiBr have very different trend from that of MSA in the recent period. Currently they are in the supplementary, but without OWIP trend in the same figure.

enrBr(Na) and nsiBr have been added to figs 6 and 7.

4. Please show enrBr(Na) and nsiBr in the main text, not in the supplementary, because enrBr is a sea ice proxy published by previous studies, and to strengthen the conclusion on the findings between enrBr/nsiBr and sea ice trends.

enrBr(Na) and nsiBr have been added to figs 6 and 7 as per #3.

5. It would be better to add a few words to the final line of the manuscript "leaving room for the possibility that bromine may still be an effective proxy for local Antarctic sea ice conditions" “\*and for preindustrial sea ice reconstructions\*.”

This has been added to the final line.

Non-public comments to the Author:  
Dear Dr. Maselli,

I have the following minor editorial comments. Please revise the manuscript following them.

1. Line 82:  $\sim 0.22$  m yr<sup>-1</sup>. This needs a reference

This value was determined from the ice core record. This has been stated in the manuscript

2. Line 86:  $\sim 0.11$  m yr<sup>-1</sup>. This needs a reference.

This value was determined from the ice core record. This has been stated in the manuscript

3. Line 114: a peristaltic pump. Information on the make and company is necessary.

Reference to the pump was removed

4. Line 117: M6 pump. What pump is this? A peristaltic pump?

Syringe-free liquid handling pump – this was added to the manuscript

5. Lines 124-125. “The analysis... (Saltzman et al., 2006)” should be moved to Line 116.

Done

6. Lines 135- 148. Please define suffixes obs, dust, seaweater and enrich.

done

7. Line 176. Please explain how outliers were removed.

Technique references Sigl 2013. Sentence reworded to remove the ambiguity.

8. In Methods section, please show how you define each month for the ice core data.

Original wording :

‘The Summit-2010 and Tunu cores were dated using well-known volcanic horizons in sulfur (S). The dating of Summit-2010 was refined by annual layer counting using seasonal cycles in the ratio of non-sea salt S/Na (Sigl et al., 2015).’

Changed to :

‘The Summit-2010 and Tunu cores were dated using volcanic horizons in sulfur (S) from well dated historic eruptions (e.g., 1815, 1835, 1846, 1854, 1873, 1883, 1912). The dating of both cores was refined by annual layer counting using seasonal cycles in Na, Ca, and the ratio of non-sea salt S/Na as described in more detail for another Greenland ice core (NEEM-2011-S1) by Sigl et al., (2013, 2015). Annual-layer boundaries (nominal January) were defined as the minimum value in the ratio of non-sea salt S/Na following Sigl et al. (2013). The seasonal cycles in Na and Ca (from sea-salt and mineral dust emissions peaking in winter months) remain largely unaffected by rising anthropogenic emissions during the industrial period and thus can be used for annual layer counting for the entire record. The minimum in hydrogen peroxide was also used as a winter marker in the upper section of the Summit-2010 core. Timing was evaluated for consistency against other parameters including insoluble particle counts and black carbon. Monthly values were calculated assuming a constant distribution of snowfall within each year. Because of the lower accumulation rate and strong katabatic winds at the Tunu site, constraints from volcanic synchronization played a more important role in the developing the depth-age scale for the Tunu core compared with Summit-2010. First the Tunu non-sea salt S record was synchronized to the NEEM-2011-S1 volcanic record (Sigl et al., 2015) and then the required number of annual layers between volcanic horizons picked from the high-resolution chemistry.

The annual-layer dating for these ice cores resulted in a plutonium record that is consistent with other ice cores from Greenland between 1950 and 1970 and with the emission histories from nuclear weapon testing in the Northern Hemisphere (Arienzo et al., 2016). The error in the dating of the ice core records was estimated as  $\pm 0.33$  years for the Summit-2010 record and  $\pm 1$  years for the Tunu record.

9. Lines 298-299. I think  $H_2SO_4$  and  $HNO_3$  could be formed not only after deposition on the ice/snow, but also during transportation.

I agree – included adsorption onto aerosols:

‘ $SO_2$  and  $NO_x$  from the haze are adsorbed onto aerosols or deposited directly on the ice/snow and oxidised to sulfuric ( $H_2SO_4$ ) and nitric acid ( $HNO_3$ )’

10. Lines 319-320: I think coal burning is one kind of fossil fuel combustion.

Changed to:

global  $SO_2$  emissions with maxima from coal (~1920 C.E.) and coal plus petroleum combustion (~1970 C.E.),

11. Line 340: at heights of 500m and 10,000 m. I don’t think the latter is correct. The latter should be total column trajectory

changed to:

“calculated for Summit-2010 up to heights of 500 and 10,000m (total column trajectory, Fig. 5a, S8a)”

12. Line 371, OWIP is stable until ~1970. To my eyes, OWIP seems to have started to decrease earlier than 1970 at Summit.

Changed to:

“For both ice cores the source region OWIP trend is followed by the MSA.”

13. Line 473: Mirabolite should be mirabilite.

Done

14. Line 488: was less than 1nM. At Tunu, the exPb peak is close to 2nM (only slightly lower than 2nM). If this is corrected, 0.67M in Line 490 needs to be corrected, too.

The 1 nM reference is to the coal burning era – which peaks in 1920. The plots are consistent with this statement. At the height of the fossil fuel burning era (~1970) the exPb peak close to 2nM as the editor notes.

15. Line 531. Please remove “,” between “reactive” and “species”.

Done

16. Please check the references more carefully. I found the following errors, though I haven’t checked the references very carefully.

Thanks, the reference list needed to be refereshed.

- Jaffrezo et al. (1994) (Line 258) is missing from the reference list. Updated  
added

- Line 446 Macias Fauria et al (2010): Is Macias Fauria a family name? Though this is consistent with the reference list, I wonder if this is correct.

Yes it is correct

- Line 483 McConnell et al. (2008, 2007):McConnell et al. (2008) is missing from the reference list.  
This was Mcconnell and Edwards 2008. Ref removed.

Line 809, Science (80-): Something missing? fixed

Line 615, Morin (2008): Is this Morin et al. (2008)? Updated

Figs. 5 and S8. In some of the maps, “month” can’t be seen. Month labels updated

Caption of Fig. S4. I couldn’t understand the meaning of the sentence “The time-series... (C.E.).  
This sentence has been removed from fig s4 and s15, it is not essential.

Caption of Fig.S6. ‘overlap’ ice cores. Does ‘ice cores’ mean “ice sticks” or “ice pieces”?

Changed to: Two different depths of the Tunu ice core are shown where the replicate analysis was performed by melting a secondary stick of ice cut from the same ice core and overlapping in depth (‘overlap’ ice sticks) : (a) Six ‘overlap’ ice sticks were melted sequentially to replicate the MSA record over the depth 8-14 m.(b) Two ‘overlap’ ice sticks were melted sequentially over the depth 186.2-187.9 m.

Fig. S10. The maps are too small to see. Maps enlarged

1. Please state in more detail how you dated the cores, and how you defined a year and months.

- As for the Summit core, annual layer counting seems to have been done using nssS/Na ratio (Lines 88-89), and the manuscript refers to Sigl et al. (2015). But Sigl et al (2015) seems to have used not only nssS/Na ratio but also other parameters as well. If you used only nssS/Na, how



did you deal with the change of seasonality in nssS due to anthropogenic S input?

This has been address in #8.

-Was the Tunu core dated only by volcanic sulfur horizons?

This has been address in #8.

2. Please add the average seasonal cycle of water stable isotopes to Fig. 3.

The d18O annual cycle averaged over the 1900-2010 period has been added to the figure 3. And reference to the technique added to the manuscript. The record earlier than 1900 was not included as the record has not been corrected for back diffusion.

1 **Sea ice and pollution-modulated changes in Greenland ice core**  
2 **methanesulfonate and bromine**

3 **O.J. Maselli<sup>1\*</sup>, N.J. Chellman<sup>1</sup>, M. Grieman<sup>2</sup>, L. Layman<sup>1</sup>, J. R. McConnell<sup>1</sup>, D. Pasteris<sup>1</sup>,**  
4 **R.H. Rhodes<sup>3</sup>, E. Saltzman<sup>2</sup>, M. Sigl<sup>1</sup>**

5 [1] {Desert Research Institute, Department of Hydrologic Sciences, Reno, NV, USA}

6 [2] {University of California Irvine, Department of Earth System Science, Irvine, CA, USA}

7 [3] {University of Cambridge, Department of Earth Sciences, Cambridge, UK}

8 [\*] {now at: The University of Adelaide, Australia, 5000}

9 *Correspondence to:* Olivia Maselli (olivia.maselli@adelaide.edu.au)

10

11 Keywords: bromine, MSA, nitrate, sea ice, pollution, acidification, Arctic, Greenland, cryosphere

12

13 **Abstract**

14 Reconstruction of past changes in Arctic sea ice extent may be critical for understanding its future  
15 evolution. Methanesulphonate (MSA) and bromine concentrations preserved in ice cores have both  
16 been proposed as indicators of past sea ice conditions. In this study, two ice cores from central and NE  
17 Greenland were analysed at sub-annual resolution for MSA ( $CH_3SO_3H$ ) and bromine, covering the time  
18 period 1750-2010. We examine correlations between ice core MSA and the HadISST1 ICE sea ice  
19 dataset and consult back-trajectories to infer the likely source regions. A strong correlation between the  
20 low frequency MSA and bromine records during preindustrial times indicates that both chemical species  
21 are likely linked to processes occurring on or near sea ice in the same source regions. The positive  
22 correlation between ice core MSA and bromine persists until the mid-20th century, when the acidity of  
23 Greenland ice begins to increase markedly due to increased fossil fuel emissions. After that time, MSA  
24 levels decrease as a result of declining sea ice extent but bromine levels increase. We consider several  
25 possible explanations and ultimately suggest that increased acidity, specifically nitric acid, of snow on  
26 sea ice stimulates the release of reactive Br from sea ice, resulting in increased transport and deposition  
27 on the Greenland ice sheet.

29 **1 Introduction**

30 Atmospheric chemistry in the polar regions is strongly modulated by physical, chemical, and biological  
 31 processes occurring in and around sea ice. These include sea salt aerosol generation, biogenic emissions  
 32 of sulfur-containing gases and halogenated organics, and the photochemical/heterogeneous reactions  
 33 leading to release of volatile, reactive bromine species. The resulting chemical signals influence the  
 34 chemistry of the aerosol deposited on polar ice sheets. For this reason ice core measurements of sea salt  
 35 ions, methanesulphonate (MSA), and bromine have been examined as potential tracers for sea ice extent  
 36 (Abram et al., 2013; Spolaor et al., 2013b, 2016; Wolff et al., 2003). The interpretation of such tracers  
 37 is complicated by the fact that their source functions reflect changes in highly complex systems, and  
 38 signals are further modified by patterns of atmospheric transport and deposition.

39 MSA is produced by the atmospheric oxidation of DMS ( $(CH_3)_2S$ ). DMS is produced throughout the  
 40 world's oceans as a breakdown product of the algal metabolite DMSP,  $((CH_3)_2S^+CH_2CH_2COO^-)$ .  
 41 DMS emissions are particularly strong in marginal sea ice zones (Sharma et al., 2012), and this source  
 42 is believed to be a dominant contributor to the MSA signal in polar ice (Curran and Jones, 2000). Ice  
 43 core MSA records have been used extensively in Antarctica as a proxy for local sea ice dynamics.  
 44 Although the specifics of the relationship are highly site-dependent (Abram et al., 2013; Curran et al.,  
 45 2003) MSA has been proven to be a reasonably good proxy for sea ice conditions (e.g., (Curran and  
 46 Jones, 2000)). In the Arctic, the relationship between MSA and sea ice conditions is less straightforward  
 47 due to the likelihood of multiple source regions with different sea ice conditions contributing to the ice  
 48 core archived MSA (Abram et al., 2013). Until now, a significant, ( $r = -0.66$ ) relationship between ice  
 49 core MSA and Arctic sea ice extent (specifically August in the Barents sea) has only been established  
 50 for a short record from a Svalbard ice core (O'Dwyer et al., 2000). In this study we analyse the direct  
 51 correlations between the MSA records from two Greenland ice core sites and the surrounding sea ice  
 52 conditions in order to demonstrate the utility of MSA as a local sea ice proxy.

53 In this study, all dissolved or suspended bromine species are measured (including organic bromine) and  
 54 shall be referred to as "bromine". The primary source of total inorganic bromine (e.g.  $Br_2$ ,  $Br^-$ ,  $HBr$ )  
 55 in the marine boundary layer (MBL) is the ocean (Parrella et al., 2012; Sander et al., 2003). At  
 56 concentrations of less than 0.2% that of sodium (Na), bromide ( $Br^-$ ) makes a small contribution to  
 57 ocean salinity.  $Br^-$  can be concentrated in the high latitude oceans when the sea water is frozen, since  
 58 the formation of the ice matrix exudes the sea-salts in the form of brine (Abbatt et al., 2012). Small, sea-  
 59 salt aerosol particles blown from the surface of sea ice are typically enriched with bromine (Sander et

Deleted: ph

Deleted: but rather weak

Deleted: 37

Deleted: c

Deleted: (Parrella et al., 2012; Sander et al., 2003)

Deleted: (Sander et al., 2003)

al., 2003) and satellite imagery has revealed that plumes of bromine (as BrO) are photo-chemically released from sea-ice zones in spring (Nghiem et al., 2012; Schönhardt et al., 2012; Wagner et al., 2001). Recently, studies have begun to link ice core records of bromide enrichment (relative to sea water  $Na$  concentrations) preserved in polar ice sheets to that of local sea ice conditions (Spolaor et al., 2013a, 2013b, 2014). Spolaor and co-workers demonstrated the spring-time  $Br^-/Na$  that is preserved in the ice core is a record of bromine explosion events over adjacent seasonal sea ice. A  $Br^-/Na$  enrichment would therefore indicate a larger seasonal sea ice extent or conversely a shorter distance between the ice edge and the ice core site due to decreased multi-year sea ice (Spolaor et al., 2013a). However, like MSA, it is likely that the bromine – sea-ice relationship in the Arctic is complicated by the myriad of bromine source regions which influence an ice core record in addition to factors which influence the degree of enrichment of the aerosol as it travels to the ice core site. In this study we compare ice core records of bromine to those of MSA and other common MBL species in order to determine the influence of sea ice conditions and other factors on bromine concentrations.

Here we present measurements of MSA, bromine, and elemental tracers of sea salt and crustal input in two Greenland ice cores covering the time period 1750-2010 C.E.. These ice core records represent the first continuous, sub-annual resolution records of bromine in polar ice to extend beyond the satellite era. We examine the relationship between these two sea ice-modulated tracers, their relationship to independent historical estimates of sea ice distribution, and the influence of industrialization on atmospheric and ice core chemistry.

## 2 Methods

### 2.1 Ice cores

The 87 m ‘Summit-2010’ ice core was collected in 2010 close to Summit Station, Greenland (72°20'N 38°17'24"W, Fig. 1). The average snow accumulation at Summit, as determined from the ice core record, is  $\sim 0.22 \text{ m yr}^{-1}$  water equivalent, with few instances of melt. Due to the relatively high snow accumulation rate, seasonal analysis of the sea salt species concentrations was feasible. The 213 m Tunu core was collected in 2013 (78° 2' 5.5"N, 33° 52' 48"W, Fig. 1), approximately 3 km east of the Tunu-N automatic weather station, part of the Greenland Climate Network. The average snow accumulation at Tunu, as determined from the ice core record, is  $\sim 0.11 \text{ m yr}^{-1}$  water equivalent. The Summit-2010 and Tunu cores were dated using volcanic horizons in sulfur (S) from well dated historic eruptions (e.g., 1815, 1835, 1846, 1854, 1873, 1883, 1912). The dating of both cores was refined by annual layer counting using seasonal cycles in Na, Ca, and the ratio of non-sea salt S/Na as described

**Deleted:** ). The average snow accumulation at Summit is  $\sim 0.22 \text{ m yr}^{-1}$  water equivalent, with few instances of melt. Due to the relatively high snow accumulation rate, seasonal analysis of the sea salt species concentrations was feasible. The 213 m Tunu core was collected in 2013 (78° 2' 5.5"N, 33° 52' 48"W), approximately 3 km east of the Tunu-N automatic weather station, part of the Greenland Climate Network. The average snow accumulation at Tunu is  $\sim 0.11 \text{ m yr}^{-1}$  water equivalent. The Summit-2010 and Tunu cores were dated using well-known volcanic horizons in sulfur (S). The dating of Summit-2010 was refined by annual layer counting using seasonal cycles in the ratio of non-sea salt S/Na (Sigl et al., 2015).

**Deleted:**

in more detail for another Greenland ice core (NEEM-2011-S1) by Sigl et al., (2013, 2015). Annual-layer boundaries (nominal January) were defined as the minimum value in the ratio of non-sea salt S/Na following Sigl et al. (2013). The seasonal cycles in Na and Ca (from sea-salt and mineral dust emissions peaking in winter months) remain largely unaffected by rising anthropogenic emissions during the industrial period and thus can be used for annual layer counting for the entire record. The minimum in hydrogen peroxide was also used as a winter marker in the upper section of the Summit-2010 core. Timing was evaluated for consistency against other parameters including insoluble particle counts and black carbon. Monthly values were calculated assuming a constant distribution of snowfall within each year. Because of the lower accumulation rate and strong katabatic winds at the Tunu site, constraints from volcanic synchronization played a more important role in the developing the depth-age scale for the Tunu core compared with Summit-2010. First the Tunu non-sea salt S record was synchronized to the NEEM-2011-S1 volcanic record (Sigl et al., 2015) and then the required number of annual layers between volcanic horizons picked from the high-resolution chemistry. The annual-layer dating for these ice cores resulted in a plutonium record that is consistent with other ice cores from Greenland between 1950 and 1970 and with the emission histories from nuclear weapon testing in the Northern Hemisphere (Arienzo et al., 2016). The error in the dating of the ice core records was estimated as  $\pm 0.33$  years for the Summit-2010 record and  $\pm 1$  years for the Tunu record.

## 2.2 Sampling and analysis

The ice cores were sampled from 33x33 mm cross-section sticks using a continuous melter system (McConnell et al., 2002). The silicon carbide melter plate provides three streams from concentric square regions of the ice core sample: an innermost stream (with a cross sectional area of 144 mm<sup>2</sup>), an intermediate stream (340 mm<sup>2</sup>) and an outer stream that was discarded along with any contaminants obtained from handling of the ice core. The innermost melt stream was directed to two inductively coupled plasma-mass spectrometers (ICP-MS, Thermo Element II high resolution with PFA-ST concentric Teflon nebulizer (ESI)) run in parallel. All calibrations and runtime standards were run on both instruments and several elements were also measured in duplicate (Na, Ce, Pb) to ensure tracking between both ICP-MS. In addition, an internal standard of yttrium flowed through the entire analytical system and was used to observe any change in system sensitivity. The instrument measuring bromine was run at medium resolution, and there were no mass interferences observed at the bromine isotope mass monitored (79 amu). The sample stream was acidified to 1% HNO<sub>3</sub> to prevent loss of less soluble species, degassed just prior to analysis to minimize mixing in the sample line and sampled at a rate of 0.45ml min<sup>-1</sup> (McConnell et al., 2002; Sigl et al., 2013). The following elements were measured by

Deleted: low

Deleted: to get the highest sensitivity

143 ICP-MS: Br, Cl, Na, Ca, S, Ce, and Pb. Calibration of the ICP-MS was based on a series of 7 mixed  
144 standards measured at the start and end of each day for all elements except for the halides. Due to the  
145 high volatility of acid halides, a set of 4 bromine and chlorine standards were made individually in a  
146 1% UHP  $HNO_3$  matrix from fresh, non-acidified intermediate stock solution (Inorganic Ventures) every  
147 day. The intermediate melt stream was directed to a continuous flow analysis (CFA) system on which  
148 nitrate ion ( $NO_3^-$ ) and snow acidity (sum of soluble acidic species) were measured using the technique  
149 described by Pasteris (2012) in addition to other atmospheric species of interest (Röthlisberger et al.,  
150 2000). Stable water isotopes records were also collected using the CFA system according to the method  
151 described by Maselli et al. (2013)

152 The analysis of MSA by batch analysis using ESI/MS/MS has been reported previously (Saltzman et  
153 al., 2006). A portion of the debubbled CFA melt stream ( $150\ \mu\text{l min}^{-1}$ ) was subsampled for continuous  
154 on-line analysis of methanesulfonate by electrospray triple-quad mass spectrometer (ESI/MS/MS;  
155 Thermo-Finnigan Quantum). This subsample was mixed with pure methanol ( $50\ \mu\text{l min}^{-1}$ ) delivered  
156 using an M6 pump (syringe-free liquid handling pump, VICI). The methanol was spiked with an  
157 internal standard of deuterated MSA ( $CD_3SO_3^-$ ; Cambridge Isotopes) at a concentration of 52 nM. The  
158 internal isotope standard was used to correct for any changes in instrument response due to variations  
159 in water chemistry (such as acidity). The isotope standard was calibrated against non-deuterated MSA  
160 standards prepared in water from non-deuterated MSA ( $CH_3SO_3^-$ ; Sigma Aldrich). MSA was detected  
161 in negative ion mode using the  $CH_3SO_3^-/SO_3^-$  transition (m/z 95/80) and  $CD_3SO_3^-/SO_3^-$  (m/z 98/80). The  
162 concentration of MSA in the sample flow was determined from the ratio of the non-deuterated and  
163 deuterated signals after minor blank corrections. This study is the first use of the technique for ice core  
164 MSA analysis in a continuous, online mode. The uncertainty in the MSA intensity as calculated from  
165 the standard calibrations is 1%.

166 A second portion of the debubbled CFA melt stream was directed to an autosampler collection system  
167 to collect a discretely sampled archive of the melted ice cores. The collected samples were frozen at the  
168 end of each day and later analysed for MSA again using ion chromatography and ESI/MS/MS.

### 169 2.3 Calculation of anthropogenic Pb, non sea-salt S, and Br enrichment

170 The Pb derived from anthropogenic sources (exPb) was calculated as the difference between total lead  
171 measure in the ice core,  $[Pb]_{obs}$ , and that from dust sources. The Pb from dust was calculated as a  
172 fraction of the dust proxy cerium,  $([Ce]_{obs})$ .

**Moved down [1]:** The methanol was spiked with an internal standard of deuterated MSA ( $CD_3SO_3^-$ ; Cambridge Isotopes) at a concentration of 52 nM. The isotope standard was calibrated against

**Moved down [2]:** The isotope standard was calibrated against non-deuterated MSA standards prepared in water from non-deuterated MSA ( $CH_3SO_3^-$ ; Sigma Aldrich). MSA was detected in negative ion mode using the  $CH_3SO_3^-/SO_3^-$  transition (m/z 95/80) and  $CD_3SO_3^-/SO_3^-$  (m/z 98/80). The concentration of MSA in the sample flow was determined from the ratio of the non-deuterated and deuterated signals after minor blank corrections.

**Deleted:** A portion of the debubbled CFA melt stream ( $150\ \mu\text{l min}^{-1}$ ) was subsampled using a peristaltic pump for continuous on-line analysis of methanesulfonate by electrospray triple-quad mass spectrometer (ESI/MS/MS; Thermo-Finnigan Quantum). This subsample was mixed with pure methanol ( $50\ \mu\text{l min}^{-1}$ ) delivered using an M6 pump (VICI).

**Deleted:**

**Formatted:** Font color: Text 1

**Moved (insertion) [1]**

**Formatted:** Font color: Text 1

**Moved (insertion) [2]**

**Deleted:** This study is the first use of the technique for ice core MSA analysis in a continuous, on-line mode. The uncertainty in the MSA intensity as calculated from the standard calibrations is 1%.

**Deleted:**

**Deleted:**



$$exPb = [Pb]_{obs} - [Ce]_{obs} \times \left( \frac{[Pb]}{[Ce]} \right)_{dust}$$

Deleted: [Ce]<sub>obs</sub>

(1)

Formatted: Font:Bold

Formatted: Font:12 pt

Where the relative amount of Pb in dust,  $([Pb]/[Ce])_{dust}$ , has the constant mass ratio of 0.20588 (Bowen, 1979).

Formatted: Normal, Tabs:Not at 16.5 cm

Deleted:  $([Pb]/[Ce])_{dust}$  mass ratio

Deleted: value

Similarly the amount of non-sea salt sulfur (nssS) was calculated relative to the sea-salt sodium, ssNa:

Deleted:

Deleted: ph

$$nssS = [S]_{obs} - [ssNa] \times \left( \frac{[SO_4^{2-}]}{[Na]} \right)_{seawater}$$

Deleted:  $nssS = [S]_{obs} - [ssNa] \times \left( \frac{[SO_4^{2-}]}{[Na]} \right)_{seawater}$

(2)

Where the amount of sulfur relative to Na in sea-water,  $([SO_4^{2-}]/[Na])_{seawater}$  has the constant mass ratio of 0.252 (Millero, 1974). ssNa was calculated by comparison with calcium as both have sea salt and dust origins (Röthlisberger et al., 2002):

Deleted:  $\left( \frac{[SO_4^{2-}]}{[Na]} \right)_{seawater}$  mass ratio

Deleted: value

$$ssNa = \frac{[Na_{obs}] \times R_t - [Ca_{obs}]}{[R_t - R_m]}$$

(3)

Where  $R_t$  and  $R_m$  are the Ca/Na mean crustal and mean marine mass ratios of 1.78 and 0.038, respectively, (Millero, 1974).

Bromine enrichment factors relative to sea water concentrations were calculated using the following:

$$enrBr(Na) = \left( \frac{[Br]}{[Na]} \right)_{obs} / \left( \frac{[Br]}{[Na]} \right)_{seawater}$$

Deleted:  $Br_{enrich} = \left( \frac{[Br]}{[Na]} \right)_{obs} / \left( \frac{[Br]}{[Na]} \right)_{seawater}$

(4)

where the  $([Br]/[Na])_{seawater}$  mass ratio is 0.00623 (Millero, 1974).

## 2.4 Air mass back trajectories

Deleted: -

To identify the likely sea ice source regions of MSA and Br deposited at the ice core sites, we perform 10 day air mass back trajectories of boundary layer air masses from each ice core site using the GDAS1 archive dataset in the Hysplit4 software (Draxler and Hess, 1998). The starting height of the back trajectories was 500 m to ensure that the monitored air masses travelled close enough to the surface at the ice core site to potentially deposit aerosols. The vertical velocity field was taken from the

Deleted: -

230 meteorological data files. Air mass back trajectories were started every 12 hours and allowed to travel  
231 for 10 days (total number of trajectories hours = 14400 hours per month). The number of hours that the  
232 trajectories spent in a 2°x2° degree grid was summed over all of the trajectories for that month between  
233 the years 2005-2013. Previous work showed that the rapid advection of MBL air was the likely source  
234 of reactive halogens at Summit (Sjostedt et al., 2007).

235 **2.5 Sea Ice Correlation mapping**

236 In order to assess the relationships between sea ice conditions and ice core chemistry, correlation maps  
237 were generated between annual MSA concentrations and monthly sea ice using the HadISST1 ICE  
238 dataset at 1° latitude-longitude monthly resolution (Rayner, 2003). Pre-1979 sea ice datasets were  
239 interpolated from sea ice extent maps compiled by Walsh (1978) which incorporate a variety of  
240 empirical observations. The data were later bias corrected using modern satellite data (Rayner, 2003).  
241 Correlations were performed separately for the satellite period (1979-2012) and for the extended record  
242 (1900-2012), excluding the period 1940-1952 when the record has no variability due to scarcity of data  
243 (Rayner, 2003). Because strong DMS emissions occur in marginal sea ice zones (Sharma et al., 2012),  
244 we considered both sea ice concentration (SIC) and the area of open water in the sea ice pack (OWIP)  
245 which represents the size of the marginal sea ice zone. OWIP is defined as the difference between sea  
246 ice area (calculated from sea ice concentration over the area of the grid cell) and sea ice extent (NSIDC).  
247 A SIC of 15% was used as the threshold for a grid cell to contribute to sea ice extent. The area of OWIP  
248 was calculated within the coastal areas as defined by the results of the air mass back trajectories (Sect.  
249 3.4).

250 Outliers were removed from the MSA time series (see Fig. 2) before the correlations were performed.  
251 The outliers were removed using the technique described by Sigl (2013) for identifying volcanic signals  
252 using a 25 year running average filter. Correlations were performed on an annual rather than seasonal  
253 basis because the seasonality of ice core MSA is distorted due to post-depositional migration of MSA  
254 signal at depth in the snow pack (Mulvaney et al., 1992) (Fig. 3, S1).

256 **3 Results**

257 **3.1 Bromine**

258 Ice core measurements of bromine at Summit and Tunu covering the period 1750-2010 are shown in  
259 Fig. 2. Ice core Br levels at each site were stable until ~1820 at Summit and ~1840 at Tunu when they

Deleted:

Deleted: -

Deleted: 3.4

Formatted: English (AUS)

Moved (insertion) [3]

Deleted: Correlations were performed on an annual rather than seasonal basis because the seasonality of ice core MSA is distorted due to post

Moved down [4]: depositional migration of MSA signal at depth in the snow pack (Mulvaney et al., 1992) (Fig. 3,

Deleted: S3).

Moved up [3]: Outliers were removed from the MSA time series (see Fig.

Deleted: 2) before the correlations were performed

Moved (insertion) [4]

Deleted: 1830

273 both decreased by ~1 nM, establishing a new baseline that was stable until the mid 1900s. Both ice cores  
274 also show a Br peak in the late 20<sup>th</sup> century. The concentration values and the timing of inflections in  
275 concentrations were determined by a 3 step linear regression of the data set. The analysis was performed  
276 by simultaneous linear least squares fitting of 3 straight lines joined by 'inflection points' to the data  
277 set. The variables of the fitting procedure were the slopes and intercepts of each line as well as the x-  
278 axis locations at which the total function switched from one linear section to the next (the inflection  
279 points). Initial guess values were supplied for each variable to help the fitting procedure reach  
280 reasonable values. A summary of the regression results can be found in Table S1.

Deleted: early

Deleted: A summary of

Deleted: and

281 Sea-salt transport onto the Greenland ice sheet occurs predominantly during winter. Historically the  
282 winter-time sea-salt maximum was believed to be due to increased cyclonic activity over the open  
283 oceans (Fischer and Wagenbach, 1996) though more contemporary studies show that blowing snow  
284 from the surface of sea-ice may be a significant source (Rankin et al., 2002; Xu et al., 2013; Yang et al.,  
285 2008, 2010). At Summit, a winter-time maximum is observed in the most abundant sea salts, Na and Cl  
286 (Fig. 3). Bromine also shows a significant winter-time signal, however the annual maximum appears in  
287 mid-summer - at concentrations ~70% above winter levels (Fig. 3a). Comparison with Br measured in  
288 weekly surface snow samples collected from Summit (from 2007-2013; GEOSummit project) confirms  
289 that this summer signal is real and not a result of post-depositional modification of seasonality of the  
290 bromine signal (Fig. S2). The results from that study confirm that total Br concentrations peak in  
291 summer on the ice sheet closely following the Br cycle observed in the Summit-2010 ice core. In  
292 addition to the comparison with the Geosummit data, in the ice cores studied here there are routinely  
293 more than 10 measurements made within a yearly layer of snow giving confidence to the allocation of  
294 a summer maximum in bromine at Summit. Analysis of the annual cycle of bromine in the Tunu ice  
295 core also shows a summer maximum when averaged over the entire ice core time series but with  
296 significantly larger error than observed at Summit. The timing of this peak suggests a predominant  
297 summer-time deposition of bromine that dwarfs that from winter sea salt sources.

Deleted: S1

298 The shape of the annual bromine cycle does change slightly over the course of the Summit record (see  
299 Fig. 3). Starting in the early 1900s the annual bromine cycle slowly becomes broader. A slight shift in  
300 the maximum from a solely summer peak in the preindustrial era towards a broad summer-spring peak  
301 by 1970 is observed (Fig. 3 lower plot). Comparison with the sea salt tracer, sodium, which does not  
302 undergo the large temporal shift and broadening of its seasonal cycle shows that this change in bromine  
303 seasonality is not linked to changes in production or transport of sea-salt aerosols or even dating  
304 uncertainties in the ice core but perhaps the introduction of an additional, smaller bromine source in the  
305 spring-time during the industrial era.

Deleted: source

Both ice cores show a predominantly positive Br enrichment throughout the year (Fig. S3, S4) relative to both sea salt elements chlorine and sodium. This enrichment reaches a maximum in mid to late summer at Summit (Fig. 3). We assume that this enrichment reflects Br enrichment in the aerosol transporting Br to the ice sheet. In a comprehensive review of global aerosol Br measurements, Sander et al. (2003) concluded that in general, aerosols which showed positive Br enrichment factors were of sub-micrometer size. These small aerosols can travel further (lifetimes of around 5-10 days) and due to their larger surface/volume ratio may experience more atmospheric processing than larger aerosols, resulting in the positive enrichment. However, post-depositional reduction of the bromine concentration is a possibility during the summer months due to photolytic processes at the snow surface. This may be the cause of the noisiness of the bromine signal within the lower accumulation, Tunu core. However, the increased snow accumulation that occurs during the summer months in both central and northern Greenland (Chen et al., 1997) should act to minimise these bromine depleting effects driven by increased insolation in summer, and indeed Weller (2004) has shown that accumulation rates of this size are large enough to prevent the post-deposition loss of other species such as nitrate and MSA.

Both sites also show a (small) positive enrichment of chlorine relative to sodium, which is amplified at small sodium concentrations. Chlorine containing aerosols are expected to undergo similar chemical processing to bromine containing aerosols but the enrichment factors of bromine (relative to sodium) are much larger which is likely due to the high solubility of bromine species such as HBr (Sander et al., 2003). Alternatively, the chlorine enrichment could be interpreted as a sodium depletion of the aerosols particularly in those of small diameter where both concentrations are low; this would amplify the bromine enrichment (relative to sodium) but would not explain the bromine enrichment relative to chlorine. It is likely that both halogens undergo some degree of enrichment and the sodium undergoes some depletion in the aerosols though it is difficult to determine this from the data.

A summer-time maximum in Br enrichment was also observed by Spolaor (2014) in a short segment of Antarctic Law Dome ice core as well as two Arctic ice cores. Spolaor et al. believe that the main source of the inorganic bromine originated from spring-time bromine explosion events above sea ice and the summer-time maximum could possibly be an indication of lag-time between bromine containing particles becoming airborne and their deposition. Further investigation is needed to definitively establish the seasonality of bromine deposition at the poles. However the results of the Arctic ice cores studied here suggest that the summer maximum in bromine deposition is indeed real.

In the Tunu ice core, 11% of the monthly bromine enrichment measurements relative to Na were negative (less than the Br/Na seawater ratio, Fig. S3) and 12% were negative relative to Cl. It is possible

Deleted: S2

Deleted: 3). We assume that this enrichment reflects Br enrichment in the aerosol transporting Br to the ice sheet.

Deleted: .

Deleted:

Deleted: summertime

Deleted: In the Tunu ice core, 2% of the monthly bromine enrichment measurements (relative to Cl) were negative (less than the Br/Cl seawater ratio, Fig S2). In a comprehensive review of global aerosol Br measurements, Sander (2003) concluded that in general, aerosols which showed positive Br enrichment factors were of sub-micrometer size. These small aerosols can travel further (lifetimes of around 5-10 days) and due to their larger surface/volume ratio may experience more atmospheric processing than larger aerosols, resulting in the positive enrichment.

358 that the negative enrichment values observed in the Tunu ice core are therefore a result of larger aerosols  
359 (> micrometer) reaching the site due to its proximity to the coast (and thus the likely sea ice aerosol  
360 source region) in comparison to Summit.

### 361 3.2 MSA

362 The Summit-2010 MSA record (Fig. 2) replicates that measured by Legrand in 1993 (Legrand et al.,  
363 1997) and extends it an additional 17 years, (see Fig. S5). The mean Summit-2010 MSA measurements  
364 over the period 1984-1992 ( $2.0 \pm 0.7$  ( $1\sigma$ ) ppb) also compare well with the results of the sub-annually  
365 sampled Summit snow pit study performed by Jaffrezo et al., (1994);  $2.1 \pm 1.8$  ( $1\sigma$ ) ppb. Both the Legrand  
366 and Jaffrezo studies measured MSA using ion chromatography of discretely sampled snow and ice. The  
367 similarity between the Summit-2010 measurements and the results of these studies demonstrates that  
368 the new, continuous technique is able to achieve a comparable accuracy in MSA measured  
369 concentrations to the traditional, discrete technique. It also demonstrates that negligible amounts of  
370 MSA are being lost by using the continuous melt method.

371 The Tunu measurements represent the first MSA profile at this location. Replicate measurements of the  
372 entire Tunu ice core were performed with the on-line, continuous technique by melting a secondary  
373 stick of ice cut from the original Tunu ice core. The replicate measurements closely followed the original  
374 MSA measurements demonstrating the reproducibility, stability and high precision of the continuous  
375 MSA technique (Fig. S6). The Tunu MSA record was also reproduced using discrete samples collected  
376 from the CFA system (Fig. S7).

377 At Summit, MSA concentrations averaged 48 nM in the late 18<sup>th</sup> century, compared with just 27 nM at  
378 Tunu. From 1878-1930 MSA concentrations at Summit plateaued at 36 nM after which they began to  
379 drop rapidly, at a rate of 0.27 nM/year, reaching 18 nM by 2000 C.E. Large fluctuations in the MSA  
380 record after this time make it difficult to assess the most recent trend in Summit MSA concentrations.  
381 MSA concentrations in the Tunu core showed a similar temporal variability to those in the Summit  
382 record, and until the mid-20<sup>th</sup> century, were consistently lower in magnitude. MSA concentrations only  
383 began to decline consistently at Tunu after 1984, almost 50 years after the rapid decline observed in the  
384 Summit record. After 2000 C.E., large fluctuations in concentration were again observed making the  
385 modern-day trend in MSA concentration at Tunu difficult to establish.

386 Comparison with the total sulfur record (Fig. 4) reveals that during the preindustrial period, MSA  
387 contributes to ~12% and ~7% of the total sulfur signal at Summit and Tunu, respectively, compared  
388 with < 2% at the height of industrial period (1970 C.E.) at both sites.

Deleted: . The Tunu measurements represent the first MSA profile at this location.

Deleted:

Deleted: .

Deleted: ,

394 The low frequency, preindustrial trend in MSA concentrations seen in these ice core records closely  
395 follows that of bromine; particularly distinct is the decrease in both MSA and bromine at both sites in  
396 the early to mid 1800s (Tables S1 and S2). In the 1900s, however, both sites show a divergence between  
397 the MSA and Br records—as MSA begins to decline, Br concentrations increase.

Deleted: S1 and  
Deleted: early

398 A dramatic shift in the ‘timing’ of the annual MSA maximum in Summit-2010 ice core is illustrated in  
399 Figs. 3c and S1. The signal shifts gradually and continuously along the length of the the entire Summit-  
400 2010 record from a spring to winter maximum (Fig. S1). This phenomenon has previously been  
401 observed in several Antarctic ice cores and has been attributed to post-depositional migration within the  
402 ice due to salt gradients (Mulvaney et al., 1992; Weller, 2004). At very low accumulation ice core sites  
403 post-depositional loss of MSA (and nitrate) must also be considered. Extrapolation of data collected by  
404 Weller (2004) from a series of East Antarctic ice cores predicts that sites with annual average  
405 accumulations of greater than 105 kg m<sup>-1</sup> yr<sup>-1</sup> (0.105 m yr<sup>-1</sup>) will not show post-depositional loss of  
406 MSA (or nitrate). Both ice cores in this study have sufficient average annual accumulation that post-  
407 depositional loss of MSA (and nitrate) is predicted to be negligible and so is not discussed further.

Deleted: S3

Deleted: S3

### 408 3.3 Acidic Species

409 In winter, with the collapse of the polar vortex, polluted air masses enter the Arctic region as the  
410 phenomenon known as the Arctic haze (Barrie et al., 1981; Li and Barrie, 1993).  $SO_2$  and  $NO_x$  from the  
411 haze are adsorbed onto aerosols or deposited directly on the ice/snow and oxidised to sulfuric ( $H_2SO_4$ )  
412 and nitric acid ( $HNO_3$ ). There are also natural sources of  $SO_2$  (biomass burning, volcanic eruptions,  
413 oceans (Li and Barrie, 1993; McConnell et al., 2007; Sigl et al., 2013) and  $NO_x$  (microbial activity in  
414 soils, biomass burning, lightning discharges (Vestreng et al., 2009) as well as other snow/ice acidifiers  
415 including MSA, hydrogen chloride and organic acids released from biogenic or biomass burning sources  
416 (Pasteris et al., 2012).

Deleted: ph

Deleted: (Li and Barrie, 1993; McConnell et al., 2007; Sigl et al., 2013)

Deleted: (

417 The annual cycle for nitrate ( $NO_3^-$ ) is shown in Fig. 3d. Before 1900 C.E. the nitrate shows a seasonal  
418 maximum in late summer/early fall after which the maximum shifts to late spring/early summer.  
419 Although there are biological sources of nitrate in the ice core aerosol source regions, in a recent study  
420 focused on the  $NO_3^-$  and  $\delta^{15}N - NO_3^-$  record in the Summit-2010 ice core, Chellman et al. (2016)  
421 concluded that the preindustrial (1790-1812 C.E.)  $NO_3^-$  seasonal cycle was driven by biomass burning  
422 emissions. However, in the modern era (1930-2002 C.E.) oil-burning emissions became the dominant  
423 source of  $NO_3^-$  in the snow-pack. The change in the dominant  $NO_3^-$  source due to industrialisation is the  
424 cause of the shift in timing of the seasonal cycle.

133 Total snow acidity was stable at both sites from 1750 through to ~1900 C.E. except for sporadic, short-  
 134 lived spikes due to volcanic eruptions. The average preindustrial acidity was the same at both sites (~1.8  
 135  $\mu\text{M}$ ). Both records also show two distinct maxima in acidity centred on 1920 and 1970 C.E. (Fig. 4)  
 136 with Tunu displaying higher acidity than Summit over the entire industrial period. Overlaid with the  
 137 acidity is the total sulfur (S) record for both ice cores. The high correlation between the acidity and S  
 138 records illustrates that the sulfur species are the dominant natural and anthropogenic acidic species in  
 139 the ice cores. The trend in acidity closely follows the global  $\text{SO}_2$  emissions with maxima from coal  
 140 (~1920 C.E.) and coal plus petroleum combustion (~1970 C.E.), respectively (Smith et al., 2011). After  
 141 1970 the records of acidity and S deviate. This deviation can be attributed to the presence of nitric acid  
 142 that remains at a relatively high concentration in the late 20<sup>th</sup> century whilst sulfur species reduce in  
 143 concentration (Fig. 4).

144  $\text{NO}_3^-$  concentrations show no trend during the preindustrial era in either ice core records, averaging  
 145  $1.1(\pm 0.02) \mu\text{M}$  and  $1.3(\pm 0.03) \mu\text{M}$  for Summit and Tunu, respectively. The higher signal-to-noise ratio  
 146 in the Summit-2010 record reveals a small peak in  $\text{NO}_3^-$  concentrations centred on ~1910. The Tunu  
 147 record also shows elevated  $\text{NO}_3^-$  concentrations over this period. However the large variability in the  
 148 signal makes it difficult to establish a higher resolution temporal trend. Both records clearly show a  
 149 large increase in  $\text{NO}_3^-$  after 1950, peaking in ~1990 and followed by a general decreasing trend with the  
 150 average  $\text{NO}_3^-$  levels still double that of preindustrial concentrations:  $2.1 \mu\text{M}$  and  $2.3 \mu\text{M}$  at Summit and  
 151 Tunu, respectively.

152 The nitrate records from both sites follow the trend in northern hemisphere  $\text{NO}_x$  emissions with a peak  
 153 in ~1910 and 1990 C.E.– a result of emissions from increases in both Northern Hemisphere fertilizer  
 154 usage and biomass and fossil fuel combustion (Felix and Elliott, 2013).

### 155 3.4 Air mass back trajectories

156 Air mass back trajectory results demonstrate that air masses reaching the Summit-2010 site between  
 157 March and July originate primarily from the South/South-East of the ice core site (Fig. 5a). Previous  
 158 back trajectory analyses by Kahl *et al.* (1997) also linked individual spikes in their Summit MSA record  
 159 to air masses that had passed over this same region of coast (SE Greenland) within the previous 1-3  
 160 days. Similar back trajectories were calculated for Summit-2010 up to heights of 500 and 10,000m (total  
 161 column trajectory, Fig. 5a, S8a) illustrating that air masses that travel in the free troposphere and lower  
 162 troposphere follow similar back trajectories and likely share the same source regions.

Deleted: ph

Deleted: ph

Deleted: )

Deleted: fossil fuel

Deleted: ),

Deleted: ph

Deleted: until 2010 C.E.

Deleted: at

Deleted: 4



The results for Tunu indicate that air masses arrive primarily from the west coast of Greenland, passing over the Baffin Bay area, but there is also significant contribution from both the SE and NE (in May) coastal areas (Fig. ~~5b, S8b~~). Of these two secondary areas it is likely that aerosols transported from the NE would have a greater influence on the ice core concentrations due to proximity to the ice core site. Aerosol deposited at Tunu therefore represents a mixture of source regions, but are likely dominated by the NW Greenland, Baffin Bay coastal region.

### 3.5 MSA - Sea Ice correlations

Locations which showed a sea ice concentration (SIC) variability greater than 10% (the average estimated range of uncertainty in the satellite measurements) and have a significant correlation to MSA (t-test,  $p < 0.05$ ) are displayed in ~~Figs S9 and S10 for the months of March-July~~. A greater weight must be placed on the post-1979 sea ice concentration maps as these were derived from passive microwave satellite data and, where available, operational ice chart data. The likely air mass source regions, as defined by the results of the air mass back trajectories, are indicated by the black bordered regions. Within these areas there is generally a negative correlation between SIC and MSA, particularly in the spring months, ~~and only small patches that show large correlation ( $>0.4$ )~~. The large areas of positive correlation along the east coast and in the western Barents Sea are striking ~~for the Summit-2010 record~~, however, these areas are outside of the defined air mass source region and thus are unlikely to be contributing to the ice core aerosol records. The positive correlation is likely an artefact of the negative autocorrelation between sea ice conditions in this region and the SE coast source region (Fig. ~~S11~~).

~~The effect of the estimated error in dating of the MSA records on the SIC correlation maps is explored in Fig. S12. By shifting the dating of the MSA records to either extreme of the dating error estimate and replotting the SIC correlation plots it is clear the error in the dating of the MSA records does not affect the sign of the correlations displayed on the maps but can have an affect on the magnitude of the correlation found in different locations. This is likely a result of the peaks in the MSA record being shifted in or out of temporal coherence with peaks in SIC at the different locations.~~

Over the period 1900-2010 C.E. highly significant correlation (t-test,  $p < 0.001$ ) is found between the annual ice core MSA and the amount of open water in the ice pack (OWIP, representing the area of the marginal sea ice zone, Figs. 6a and 7a: lower plots) in these aerosol source areas. For both ice cores the source region OWIP trend is followed by the MSA. ~~In the Summit-2010 ice core the highest correlation between annual MSA and monthly OWIP occurs in May ( $r=0.58$ ,  $p < 0.001$ ) though the following months through to July all show highly significant correlations (July  $r=0.53$ ,  $p < 0.001$ ). For comparison, the May~~

Deleted: 6b, S4b

Deleted: Fig. 6

Deleted: 7.

Deleted: (Fig. 6b, Fig. 7b)

Deleted: -

Deleted: -

Deleted: in Figs. 6 and 7

Deleted: .

Deleted: -

Deleted: S5

Deleted: , Fig.

Deleted: is stable until ~1970, when it begins to decline; a

Deleted: Over the shorter, satellite era (1979–2010), both

Deleted: and Tunu sites show strongest

Deleted: March – when the break-up of the winter sea ice begins

Formatted: Font:Not Italic

Deleted: =

Deleted: 33

Formatted: Font:Not Italic

Deleted: 0.1;  $r = 0.37$

Formatted: Font:Not Italic

Deleted: 05, Fig. 7b, Fig. 8b). The significance of the Tunu

522 SIC correlation map is also shown as the upper plots in Figs. 6a. Figs. 3f and S13 demonstrate that this  
 523 time period (May-July) corresponds to the peak and then rapid decline in the amount of annual OWIP  
 524 within the Summit-2010 aerosol source area because of the decreasing extent of sea ice. Rapid loss of  
 525 sea ice reveals areas of biological activity previously capped by the ice allowing surface-atmosphere  
 526 exchange of DMS, resulting in the seasonal peak in atmospheric MSA correlation with the peak in the  
 527 area of OWIP.  
 528 At Tunu the highest correlation over the 1900-2012 C.E. period is found between annual MSA and  
 529 annual OWIP ( $r=0.59$ ,  $p<0.001$ ), though the July OWIP shows the highest monthly correlation and is  
 530 also highly significant ( $r=0.41$ ,  $P<0.002$ ). For comparison, the July SIC correlation map is also shown  
 531 as the upper plots in Figs. 7a. Due to the more northerly location of the Tunu aerosol source region, the  
 532 sea ice pack in this region is generally less fractured and break-up occurs later in the year, with a sharp  
 533 peak in OWIP occurring in July (Fig. S13). The higher stability of the ice pack throughout the year  
 534 compared to that in the Summit-2010 source region is the likely reason the Tunu MSA shows highest  
 535 correlation with the annual average of the OWIP. However, like Summit-2010 the highest monthly  
 536 OWIP correlation occurs between the annual MSA and the timing of the maximum in annual OWIP  
 537 (July).  
 538 Over the shorter, satellite era (1979–2012 C.E.) again Tunu shows strongest correlation between annual  
 539 MSA and annual OWIP though at a much lower significance ( $r=0.32$ ,  $p<0.05$ ), and the highest monthly  
 540 correlation occurs in March ( $r=0.2$ ,  $p<0.1$ ) albeit with low significance. The significance of the Tunu  
 541 correlation over this period can be dramatically increased (annual OWIP  $r=0.54$ ;  $p<0.001$ , March OWIP  
 542  $r=0.63$ ,  $p<0.001$ ) if the closer, secondary aerosol source region (NE Greenland,  $80^{\circ}$ – $73^{\circ}$ N,  $20^{\circ}$ – $0^{\circ}$ W)  
 543 is assumed to also influence the site in equal proportion. March corresponds to the timing of increased  
 544 insolation and thus the rapid increase in ice algal production (Leu et al., 2015). The shift from a July to  
 545 March peak in the correlation of OWIP with annual Tunu MSA may be a result of the reduced overall  
 546 SIE (and thus OWIP) influencing the timing of MSA production. Unfortunately, the post-depositional  
 547 migration of the MSA signal within the ice cores masks any evidence of true seasonal MSA shifts.  
 548 Summit-2010 also shows a much less significant monthly OWIP correlation with the annual MSA signal  
 549 over this time period, with the most significant correlation again occurring in March ( $r=0.4$ ,  $p<0.02$ ).  
 550 The greater significance of both the SIC-MSA and OWIP-MSA correlations at both sites over the longer  
 551 time period is likely a result of the averaging of any MSA production or transport variability as well as  
 552 the dominance of the low frequency variability of both time series on the overall correlation.

Deleted: over this period can be dramatically increased ( $r = 0.58$ ;  $p<0.001$ ), if the closer, secondary source region (NE Greenland)  
 Deleted: assumed to  
 Deleted: influence  
 Deleted: site (not shown).

558 **3.6 MSA and bromine relationship**

559 In an era where climate is driven by only natural forcings, chemical species that share a common source  
560 should show broadly consistent variability. This is evident in the preindustrial section of both ice core  
561 records where the relationship between MSA and Br (monitored as Br/MSA) remains constant over the  
562 entire period (Fig. 4) despite individual records going through step function changes. Using a 25 year  
563 running average on all records, the correlation between MSA and Br over the preindustrial period was  
564 calculated as: Summit-2010:  $r=0.282$  ( $p=0.0008$ ); Tunu:  $r= 0.298$  ( $p = 0.0004$ ),  $n= 138$ . After ~1930  
565 C.E., relative increases in Br concentrations cause the Br/MSA ratio to increase above the stable  
566 preindustrial levels by more than 160%, reaching a peak in ~2000 C.E. at both sites.

567 Bromine in excess of what is expected from a purely sea ice source (non sea ice bromine, nsiBr) was  
568 calculated by comparison to the other sea ice proxy, MSA. A linear regression of MSA versus Br was  
569 performed with the preindustrial data (1750-1880 C.E.) to establish the relationship between the two  
570 proxies during an era free of anthropogenic forcing (Figure S14a,b). This relationship was then  
571 extrapolated into the period after 1880 C.E. in order to estimate the amount of bromine sourced only  
572 from sea ice sources during the industrial era. The MSA record was smoothed with a 9<sup>th</sup> order  
573 polynomial function before being used in the extrapolation to reduce the noise in the resultant record  
574 whilst maintaining the low frequency trends (Figure S14c,d). nsiBr is thus the difference between the  
575 total bromine measured and the calculated, natural sea ice bromine (Figs. 8 and S14e,f); in contrast to  
576 Br<sub>exc</sub> defined by Spolaor (2016) as the amount of bromine in excess of the Br/Na seawater ratio.  
577 An estimate of the nsiBr is shown in Figs. 6, 7 and 8. By definition, nsiBr is essentially constant during  
578 the preindustrial period, but during the industrial period nsiBr peaks, reaching a broad maximum  
579 between 1980-2000 C.E. of ~3.4nM and 1.9nM at Summit and Tunu, respectively.

580 **4 Discussion**

581 The significant correlation between variability of marginal sea ice zone (OWIP) area within the  
582 identified source regions and the MSA records suggests that MSA records can be used as a proxy for  
583 modern sea ice conditions in these areas. North Atlantic Oscillation (NAO) proxy records developed in  
584 Greenland ice core records (Appenzeller et al., 1998) suggest that although the northern hemisphere  
585 climate phenomenon has shown variability over the past 200 years, its effect is damped in Northern  
586 Greenland (Appenzeller et al., 1998; Weißbach et al., 2015), so we can assume that no major changes in  
587 atmospheric circulation patterns have occurred to change the source regions for the marine aerosols  
588 between the preindustrial and industrial periods. If this assumption is true, our identification of MSA as  
589 a sea ice proxy (specifically a marginal sea ice zone proxy) may be valid for time periods both before

Deleted: ,

Deleted: exBr

Deleted: Br

Deleted: MSA

Deleted: .

Deleted: 5

Deleted: -

Deleted: 264 point Stineman

Deleted: . exBr

Deleted: ).

Deleted: amount of bromine measured in excess of what is expected from a purely sea ice source (exBr)

Deleted: is Fig.

Deleted: exBr

Deleted: exBr

Deleted: 2nM

Deleted: 5nM

Deleted: Assuming that no major changes in atmospheric circulation patterns occurred to change the source regions for the marine aerosols between the preindustrial and industrial periods, our identification of MSA as a sea ice proxy (specifically a marginal sea ice zone proxy) may be valid for time periods both before and after 1850 at each ice core site. One major Northern Hemisphere climate phenomena is the North Atlantic Oscillation (NAO). NAO

Deleted: NAO

Deleted: .

516 and after 1850 at each ice core site.

517 The MSA records reveal that after 1820 C.E. a gradual decline in sea ice occurred along the southern  
518 Greenland coast (reflected in the Summit-2010 core) and that this decline in sea ice did not extend  
519 significantly to the most northern Greenland coastline (reflected in the minimal change in Tunu MSA  
520 during this period). It is not unexpected that the Summit-2010 record would show the most dramatic  
521 changes in sea ice since we have demonstrated that the Summit sea ice proxy (MSA) is sourced from  
522 the south-east Greenland coast – an area sensitive to climate changes as it is primarily covered by young,  
523 fragile sea ice. The timing of the sea ice decline is coincident with the end of the Little Ice Age, identified  
524 from  $\delta^{18}\text{O}$  ice core records as spanning the period 1420-1850 C.E. in Greenland (Weißbach et al., 2015).  
525 The dramatic dip in sea ice reflected in both the Tunu MSA and Br records at 1830 C.E. (and also seen  
526 less dramatically in Summit) also appears in the multi-proxy reconstruction of sea ice extent in the  
527 Western Nordic Seas performed by Macias Fauria et. al. (2010). This may be evidence of a 1830 C.E.  
528 sea ice decline event isolated to the east Greenland coast as the ice core records do not replicate the  
529 other dramatic, early 20<sup>th</sup> century fluctuations observed in the latter part of the Western Nordic Seas  
530 reconstruction.

Deleted: A.D

Deleted: A.D

531 From the ice core records it appears that the greatest decline in Greenland sea ice began in the mid 20<sup>th</sup>  
532 century, dropping to levels that are unprecedented in the last 200 years. This decline is observed along  
533 the entirety of the Greenland coast. Sea ice declined first around the southern coast (from 1930 C.E.,  
534 reflected in Summit-2010) followed 54 years later by the more northern coastline (reflected in the Tunu  
535 record, see infection timings in Table S1). This sea ice decline is coincident with the sustained increase  
536 in greenhouse gases which has been identified as the major climate forcing and driver of increased  
537 global temperatures during the 20<sup>th</sup> century (Mann et al., 1998) and follows the same general trend in  
538 Arctic wide sea ice extent observed by Kinnard (2008).

Deleted: A.D

539 Bromine (more specifically bromine enrichment (Spolaor et al., 2014) and bromine excess (Spolaor et  
540 al., 2016)) has also been suggested as a possible proxy for sea ice conditions, however the timing of the  
541 largest bromine aerosol deposition, in summer, does not coincide with the largest growth or extent of  
542 new sea ice. Sea ice begins to increase only at the end of summer as the fractures in the ice cover are  
543 re-laminated and the ice edge begins to advance southward (see Fig. 3f). Fig. S4 compares the record  
544 of total bromine and bromine enrichment (calculated relative to sodium, enrBr(Na)) from the Summit-  
545 2010 ice core. The major discrepancies between the two records occur when the total sodium signal has  
546 sharp maxima causing dips in the enrBr(Na) record in ~1954 and 1990 C.E. and the magnitude of the  
547 low frequency variability in enrBr(Na) is not as great as in the total bromine record. This is also

Moved (insertion) [5]

Moved (insertion) [6]

demonstrated in figs. 6 and 7 where the enrBr(Na) records are compared with the OWIP records. Whilst both series share high frequency temporal features, over the longer term (1900-2010) the low frequency trend is dramatically different. We are not discounting enrBr(Na) as a viable proxy for sea ice conditions, however the use of Na to try and extract the pure sea water component of the Br is complicated by the fact that a lot of Na comes from the sea ice surface as well as from the open ocean. Na itself has been used as a sea ice proxy in several prominent studies (Wais Divide Project Memembers, 2013; Wolff et al., 2003) because, like Br, Na is incorporated into the snow on the surface of the sea ice and can be subsequently blown aloft to produce the atmospheric Na signal seen in the ice core. In addition, the Na concentration is fractioned upon the formation of the ice when mirabilite ( $\text{Na}_2\text{SO}_4$ ) is precipitated out of the brine solution at  $-8^\circ\text{C}$  (Abbatt et al., 2012).

The calculated, non-sea ice bromine records (nsiBr) for both ice cores are shown in figs. 6 and 7. Like the enrBr(Na) records, the nsiBr records share some of the high frequency features of the OWIP records, however there is no significant correlation between nsiBr and the selected OWIP records over the short time period. This supports the supposition that the nsiBr record is indeed an extraction of the non-sea ice component of bromine from the total bromine record. Over the longer time period there is a significant negative correlation between OWIP and nsiBr at both sites (Summit-2010:  $r=-0.7$ ,  $p<0.001$ , Tunu:  $r=-0.22$ ,  $p<0.02$ ). This result is likely an artifact of the positive correlation from the MSA records used to generate the nsiBr records.

So what is the summer-time source of bromine? What is the cause of the increase in spring-time bromine explosion events in the industrial era? (see Fig. 3, lower panel) and why does the bromine record deviate from the sea ice proxy record (MSA) around the same time? Possible sources of bromine and the factors which may effect the resultant bromine deposition flux are discussed below.

#### 4.1 Alternate sources of bromine

##### 4.1.1 Combustion of coal

Bromine is present in coal (Bowen, 1979; Sturges and Harrison, 1986) and coal burning is therefore a potential source of increased bromine deposition on the Greenland ice sheet over the period 1860-1940 (McConnell and Edwards, 2008). McConnell et al. (2007) demonstrated that pollution from the Northern American coal burning era was deposited all over Greenland leaving as its fingerprint large amounts of black carbon and toxic heavy metals. Sturges (1986) measured the relative concentrations

Moved (insertion) [7]

Formatted: Font:Times, Font color: Text 1, English (US)

Deleted: Bromine has also been suggested as a possible proxy for sea ice conditions, however the timing of the largest bromine aerosol flux, in summer, does not coincide with the largest growth or extent of new sea ice.

Moved up [5]: Sea ice begins to increase only at the end of summer as the fractures in the ice cover are re-laminated and the ice edge begins to advance southward (see Fig. 3f).

Moved up [7]:  
So what is the summer-time source of bromine? What is the cause of the increase in spring-time bromine explosion events in the industrial era? (see Fig. 3, lower panel) and why does the bromine record deviate from the sea ice proxy record (MSA) around the same time? Possible sources of bromine and the factors which may effect the resultant bromine

Formatted: Font:Times, Font color: Text 1, English (US)

Deleted: flux are discussed below.

Deleted: (Bowen, 1979; Sturges and Harrison, 1986)

Deleted: (2008; 2007) demonstrated that pollution from the Northern American coal burning era was deposited all over Greenland leaving as its fingerprint large amounts of black carbon and toxic heavy metals.

of Br and Pb in particulates emitted from the stacks of coal fired power stations and found a molar ratio (Br:Pb) ranging between 0.36-0.67:1. Figure 8 illustrates that at both Summit and Tunu the exPb (lead not from dust sources) preserved in the ice cores over the coal burning era (~1920) was less than 1nM. This concentration implies that the upper limit to the amount of bromine deposited from coal combustion would be 0.67nM (assuming no loss of bromine from the particulates during transportation). This is an insignificant amount compared to the total Br signal preserved in the ice at this time. Coal combustion is not the major cause of the elevated industrial Br concentration.

#### 4.1.2 Leaded Gasoline

The largest global, historical, anthropogenic source of bromine is thought to be the combustion of leaded gasoline. Large quantities of 1,2-dibromoethane (DBE) were added to leaded fuel as a scavenger for Pb preventing lead oxide deposition by converting it to volatile lead bromide salts as well as  $CH_3Br$  (Berg et al., 1983; Nriagu, 1990; Oudijk, 2010). In 1925 C.E. gasoline had a Br:Pb molar ratio of 2:1 in a formulation which is now called “aviation fluid”. The Br:Pb molar ratio was reduced to 1:1 in the 1940s except in places such as the Soviet Union which continued to use “aviation fluid” for motor gasoline (Thomas et al., 1997). Although the consumption of leaded gasoline has been well documented, particularly in North America, the estimates of the emissions of bromine compounds from the combustion process are still unclear. Estimates of the amount of DBE that is converted into gaseous  $CH_3Br$  range from 0.1% to 25% (Bertram and Kolowich, 2000) and direct measurements of exhaust fumes across NW England found a Br:Pb ratio of between (0.65-0.8):1 in the airborne particulates (Sturges and Harrison, 1986).

The ratio of Br:Pb in the gasoline formulae can therefore be used only as an upper limit to predict the Br:Pb ratio in gasoline combustion aerosols transported to the ice core sites. Figure 8 shows a comparison between  $\psi$ siBr and exPb measured in each ice core. Also illustrated is the upper limit of the amount of bromine expected from gasoline sources assuming the 2:1 Br:Pb ratio for aviation gasoline over the whole leaded gasoline era. World-wide leaded gasoline emissions were estimated to have peaked in 1970 C.E. (Thomas et al., 1997)—an assumption that is supported by the observed timing of the exPb maximum observed in both ice cores. Whilst it is likely that leaded fuel contributed to the increased bromine observed between 1925 and 1970, it is clear that it was not the only contributor to the  $\psi$ siBr record, particularly after 1970 when the  $\psi$ siBr record continues to rise despite a worldwide decline in leaded fuel consumption. The disparity between the exPb and  $\psi$ siBr records suggests the driving force for the enhanced emission of Br was still active and increasing after 1970.

Deleted: , diethyl bromide (DEB)

Deleted: (Oudijk, 2010;Nriagu, 1990;Berg et al., 1983). In 1925

Deleted: (Thomas et al., 1997).

Deleted: E

Deleted: exBr

Deleted: (blue) and just between 1925 and 1940 (green; representing source regions outside the Soviet Union).

Deleted: exBr

Deleted: exBr

Deleted: exBr

Deleted: ing

743 **4.1.3 Seasonal salinity changes**

744 Younger sea ice surfaces such as frost flowers, new and 1<sup>st</sup> year sea ice have a higher salinity and thus  
745 have higher bromine concentrations than older sea ice surfaces (Hunke et al., 2011) . The salinity of sea  
746 ice is at its maximum at the start of the winter season after which surface salinity slowly diminishes due  
747 to gravitational draining (Hunke et al., 2011). As summer approaches, ice continues to undergo  
748 desalination due to melting of surface snow which percolates through the ice (Hunke et al., 2011).  
749 Satellite observations that the BrO flux from the sea ice declines over summer (despite increasing  
750 insolation) is likely due to the combined reduction in young sea ice area and in ice salinity. Ocean  
751 surface salinity decreases in the summer due to the increased meteoric water flux and melting of  
752 desalinated sea ice. Salinity increases are therefore unlikely to be the sole cause of the psiBr flux  
753 observed in the ice core records and the observed summer maximum in bromine.

Deleted: exBr

754 **4.1.4 Organic bromine species**

755 Gaseous bromocarbons can be a source of inorganic bromine to the snow pack when they react with  
756 •OH or to a lesser extent with •NO<sub>x</sub> or by photolysis (Kerkweg et al., 2008; WMO, 1995) to form the  
757 less reactive species HBr, BrNO<sub>3</sub> and HOBr. These species can then be washed out of the atmosphere  
758 and deposited on the snow surface due to their high solubility (Fan and Jacob, 1992; Sander et al., 1999;  
759 Yung et al., 1980).

Deleted: (Kerkweg et al., 2008; WMO, 1995)

Deleted: ,

760 The predominant source of gaseous bromine in the atmosphere is methyl bromide, CH<sub>3</sub>Br (WMO,  
761 2002). The major modern sources of CH<sub>3</sub>Br are fumigation, biomass burning, leaded fuel combustion,  
762 coastal marshes, wetlands, rapeseed and the oceans (WMO, 2002). The ocean is also a major sink for  
763 CH<sub>3</sub>Br, the temperature sensitive dissolution occurring through hydrolysis and chloride ion substitution  
764 to form bromide (WMO, 1995). ~30% of CH<sub>3</sub>Br was from industrial emissions at the time of the global  
765 peak in the CH<sub>3</sub>Br mixing ratio (1996-1998) (Montzka and Reimann, 2010). The timing of the massive  
766 increases in psiBr seen at both ice cores sites coincides with the timing of maximum anthropogenic  
767 emissions of CH<sub>3</sub>Br. However, the estimated 2.7 ppt increase in global tropospheric CH<sub>3</sub>Br above  
768 preindustrial levels equates to only ~ 3.7 ppt (0.05nM) Br incorporated into the snow pack (assuming  
769 100% conversion efficiency of CH<sub>3</sub>Br in soluble Br species). This level is far less than the 2-5 nM  
770 increase in psiBr observed in the ice cores during the industrial period.

Deleted: (Montzka and Reimann, 2010).

Deleted: inorganic bromine

Deleted: exBr

771 Bromoform (CHBr<sub>3</sub>) is emitted from vegetation such as marine phytoplankton and seaweed. It has the  
772 largest globe flux of all the bromocarbons (estimated at almost 5 times that of CH<sub>3</sub>Br (Kerkweg et al.,  
773 2008). However, it is very short-lived (atmospheric lifetime of ~ 17 days (Ordóñez et al., 2012) and

Deleted: (Kerkweg et al., 2008)



thus is confined to the marine boundary layer. Inorganic bromine formed from the destruction of  $CHBr_3$  would therefore be representative of only local sources of organic bromine. The biological seasonal cycle maximises the production of  $CHBr_3$  in summer and concentrations are greatly reduced but not negligible in winter (tidal forcing also influences bromocarbon emission by allowing coastal algae to dry-out (Kerkweg et al., 2008). The season of Arctic sea ice algae productivity is confined by limitations in available sunlight and nutrients resulting in a mid-to-late spring maxima – depending upon site location (Leu et al., 2015) – as is reflected in the seasonality of the MSA record. Direct transport of bromine enriched aerosols from these algal sources to the ice core sites again cannot explain the summer maximum of bromine observed in the ice. In addition to the incoherence of the seasonality of the bromine ice core signal, to-date biogenic sources have been considered insignificant sources of bromine in the Arctic marine boundary layer compared with the inorganic bromine source from sea salts (Simpson et al., 2007).

**Deleted:** (Kerkweg et al., 2008)

**Deleted:** The summer maximum in inorganic bromine at Summit (

**Moved up [6]:** Fig.

**Deleted:** 3a) suggests that a biogenic source of bromine is dominant. However to-date biogenic sources have been considered insignificant

**Deleted:** These results suggest that a biogenic system should be reconsidered as a major source of the natural inorganic bromine flux to the polar regions.

## 4.2 Cause of the spring-time increase in bromine flux

### 4.2.1 Bromine explosion events

Spring is the time of ‘bromine explosion’ events above sea ice. Sea salt aerosols passing through these BrO plumes can become enriched with bromine by adsorbing the gaseous species (Fan and Jacob, 1992; Langendörfer et al., 1999; Lehrer et al., 1997; Moldanová and Ljungström, 2001; Sander et al., 2003). Nghiem (2012) showed that these bromine rich air masses can then be elevated above the planetary boundary layer and transported hundreds of kilometres inland. Increasing the frequency and duration of the bromine explosion events would therefore likely increase the amount of bromine delivered to the ice core sites during spring without influencing the total aerosol flux, and thus explain the shift in the bromine seasonal concentrations from a purely summer to a broad spring-summer maxima (Fig. 3).

**Deleted:** (Fan and Jacob, 1992; Langendörfer et al., 1999; Lehrer et al., 1997; Moldanová and Ljungström, 2001; Sander et al., 2003)

**Deleted:** .

Spring-time field studies at Ny Ålesund, Svalbard have shown positive correlation between atmospheric filterable bromine species and elevated levels of sulfate and nitrate (Langendörfer et al., 1999; Lehrer et al., 1997) suggesting that acidic, anthropogenic pollution may be the driver of the observed increases in annual bromine enrichment during the industrial period and seasonal shift.

**Deleted:** sulphate and nitrate (Langendörfer et al., 1999; Lehrer et al., 1997) suggesting that acidic, anthropogenic pollution may be the driver of the observed increases in annual bromine enrichment during the industrial period

### 4.2.2 Acidity effects on debromination

In remote, relatively clean environments such as the Arctic, even small increases in acidity are thought to affect the cycling of bromine in the snow pack (Finlayson-Pitts, 2003; Pratt et al., 2013; Sander et al.,

1999). In the laboratory, increasing the acidity of frozen (Abbatt et al., 2010) and liquid salt solutions (Frinak and Abbatt, 2006; George and Anastasio, 2007) increased the yield of gas-phase  $Br_2$  whilst at the same time increasing the solubility of other bromine species, such as  $HBr$ . The uptake efficiency of  $HBr$  by acidic sulfate aerosols, for example, is estimated at 80% compared to 30% for sea salt aerosols (Parrella et al., 2012). Interestingly, Abbatt (1995) demonstrated that  $HBr$  is more than 100 times more soluble in super-cooled sulfuric acid solutions than  $HCl$ . This may explain the cause of bromine enrichment in the aerosol measured in the ice cores relative to the more abundant chlorine (Fig. S3). The results of both the laboratory and field studies suggest that increasing snow/ice acidity in the Arctic will likely enhance spring-time bromine explosion events above the sea ice whilst the increase in solubility allows the termination products of the explosion to be transported away from the sites on the surface of acidic aerosols. Increasing spring-time bromine aerosol concentrations would increase the average annual bromine concentrations deposited on the ice sheet and could explain the  $nsiBr$  records observed in both ice cores.

There are also significant periods over which the calculated  $nsiBr$  record shows negative values (e.g. 1815-1870 C.E. in Summit-2010 and 1860-1940 C.E. in Tunu). The negative values are a result of the Total Br being less than that calculated by interpolation from the smoothed MSA record. Though the sources of Br and MSA are linked – which is what provides the similarities between the general low frequency trend of the two species, the atmospheric processing, transport and deposition of the two species may be modified by different variables such as changes in atmospheric acidity, for example. These variables cause the short term differences between the MSA and Total Br records preserved in the ice so we believe it is not unreasonable to expect negative values in the calculated non-sea ice Br record when the MSA and Total Br are close (essentially no  $nsiBr$ ). The periods of negative  $nsiBr$  do correspond to the timing of increased sulfate concentrations (due to volcanic or industrial activity) and this could be an indication that the atmospheric sulfate concentrations do have some influence on the production of either the MSA or Br records.

Figure 9 illustrates that of the two dominant acidic species preserved in the ice,  $HNO_3$  (represented by nitrate) shows the highest correlation to total bromine over sub-decadal time scales at both ice core sites. Records were detrended with an 11 year running average before comparison to isolate the high frequency components of each record. The bromine – sulfuric acid (represented by sulfate) correlation is not significant. This is primarily because there is no bromine response to the dominant volcanic sulfate spikes throughout the record. The large spikes in sulfate concentrations did not cause a depletion of bromine preserved in the snowpack (Figure 9). This result might be expected if the increased acidity caused more bromine to volatilize. These results suggest that  $HNO_3$  is the most influential of the MBL

Deleted: (Abbatt et al., 2010)

Deleted: ph

Deleted: ph

Deleted: S2

Formatted: Font color: Text 1

Deleted: exBr

Formatted: Font color: Text 1

Formatted: Tabs: 16.25 cm, Left

Deleted: ph

365 acidic species in the processing and transport of Br on aerosols in the MBL.

#### 366 4.2.3 NO<sub>x</sub> and links to bromine

367 The snow and atmospheric chemistries of bromine and nitrate ( $NO_3^-$ ) are tightly linked.  $NO_3^-$  is one of  
368 the main sources of the •OH radical. The •OH radical can oxidize bromide salts and cause the release  
369 of gas-phase bromine species (Abbatt et al., 2010; Chu and Anastasio, 2005; George and Anastasio,  
370 2007; Jacobi et al., 2014). Morin et al. (2008) observed that the majority of nitrate that is deposited to  
371 the snow surface is of the form  $BrNO_3$  in coastal Arctic boundary layer.  $BrNO_3$  forms by gas-phase  
372 reaction of  $BrO$  and  $NO_2$ .  $BrNO_3$  is quickly adsorbed back onto the snow and aerosol surfaces due to  
373 its high solubility. The heterogeneous hydrolysis of  $BrNO_3$  to again release bromine species back into  
374 the gas-phase has also been observed (Parrella et al., 2012) and can occur both during sunlight hours as  
375 well as in the dark (Sander et al., 1999). However, the study of Thomas et al. (2012) into the cycling of  
376  $NO_x$  and bromine species in the snowpack at Summit concluded that the presence of snow  $NO_3^-$  would  
377 suppress the emission of  $BrO$  from the snow pack and into the interstitial air.  
378 In spring, when the greatest concentrations of  $BrO$  are observed over the sea ice the atmospheric  
379 concentrations of  $NO_x$  species is rising. After 1900 C.E. there was, on average, a 60% increase in spring  
380  $NO_3^-$  concentrations observed in Summit-2010 ice core (Fig. 3d) which, as discussed in Sect. 4.2.1, if  
381 reflected in the concentration of acidic aerosols landing on the sea ice (specifically  $HNO_3$   
382 concentrations) would enhance the emission of  $BrO$  into the MBL. Satellite imagery shows that bromine  
383 in the form of  $BrO$  is confined primarily to the atmosphere above sea ice (Schönhardt et al., 2012;  
384 Wagner et al., 2001) but the presence of measurable bromine concentration hundreds of kilometres  
385 inland preserved in the ice cores demonstrates that the bromine must be transported inland, just not in  
386 the form of  $BrO$ . The reaction of atmospheric  $NO_2$  with  $BrO$  can produce the highly soluble  $BrNO_3$   
387 which will preserve the bromine in the aerosol allowing it to be transported inland. If there are high  
388  $NO_3^-$  concentrations at the deposition site this will aid in fixing the bromine into the snow pack. This is  
389 supported by the observation that  $NO_3^-$  snow pack concentrations reach a maximum in summer,  
390 coherent with bromine snow pack concentrations even though maximum Br emission from the sea ice  
391 occurs in spring. So it appears that  $NO_x$  in its different forms, as  $NO_2$ ,  $NO_3^-$ ,  $HNO_3$  or  $BrNO_3$  is  
392 intertwined with Br as it cycles between the gas and condensed phases and as it is transported from sea  
393 ice source to deposition site. Elevated levels of  $NO_x$  over the Arctic could thus be the cause of the  
394 deviation of the bromine record from the MSA, sea ice proxy record.  
395 The high correlation between the preindustrial (1750-1850 C.E.)  $NO_3^-$  and Br records (Fig. 9) supports

Deleted:

Deleted: (Abbatt et al., 2010; Chu and Anastasio, 2005; George and Anastasio, 2007; Jacobi et al., 2014)

Deleted: in the coastal Arctic boundary layer.

Deleted:  $NO_x$  are intertwined with Br as it cycles between the gas and condensed phases

Formatted: English (US)

Deleted: The seasonality of the  $NO_3^-$  signal preserved in the ice cores is coherent with Br, showing a summer-time maximum (Fig. 3a,d). The slight shift in timing of the industrial nitrate seasonal maximum towards spring is replicated in the seasonal bromine signal preserved in the ice (Figure 3). The high correlation between the preindustrial (1750-1850)  $NO_3^-$  and Br records (Fig.

308 this observation of co-transport and sink of Br and  $NO_3^-$  into the snow pack, though the natural sources  
 309 of each are distinctly different. In the industrial era the low frequency temporal profile of the total  
 310 bromine and nitrate records differ considerably, particularly at Summit (Fig. S15), apparently  
 311 questioning the tight relationship observed before 1850. However, the positive correlation between the  
 312 nitrate and the Br/MSA (Fig. 4) and nsiBr (Fig. 8) records is striking at both sites. The large relative  
 313 increase in bromine (compared with MSA) during the era of high  $NO_x$  pollution may point to a non-sea  
 314 ice source of bromine linked to nitrate emissions or simply an increased spring-time emission and  
 315 summer-time deposition of Br from sea ice sources.

316 Bromine and  $NO_x$  species shared a common source in the 20<sup>th</sup> century through the combustion of leaded  
 317 gasoline (Sect. 4.1.2). As discussed above, we observe that leaded fuel pollution reaching the Arctic  
 318 began to decline after 1970 in-line with reduced global consumption, but the amount of bromine in-  
 319 excess of natural sources (nsiBr) continued to increase – following the trends in  $NO_x$  pollution (Fig.  
 320 8a). The continued increase in  $NO_x$  despite the decline in leaded fuel combustion is attributed primarily  
 321 to biomass burning, soil emissions and unleaded fossil fuel combustion (Lamarque et al., 2013). As the  
 322 leaded fuel source of bromine began to decline, organic bromine pollutants continued to increase, as  
 323 was discussed in Sect. 4.1.4. This can only account for a small fraction of the observed Br. The  
 324 continued correlation between nitrate and nsiBr despite the decoupling of nitrate and bromine  
 325 anthropogenic sources after 1970, suggests that nitrate pollution is likely influencing the processing of  
 326 local, natural sources of bromine in the polar MBL, in effect increasing the mobility of the bromine and  
 327 thus its flux and preservation in the ice sheet.

#### 328 4.2.4 Consequences of nitrate driven increased bromine mobility in the Arctic

329 Plumes of BrO emitted from sea ice regions have been linked to mercury deposition events which lead  
 330 to an increase in the bioavailability of toxic mercury species in polar waters (Parrella et al., 2012).  
 331 Increased spring-time mobilization of bromine from the sea ice induced by anthropogenic nitrate could  
 332 therefore increase the frequency and duration of these events and thus the mercury toxicity of the oceans.  
 333 Increased atmospheric bromine concentrations would also increase the frequency of ozone depletion  
 334 events (Simpson et al., 2007) thereby altering the oxidative chemistry of the polar MBL.

335 Whilst several studies have begun to explore bromine records from ice cores as a proxy for past sea ice  
 336 conditions, the results of this study demonstrate that in an era of massive increases in atmospheric acidity  
 337 the natural relationship between bromine and sea ice conditions can become distorted, precluding it  
 338 from being an effective modern-day Arctic sea ice proxy.

Deleted: .

Deleted: (Fig. 2)

Deleted: (Fig. 4)

Deleted: dramatically,

Deleted: exBr, Fig. 8

Deleted: 4

Deleted: exBr

Deleted: onto

347  
348  
349  
350  
351  
352  
353  
354  
355  
356  
357  
358  
359  
360  
361  
362  
363  
364  
365  
366  
367  
368  
369

5 Conclusion

In this study we have shown that high resolution MSA measurements preserved in ice cores can be used as a proxy for sea ice conditions (specifically the size of the marginal sea ice zone) along specific sections of the Greenland coast. The MSA records show that sea ice began to decline at the end of the LIA and again, more dramatically during the Industrial period. Also, unsurprisingly, the changes in sea ice conditions in the northern sites have been less dramatic than along the southern coastline. Comparison between the 260 year records of bromine and MSA presented in this study allow us to show that in the preindustrial era bromine concentrations preserved in the Greenland ice sheet are also likely linked to the local sea ice conditions. With the decline of sea ice in the modern era and the dramatic increase in acidic pollutants reaching the Arctic the sea ice-bromine connection is distorted, precluding it from being an effective, direct sea ice proxy during the industrial era. The introduction of ~~NO<sub>x</sub>~~ pollution in particular, into the clean Arctic environment promotes mobilization of bromine from the sea ice, which in turn increases the bromine enrichment of the sea salt aerosols, forcing more bromine inland (particularly in spring) than would occur naturally. Nitrate has also been linked with the mechanism for preservation of bromine in the snowpack. The summer-time maximum of nitrate may therefore be responsible for the observed summer-time bromine maximum preserved in the ice cores. Whilst Northern Hemisphere pollution may prevent bromine from being an effective modern-day sea ice proxy in the Arctic, in Antarctica the anthropogenic flux of nitrate species is thought to be small in comparison with natural sources (Wolff, 2013), leaving room for the possibility that bromine may still be an effective proxy for local Antarctic sea ice conditions and for preindustrial sea ice reconstructions.

Deleted: NO<sub>x</sub>

Formatted: Normal  
Formatted: Font:Arial, Not Bold

071 **Author contribution**

072 Manuscript written and data analysis performed by O.J.M with expert editing by E.S.. Ice cores supplied  
073 by J.R.M.. Tunu ice core was collected and processed by O.J.M, J.R.M., N.J.C, M.S., R.H.R. under the  
074 leadership of Beth Bergeron. Ice cores dated by M.S., J.R.M.. ICP-MS and CFA measurements  
075 performed by O.J.M, J.R.M., N.J.C., L.L, D.P., M.S.. MSA measurements designed and performed by  
076 M.G., E.S.

077

078 **Acknowledgements**

079 This research was funded by the National Science Foundation; grant numbers 1023672 and 1204176.

080

## References

- Abbatt, J., Oldridge, N., Symington, A., Chukalovskiy, V., McWhinney, R. D., Sjostedt, S. and Cox, R. A.: Release of gas-phase halogens by photolytic generation of OH in frozen halide-nitrate solutions: an active halogen formation mechanism?, *J. Phys. Chem. A*, 114(23), 6527–33, doi:10.1021/jp102072t, 2010.
- Abbatt, J. P. D.: Interactions of HBr, HCl, and HOBr With Supercooled Sulfuric- Acid-Solutions of Stratospheric Composition, *J. Geophys. Res.*, 100(D7), 14009–14017, 1995.
- Abbatt, J. P. D., Thomas, J. L., Abrahamsson, K., Boxe, C., Granfors, A., Jones, A. E., King, M. D., Saiz-Lopez, A., Shepson, P. B., Sodeau, J., Toohey, D. W., Toubin, C., von Glasow, R., Wren, S. N. and Yang, X.: Halogen activation via interactions with environmental ice and snow in the polar lower troposphere and other regions, *Atmos. Chem. Phys.*, 12(14), 6237–6271, doi:10.5194/acp-12-6237-2012, 2012.
- Abram, N. J., Wolff, E. W. and Curran, M. A. J.: A review of sea ice proxy information from polar ice cores, *Quat. Sci. Rev.*, 79, 168–183, doi:10.1016/j.quascirev.2013.01.011, 2013.
- Appenzeller, C., Schwander, J., Sommer, S. and Stocker, T. F.: The North Atlantic Oscillation and its imprint on precipitation and ice accumulation in Greenland, *Geophys. Res. Lett.*, 25(11), 1939, doi:10.1029/98GL01227, 1998.
- Arienzo, M. M., McConnell, J. R., Chellman, N., Criscitiello, A. S., Curran, M., Fritzsche, D., Kipfstuhl, S., Mulvaney, R., Nolan, M., Opel, T., Sigl, M. and Steffensen, J. P.: A Method for Continuous <sup>239</sup>Pu Determinations in Arctic and Antarctic Ice Cores, *Environ. Sci. Technol.*, 50(13), 7066–7073, doi:10.1021/acs.est.6b01108, 2016.
- Barrie, L. A., Hoff, R. M. and Daggupaty, S. M.: The influence of mid-latitudinal pollution sources on haze in the Canadian arctic, *Atmos. Environ.*, 15(8), 1407–1419, doi:10.1016/0004-6981(81)90347-4, 1981.
- Berg, W. W., Sperry, P. D., Rahn, K. A. and Gladney, E. S.: Atmospheric Bromine in the Arctic, *J. Geophys. Res.*, 88, 6719–6736, doi:10.1029/JC088iC11p06719, 1983.
- Bertram, F. J. and Kolowich, J. B.: A study of methyl bromide emissions from automobiles burning leaded gasoline using standardized vehicle testing procedures, *Geophys. Res. Lett.*, 27(9), 1423–1426, doi:10.1029/1999GL011008, 2000.
- Bowen, H. J. M.: Environmental chemistry of the elements / H. J. M. Bowen, BOOK, Academic Press,

**Comment [ojm1]:** Change titles with CAPS and remove hyperlinks

**Comment [ojm2]:**

Deleted: "

... [1]



London ; New York., 1979.

Chellman, N. J., Hastings, M. G. and McConnell, J. R.: Increased nitrate and decreased  $\delta^{15}\text{N-NO}_3^-$  in the Greenland Arctic after 1940 attributed to North American oil burning, *Cryosph. Discuss.*, 1–22, doi:10.5194/tc-2016-163, 2016.

Chen, Q. S., Bromwich, D. H. and Bai, L.: Precipitation over Greenland retrieved by a dynamic method and its relation to cyclonic activity, *J. Clim.*, 10(5), 839–870, 1997.

Chu, L. and Anastasio, C.: Formation of hydroxyl radical from the photolysis of frozen hydrogen peroxide, *J. Phys. Chem. A*, 109(28), 6264–6271, doi:10.1021/jp051415f, 2005.

Curran, M. A. J. and Jones, G. B.: Dimethyl sulfide in the Southern Ocean: Seasonality and flux, *J. Geophys. Res.*, 105(D16), 20451, doi:10.1029/2000JD900176, 2000.

Curran, M. A. J., van Ommen, T. D., Morgan, V. I., Phillips, K. L. and Palmer, A. S.: Ice core evidence for Antarctic sea ice decline since the 1950s., *Science*, 302(5648), 1203–1206, doi:10.1126/science.1087888, 2003.

Draxler, R. R. and Hess, G. D.: An Overview of the HYSPLIT\_4 Modelling System for Trajectories, Dispersion, and Deposition., *Aust. Meteorol. Mag.*, 47(June 1997), 295–308, 1998.

Fan, S.-M. and Jacob, D. J.: Surface ozone depletion in Arctic spring sustained by bromine reactions on aerosols, *Nature*, 359(6395), 522–524, doi:10.1038/359522a0, 1992.

Felix, J. D. and Elliott, E. M.: The agricultural history of human-nitrogen interactions as recorded in ice core  $\delta^{15}\text{N-NO}_3^-$ , *Geophys. Res. Lett.*, 40(8), 1642–1646, doi:10.1002/grl.50209, 2013.

Finlayson-Pitts, B. J.: The Tropospheric Chemistry of Sea Salt: A Molecular-Level View of the Chemistry of NaCl and NaBr, *Chem. Rev.*, 103(12), 4801–4822, doi:10.1021/cr020653t, 2003.

Fischer, H. and Wagenbach, D.: Large-scale spatial trends in recent firn chemistry along an east-west transect through central Greenland, *Atmos. Environ.*, 30(19), 3227–3238, doi:10.1016/1352-2310(96)00092-1, 1996.

Frinak, E. K. and Abbatt, J. P. D.: Br<sub>2</sub> production from the heterogeneous reaction of gas-phase OH with aqueous salt solutions: Impacts of acidity, halide concentration, and organic surfactants., *J. Phys. Chem. A*, 110(35), 10456–64, doi:10.1021/jp063165o, 2006.

George, I. J. and Anastasio, C.: Release of gaseous bromine from the photolysis of nitrate and hydrogen peroxide in simulated sea-salt solutions, *Atmos. Environ.*, 41(3), 543–553, doi:10.1016/j.atmosenv.2006.08.022, 2007.

Hunke, E. C., Notz, D., Turner, A. K. and Vancoppenolle, M.: The multiphase physics of sea ice: a review for model developers, *Cryosph.*, 5(4), 989–1009, doi:10.5194/tc-5-989-2011, 2011.

Jacobi, H. W., Kleffmann, J., Villena, G., Wiesen, P., King, M., France, J., Anastasio, C. and Staebler, R.: Role of nitrite in the photochemical formation of radicals in the snow, *Environ. Sci. Technol.*, 48(1), 165–172, doi:10.1021/es404002c, 2014.

Jaffrezo, J. L., Davidson, C. I., Legrand, M. and Dibb, J. E.: Sulfate and MSA in the air and snow on the Greenland Ice Sheet, *J. Geophys. Res.*, 99(D1), 1241–1253, doi:10.1029/93JD02913, 1994.

Kahl, J. D. W., Martinez, D. A., Kuhns, H., Davidson, C. I., Jafferezo, J. L. and Harris, J. M.: Air mass trajectories to Summit, Greenland : A 44-year climatology and some episodic events, *J. Geophys. Res. Ocean.*, 102(C12), 26861–26875, 1997.

Kerkweg, A., Jöckel, P., Warwick, N., Gebhardt, S., Brenninkmeijer, C. A. M. and Lelieveld, J.: Consistent simulation of bromine chemistry from the marine boundary layer to the stratosphere – Part 2: Bromocarbons, *Atmos. Chem. Phys. Discuss.*, 8(3), 9477–9530, doi:10.5194/acpd-8-9477-2008, 2008.

Kinnard, C., Zdanowicz, C. M., Koerner, R. M. and Fisher, D. A.: A changing Arctic seasonal ice zone: Observations from 1870-2003 and possible oceanographic consequences, *Geophys. Res. Lett.*, 35(2), 2–6, doi:10.1029/2007GL032507, 2008.

Lamarque, J.-F., Dentener, F., McConnell, J., Ro, C.-U., Shaw, M., Vet, R., Bergmann, D., Cameron-Smith, P., Dalsoren, S., Doherty, R., Faluvegi, G., Ghan, S. J., Josse, B., Lee, Y. H., MacKenzie, I. A., Plummer, D., Shindell, D. T., Skeie, R. B., Stevenson, D. S., Strode, S., Zeng, G., Curran, M., Dahl-Jensen, D., Das, S., Fritzsche, D. and Nolan, M.: Multi-model mean nitrogen and sulfur deposition from the Atmospheric Chemistry and Climate Model Intercomparison Project (ACCMIP): evaluation of historical and projected future changes, *Atmos. Chem. Phys.*, 13(16), 7997–8018, doi:10.5194/acp-13-7997-2013, 2013.

Langendörfer, U., Lehrer, E., Wagenbach, D. and Platt, U.: Observation of filterable bromine variabilities during Arctic tropospheric ozone depletion events in high (1 hour) time resolution, *J. Atmos. Chem.*, 34(1), 39–54, doi:10.1023/A:1006217001008, 1999.

Legrand, M., Hammer, C., De Angelis, M., Savarino, J., Delmas, R., Clausen, H. and Johnsen, S. J.: Sulfur-containing species (methanesulfonate and SO<sub>4</sub>) over the last climatic cycle in the Greenland Ice Core Project (central Greenland) ice core, *J. Geophys. Res.*, 102(C12), 26663, doi:10.1029/97JC01436, 1997.

Lehrer, E., Wagenbach, D. and Platt, U.: Aerosol chemical composition during tropospheric ozone depletion at Ny Ålesund/Svalbard, *Tellus B*, 49(5), doi:10.3402/tellusb.v49i5.15987, 1997.

Leu, E., Mundy, C. J., Assmy, P., Campbell, K., Gabrielsen, T. M., Gosselin, M., Juul-Pedersen, T. and Gradinger, R.: Arctic spring awakening - Steering principles behind the phenology of vernal ice algal blooms, *Prog. Oceanogr.*, 139, 151–170, doi:10.1016/j.pocean.2015.07.012, 2015.

Li, S.-M. and Barrie, L. A.: Biogenic sulfur aerosol in the Arctic troposphere: 1. Contributions to total sulfate, *J. Geophys. Res.*, 98(D11), 20613, doi:10.1029/93JD02234, 1993.

Macias Fauria, M., Grinsted, A., Helama, S., Moore, J., Timonen, M., Martma, T., Isaksson, E. and Eronen, M.: Unprecedented low twentieth century winter sea ice extent in the Western Nordic Seas since A.D. 1200, *Clim. Dyn.*, 34(6), 781–795, doi:10.1007/s00382-009-0610-z, 2010.

Mann, M. E., Bradley, R. S. and Hughes, M. K.: Global-scale temperature patterns and climate forcing over the past six centuries, *Nature*, 392(6678), 779–787, doi:10.1038/33859, 1998.

Maselli, O. J., Fritzsche, D., Layman, L., McConnell, J. R. and Meyer, H.: Comparison of water isotope-ratio determinations using two cavity ring-down instruments and classical mass spectrometry in continuous ice-core analysis., *Isotopes Environ. Health Stud.*, 49(September 2014), 387–98, doi:10.1080/10256016.2013.781598, 2013.

McConnell, J. R. and Edwards, R.: Coal burning leaves toxic heavy metal legacy in the Arctic., *Proc. Natl. Acad. Sci. U. S. A.*, 105(34), 12140–12144, doi:10.1073/pnas.0803564105, 2008.

McConnell, J. R., Lamorey, G. W., Lambert, S. W. and Taylor, K. C.: Continuous ice-core chemical analyses using inductively coupled plasma mass spectrometry., *Environ. Sci. Technol.*, 36(775), 7–11, doi:10.1021/es011088z, 2002.

McConnell, J. R., Edwards, R., Kok, G. L., Flanner, M. G., Zender, C. S., Saltzman, E. S., Banta, J. R., Pasteris, D. R., Carter, M. M. and Kahl, J. D. W.: 20th-Century Industrial Black Carbon Emissions Altered Arctic Climate Forcing, *Science*, 317, 1381–1384, doi:10.1126/science.1144856, 2007.

Millero, F. J.: The Physical Chemistry of Seawater, *Annu. Rev. Earth Planet. Sci.*, 2(1), 101–150, doi:10.1146/annurev.ea.02.050174.000533, 1974.

Moldanová, J. and Ljungström, E.: Sea-salt aerosol chemistry in coastal areas: A model study, *J. Geophys. Res.*, 106, 1271, doi:10.1029/2000JD900462, 2001.

Montzka, S. and Reimann, S.: Scientific Assessment of Ozone Depletion 2010: Scientific Summary Chapter 1 Ozone-Depleting Substances (ODSs) and Related Chemicals. [online] Available from:

<http://www.esrl.noaa.gov/csd/assessments/ozone/2010/summary/ch1.html> (Accessed 23 December 2015), 2010.

Morin, S., Savarino, J., Frey, M. M., Yan, N., Bekki, S., Bottenheim, J. and Martins, J. M. F.: Tracing the origin and fate of NO<sub>x</sub> in the Arctic atmosphere using stable isotopes in nitrate., *Science*, 322(5902), 730–2, doi:10.1126/science.1161910, 2008.

Mulvaney, R., Pasteur, E. C., Peel, D. A., Saltzman, E. S. and Whung, P.-Y.: The ratio of MSA to non-sea-salt sulphate in Antarctic Peninsula ice cores, *Tellus B*, 44(4), doi:10.3402/tellusb.v44i4.15457, 1992.

Nghiem, S. V., Rigor, I. G., Richter, A., Burrows, J. P., Shepson, P. B., Bottenheim, J., Barber, D. G., Steffen, A., Latonas, J., Wang, F., Stern, G., Clemente-Colón, P., Martin, S., Hall, D. K., Kaleschke, L., Tackett, P., Neumann, G. and Asplin, M. G.: Field and satellite observations of the formation and distribution of Arctic atmospheric bromine above a rejuvenated sea ice cover, *J. Geophys. Res. Atmos.*, 117(D17), n/a-n/a, doi:10.1029/2011JD016268, 2012.

Nriagu, J. O.: The rise and fall of leaded gasoline, *Sci. Total Environ.*, 92, 13–28, 1990.

NSIDC, National Snow and Ice Data Center, [online] Available from: <http://nsidc.org/cryosphere/seaice/data/terminology.html> (Accessed December 2013).

O'Dwyer, J., Isaksson, E., Vinje, T., Jauhiainen, T., Moore, J., Pohjola, V., Vaikmae, R. and van de Wal, R. S. W.: Methanesulfonic acid in a Svalbard ice core as an indicator of ocean climate, *Geophys. Res. Lett.*, 27(8), 1159–1162, doi:10.1029/1999GL011106, 2000.

Ordóñez, C., Lamarque, J.-F., Tilmes, S., Kinnison, D. E., Atlas, E. L., Blake, D. R., Sousa Santos, G., Brasseur, G. and Saiz-Lopez, A.: Bromine and iodine chemistry in a global chemistry-climate model: description and evaluation of very short-lived oceanic sources, *Atmos. Chem. Phys.*, 12(3), 1423–1447, doi:10.5194/acp-12-1423-2012, 2012.

Oudijk, G.: The Rise and Fall of Organometallic Additives in Automotive Gasoline, *Environ. Forensics*, 11(933126918), 17–49, doi:10.1080/15275920903346794, 2010.

Parrella, J. P., Jacob, D. J., Liang, Q., Zhang, Y., Mickley, L. J., Miller, B., Evans, M. J., Yang, X., Pyle, J. A., Theys, N. and Van Roozendael, M.: Tropospheric bromine chemistry: implications for present and pre-industrial ozone and mercury, *Atmos. Chem. Phys.*, 12(15), 6723–6740, doi:10.5194/acp-12-6723-2012, 2012.

Pasteris, D. R., McConnell, J. R. and Edwards, R.: High-resolution, continuous method for measurement

of acidity in ice cores, *Environ. Sci. Technol.*, 46, 1659–1666, doi:10.1021/es202668n, 2012.

Pratt, K. A., Custard, K. D., Shepson, P. B., Douglas, T. A., Pöhler, D., General, S., Zielcke, J., Simpson, W. R., Platt, U., Tanner, D. J., Gregory Huey, L., Carlsen, M. and Stirm, B. H.: Photochemical production of molecular bromine in Arctic surface snowpacks, *Nat. Geosci.*, 6(5), 351–356, doi:10.1038/ngeo1779, 2013.

Rankin, A. M., Wolff, E. W. and Martin, S.: Frost flowers: Implications for tropospheric chemistry and ice core interpretation, *J. Geophys. Res. Atmos.*, 107(D23), 4683, doi:10.1029/2002JD002492, 2002.

Rayner, N. A.: Global analyses of sea surface temperature, sea ice, and night marine air temperature since the late nineteenth century, *J. Geophys. Res.*, 108(D14), 4407, doi:10.1029/2002JD002670, 2003.

Röthlisberger, R., Bigler, M., Hutterli, M., Sommer, S., Stauffer, B., Junghans, H. G. and Wagenbach, D.: Technique for continuous high-resolution analysis of trace substances in firn and ice cores, *Environ. Sci. Technol.*, 34(2), 338–342, doi:10.1021/es9907055, 2000.

Röthlisberger, R., Mulvaney, R., Wolff, E. W., Hutterli, M. a., Bigler, M., Sommer, S. and Jouzel, J.: Dust and sea salt variability in central East Antarctica (Dome C) over the last 45 kyrs and its implications for southern high-latitude climate, *Geophys. Res. Lett.*, 29(20), 1–4, doi:10.1029/2003GL016936, 2002.

Saltzman, E. S., Dioumaeva, I. and Finley, B. D.: Glacial/interglacial variations in methanesulfonate (MSA) in the Siple Dome ice core, West Antarctica, *Geophys. Res. Lett.*, 33(11), 1–4, doi:10.1029/2005GL025629, 2006.

Sander, R., Rudich, Y., von Glasow, R. and Crutzen, P. J.: The role of BrNO<sub>3</sub> in marine tropospheric chemistry: A model study, *Geophys. Res. Lett.*, 26(18), 2857–2860, doi:10.1029/1999GL900478, 1999.

Sander, R., Keene, W. C., Pszenny, A. A. P., Arimoto, R., Ayers, G. P., Baboukas, E., Cainey, J. M., Crutzen, P. J., Duce, R. A., Hönninger, G., Huebert, B. J., Maenhaut, W., Mihalopoulos, N., Turekian, V. C. and Van Dingenen, R.: Inorganic bromine in the marine boundary layer: a critical review, *Atmos. Chem. Phys.*, 3, 1301–1336, doi:10.5194/acp-3-1301-2003, 2003.

Schönhardt, A., Begoin, M., Richter, A., Wittrock, F., Kaleschke, L., Gómez Martín, J. C. and Burrows, J. P.: Simultaneous satellite observations of IO and BrO over Antarctica, *Atmos. Chem. Phys.*, 12(14), 6565–6580, doi:10.5194/acp-12-6565-2012, 2012.

Sharma, S., Chan, E., Ishizawa, M., Toom-Sauntry, D., Gong, S. L., Li, S. M., Tarasick, D. W., Leaitch, W. R., Norman, A., Quinn, P. K., Bates, T. S., Lefvasseur, M., Barrie, L. A. and Maenhaut, W.: Influence of transport and ocean ice extent on biogenic aerosol sulfur in the Arctic atmosphere, *J. Geophys. Res.*

Atmos., 117(12), n/a-n/a, doi:10.1029/2011JD017074, 2012.

Sigl, M., McConnell, J. R., Layman, L., Maselli, O. J., McGwire, K., Pasteris, D., Dahl-Jensen, D., Steffensen, J. P., Vinther, B., Edwards, R., Mulvaney, R. and Kipfstuhl, S.: A new bipolar ice core record of volcanism from WAIS Divide and NEEM and implications for climate forcing of the last 2000 years, *J. Geophys. Res. Atmos.*, 118(3), 1151–1169, doi:10.1029/2012JD018603, 2013.

Sigl, M., Winstrup, M., McConnell, J. R., Welten, K. C., Plunkett, G., Ludlow, F., Büntgen, U., Caffee, M., Chellman, N., Dahl-Jensen, D., Fischer, H., Kipfstuhl, S., Kostick, C., Maselli, O. J., Mekhaldi, F., Mulvaney, R., Muscheler, R., Pasteris, D. R., Pilcher, J. R., Salzer, M., Schüpbach, S., Steffensen, J. P., Vinther, B. M. and Woodruff, T. E.: Timing and climate forcing of volcanic eruptions for the past 2,500 years, *Nature*, 523(7562), 543–9, doi:10.1038/nature14565, 2015.

Simpson, W. R., von Glasow, R., Riedel, K., Anderson, P., Ariya, P., Bottenheim, J., Burrows, J., Carpenter, L. J., Friess, U., Goodsite, M. E., Heard, D., Hutterli, M., Jacobi, H.-W., Kaleschke, L., Neff, B., Plane, J., Platt, U., Richter, A., Roscoe, H., Sander, R., Shepson, P., Sodeau, J., Steffen, A., Wagner, T. and Wolff, E.: Halogens and their role in polar boundary-layer ozone depletion, , 4375–4418, doi:10.5194/acpd-7-4285-2007, 2007.

Sjostedt, S. J., Huey, L. G., Tanner, D. J., Peischl, J., Chen, G., Dibb, J. E., Lefer, B., Hutterli, M. A., Beyersdorf, A. J., Blake, N. J., Blake, D. R., Sueper, D., Ryerson, T., Burkhardt, J. and Stohl, A.: Observations of hydroxyl and the sum of peroxy radicals at Summit, Greenland during summer 2003, *Atmos. Environ.*, 41(24), 5122–5137, doi:10.1016/j.atmosenv.2006.06.065, 2007.

Smith, S. J., van Aardenne, J., Klimont, Z., Andres, R. J., Volke, A. and Delgado Arias, S.: Anthropogenic sulfur dioxide emissions: 1850–2005, *Atmos. Chem. Phys.*, 11(3), 1101–1116, doi:10.5194/acp-11-1101-2011, 2011.

Spolaor, A., Vallenga, P., Plane, J. M. C., Kehrwald, N., Gabrieli, J., Varin, C., Turetta, C., Cozzi, G., Kumar, R., Boutron, C. and Barbante, C.: Halogen species record Antarctic sea ice extent over glacial-interglacial periods, *Atmos. Chem. Phys.*, 13, 6623–6635, doi:10.5194/acp-13-6623-2013, 2013a.

Spolaor, A., Gabrieli, J., Martma, T., Kohler, J., Björkman, M. B., Isaksson, E., Varin, C., Vallenga, P., Plane, J. M. C. and Barbante, C.: Sea ice dynamics influence halogen deposition to Svalbard, *Cryosph.*, 7(5), 1645–1658, doi:10.5194/tc-7-1645-2013, 2013b.

Spolaor, A., Vallenga, P., Gabrieli, J., Martma, T., Björkman, M. P., Isaksson, E., Cozzi, G., Turetta, C., Kjær, H. A., Curran, M. A. J., Moy, A. D., Schönhardt, A., Blechschmidt, A.-M., Burrows, J. P., Plane, J. M. C. and Barbante, C.: Seasonality of halogen deposition in polar snow and ice, *Atmos. Chem.*

Phys., 14(18), 9613–9622, doi:10.5194/acp-14-9613-2014, 2014.

Spolaor, A., Opel, T., McConnell, J. R., Maselli, O. J., Spreen, G., Varin, C., Kirchgeorg, T., Fritzsche, D., Saiz-Lopez, A. and Vallelonga, P.: Halogen-based reconstruction of Russian Arctic sea ice area from the Akademii Nauk ice core (Severnaya Zemlya), *Cryosph.*, 10, 245–256, doi:10.5194/tcd-9-4407-2015, 2016.

Sturges, W. T. and Harrison, R. M.: Bromine:Lead ratios in airborne particles from urban and rural sites, *Atmos. Environ.*, 20(3), 577–588, doi:10.1016/0004-6981(86)90101-0, 1986.

Thomas, J. L., Dibb, J. E., Huey, L. G., Liao, J., Tanner, D., Lefer, B., von Glasow, R. and Stutz, J.: Modeling chemistry in and above snow at Summit, Greenland – Part 2: Impact of snowpack chemistry on the oxidation capacity of the boundary layer, *Atmos. Chem. Phys.*, 12(14), 6537–6554, doi:10.5194/acp-12-6537-2012, 2012.

Thomas, V. M., Bedford, J. A. and Cicerone, R. J.: Bromine emissions from leaded gasoline, *Geophys. Res. Lett.*, 24(11), 1371–1374, doi:10.1029/97GL01243, 1997.

Vestreng, V., Ntziachristos, L., Semb, A., Reis, S., Isaksen, I. S. A. and Tarrasón, L.: Evolution of NO<sub>x</sub> emissions in Europe with focus on road transport control measures, *Atmos. Chem. Phys.*, 9(4), 1503–1520, doi:10.5194/acp-9-1503-2009, 2009.

Wagner, T., Leue, C., Wenig, M., Pfeilsticker, K. and Platt, U.: Spatial and temporal distribution of enhanced boundary layer BrO concentrations measured by the GOME instrument aboard ERS-2, *J. Geophys. Res.*, 106(D20), 24225, doi:10.1029/2000JD000201, 2001.

Wais Divide Project Memembers: Onset of deglacial warming in West Antarctica driven by local orbital forcing., *Nature*, 500(7463), 440–4, doi:10.1038/nature12376, 2013.

Walsh, J. E.: A data set on Northern Hemisphere sea ice extent, *Natl. Snow Ice Data Cent.*, 49–51, 1978.

Weißbach, S., Wegner, A., Opel, T., Oerter, H., Vinther, B. M. and Kipfstuhl, S.: Spatial and temporal oxygen isotope variability in northern Greenland - implications for a new climate record over the past millennium, *Clim. Past Discuss.*, 11(3), 2341–2388, doi:10.5194/cpd-11-2341-2015, 2015.

Weller, R.: Postdepositional losses of methane sulfonate, nitrate, and chloride at the European Project for Ice Coring in Antarctica deep-drilling site in Dronning Maud Land, Antarctica, *J. Geophys. Res.*, 109(D7), 1–9, doi:10.1029/2003JD004189, 2004.

WMO: Scientific Assessment of Ozone Depletion: 1994. Chapter 10: Methyl Bromide, Geneva., 1995.

WMO: Scientific Assessment of Ozone Depletion: 2002. Chapter 1: Controlled Substances and Other

Source Gases., 2002.

Wolff, E. W.: Ice sheets and nitrogen, *Philos. Trans. R. Soc. Lond. B. Biol. Sci.*, 368, doi:10.1098/rstb.2013.0127, 2013.

Wolff, E. W., Rankin, A. M. and Röthlisberger, R.: An ice core indicator of Antarctic sea ice production?, *Geophys. Res. Lett.*, 30(22), 2–5, doi:10.1029/2003GL018454, 2003.

Xu, L., Russell, L. M., Somerville, R. C. J. and Quinn, P. K.: Frost flower aerosol effects on Arctic wintertime longwave cloud radiative forcing, *J. Geophys. Res. Atmos.*, 118(23), 13282–13291, doi:10.1002/2013JD020554, 2013.

Yang, X., Pyle, J. A. and Cox, R. A.: Sea salt aerosol production and bromine release: Role of snow on sea ice, *Geophys. Res. Lett.*, 35(16), 1–5, doi:10.1029/2008GL034536, 2008.

Yang, X., Pyle, J. A., Cox, R. A., Theys, N. and Van Roozendaal, M.: Snow-sourced bromine and its implications for polar tropospheric ozone, *Atmos. Chem. Phys.*, 10(16), 7763–7773, doi:10.5194/acp-10-7763-2010, 2010.

Yung, Y. L., Pinto, J. P., Watson, R. T. and Sander, S. P.: Atmospheric Bromine and Ozone Perturbations in the Lower Stratosphere, *J. Atmos. Sci.*, 37(2), 339–353, doi:10.1175/1520-0469(1980)037<0339:ABAOPI>2.0.CO;2, 1980.



243  
244

245  
246  
247  
248

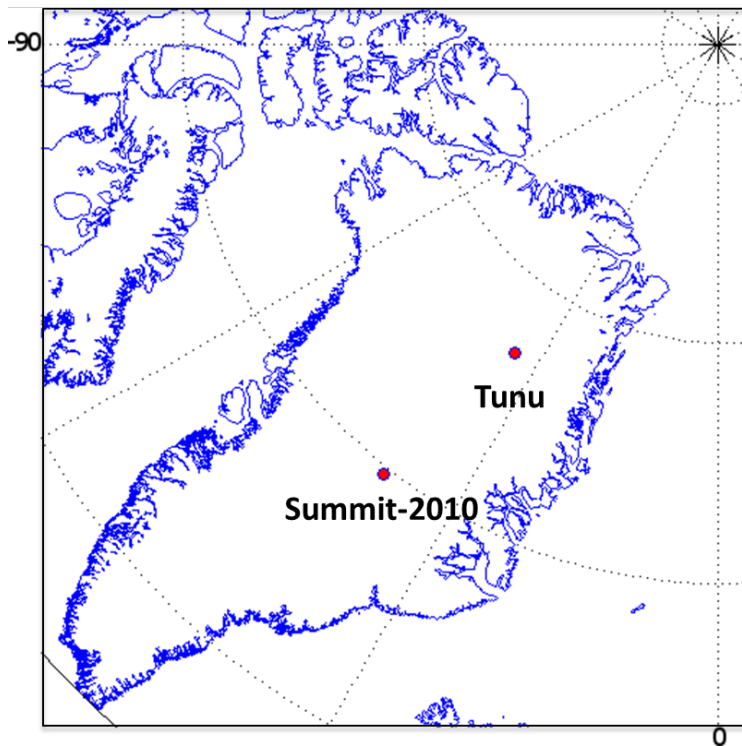


**Figure 1.** Locations of ice cores used in this study. Summit-2010: (72°20'N 38°17'24"W), Tunu: (78° 2' 5.5"N, 33° 52' 48"W)

Deleted: .  
Formatted: Font:Bold

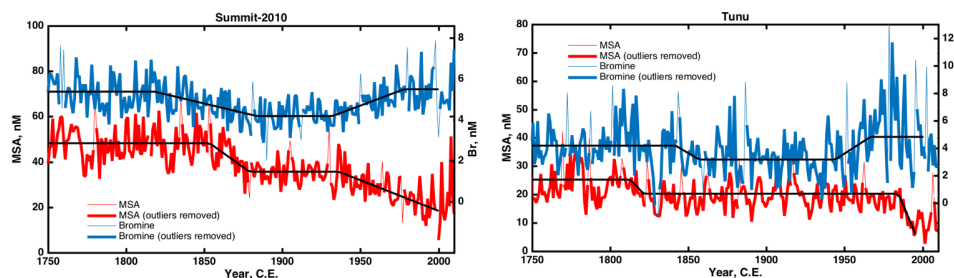
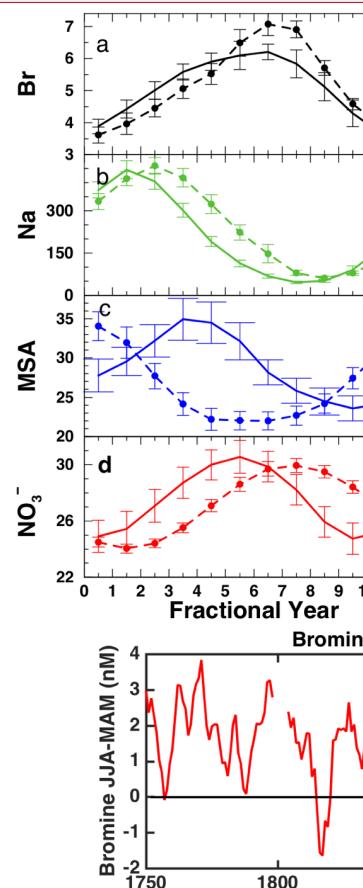


**Figure 2.** Annual record of bromine (thin blue) and MSA (thin red). Annual record of bromine (thick blue) and MSA (thick red) with outlying spikes removed using a 25 year running average filter described by Sigl et al. (2013). All records were fit with a 3 step linear regression (black) and the results of the fits which identify the timing of inflection points are summarized in Table S1. The time-series have been plotted to match the signal variability in the preindustrial era (1750-1850 C.E.).

Formatted: Font:Not Bold, Highlight



Deleted:

Formatted: Font:Bold

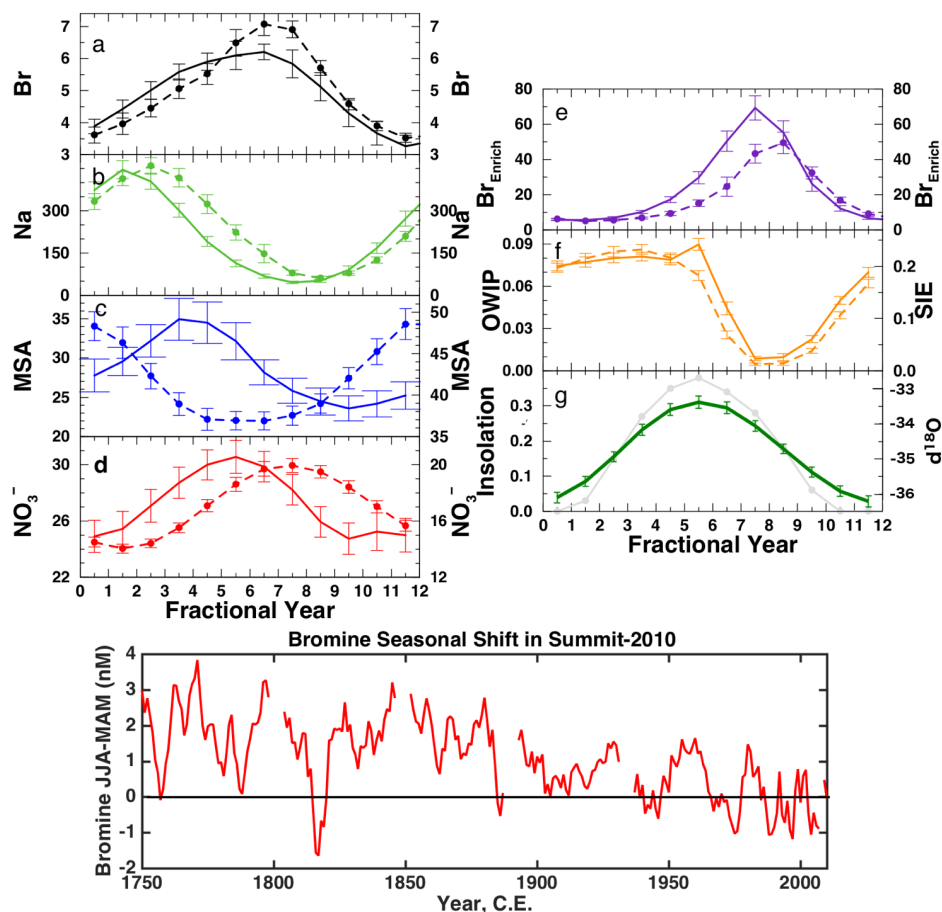


**Figure 3.** Upper plots: Average seasonal cycle of species in the Summit-2010 ice core. The left-hand Y axes are associated with the solid lines, and the right-hand Y axes associated with the dashed lines. Dashed lines (a-e): Average seasonal cycle from depths 43.5 – 87.3 m (years 1742-1900). Solid lines (a-e): Average seasonal cycle from 0-43.5 m (years 1900-2010). Error bars indicate the standard error of the monthly value. (a) Total bromine, (b) total sodium, (c) MSA, (d) nitrate. Units for (a-d) are nM. Note that the seasonal cycle in bromine appears to broaden in the 1900-2010 period (see lower panel). Note also that the MSA maximum shifts from spring in the shallowest part of the ice core (solid line) to winter in the deepest part of the ice core (dashed line) due to post-depositional effects (see Fig. S1). (e)

Formatted: Font:Bold

Deleted: S3

270 Average seasonal cycle in bromine enrichment (relative to sea salt sodium, see Eq. (4)). (f-right) The  
 271 sea ice extent (SIE,  $\times 10^6 \text{ km}^2$ ) within an area of the East Greenland coast [ $70^\circ$ – $63^\circ$  N,  $15^\circ$ – $45^\circ$  W]. (f-  
 272 – left) Area of open water within the sea ice pack (OWIP,  $\times 10^6 \text{ km}^2$ ) for the area defined by SIE. (g-  
 273 left) Solar insolation at 12 GMT at the latitude of Summit (eosweb.larc.nasa.gov). (g-right) Annual  
 274 cycle of the  $\delta^{18}\text{O}$  water signal averaged over 1900-2010 C.E. Lower plot: Broadening of bromine  
 275 seasonal cycle in the Summit-2010 ice core. The difference between the summer and spring bromine  
 276 signal (JJA-MAM) was monitored over the length of the entire ice core. In the preindustrial era (pre-  
 277 1850) bromine peaks in summer; realised as positive values of JJA-MAM. After 1900 there is a marked  
 278 broadening of the seasonal signal towards spring and by ~1970 the seasonal signal maximum is routinely  
 279 shared between summer and spring realised as an averaged JJA-MAM of approximately zero.

Deleted: ] that shows highest correlations to MSA (see Fig. 6),

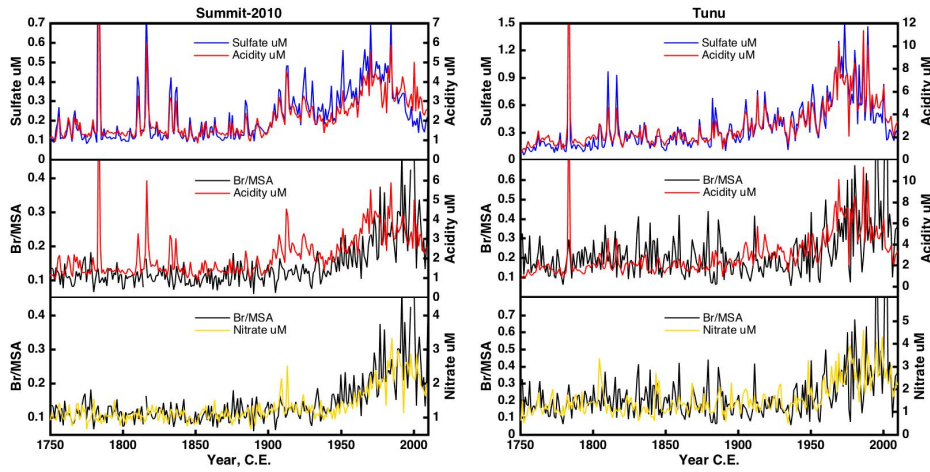


**Figure 4.** Comparison between the measured total sulfur (shown as sulfate) and acidity records from each ice core (top panels). The acidity record is dominated by the influence of the sulfur species until the early 21<sup>st</sup> century when the  $\text{NO}_x$  pollution remains elevated whilst anthropogenic sulfur sources are depleted resulting in a slight relative elevation of the total acidity relative to total sulfur concentrations. The large spikes in the acidity and sulfur records are identified as volcanic events. The ice core records cover the period of the 1783 Laki eruption as well as the Unknown 1909 eruption and Tambora eruption (Indonesia) in 1815 (Sigl et al., 2013). Comparison between Br/MSA and total acidity (center panels) and nitrate ( $\text{NO}_3^-$ , bottom panels) measured in the ice cores. The Br/MSA ratio follows the total acidity record closely except where the record is dominated by the sulfur component (e.g. early 1900s). Of the two major acidic species the Br/MSA follows the nitrate most closely at both ice core sites.

Deleted: <sp><sp>

Formatted: Font:(Default) Times

Formatted: English (US)

Deleted: NO<sub>x</sub>

Deleted: ph

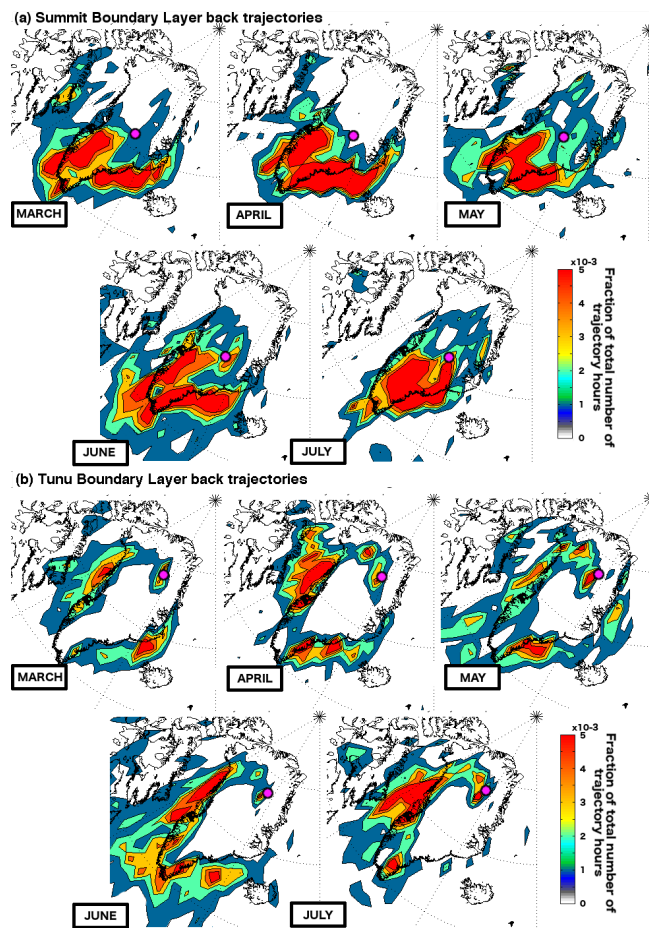
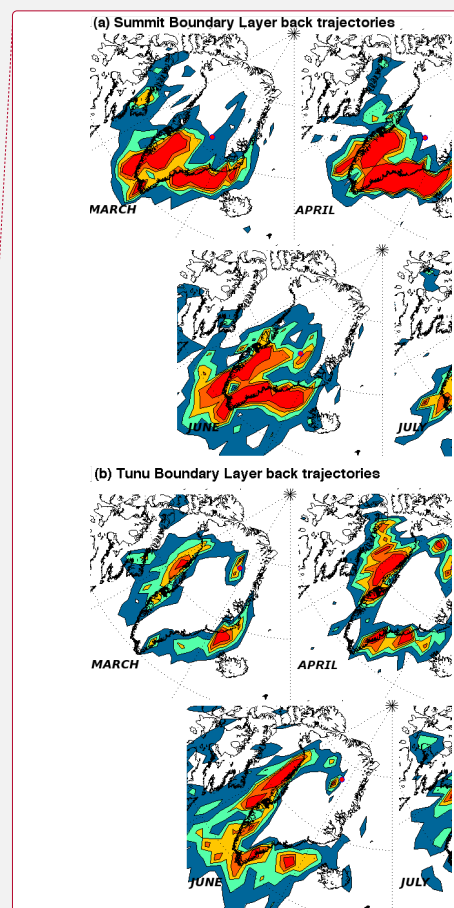


**Figure 5.** Air mass back trajectories from the (a) Summit-2010 and (b) Tunu ice core sites over the period 2005-2013 C.E. Maps display the fraction of the total number of trajectory hours (ranging between 21400-25500 hr month<sup>-1</sup>) spent at altitudes under 500 m. Back trajectories were allowed to travel for 10 days. New trajectories were started every 12 hours. Map grid resolution is 2°x 2°. Ice core locations are shown by a pink circle. Maps show that air masses consistently arrive at Summit from the SE Greenland coast with a smaller contribution from the SW coast. Air masses consistently arrive at Tunu from the western Greenland coast with a smaller contribution from the SE and NE coast. The air mass originating from the NE coast is most dominant in May and comparison with the total vertical column profile (Fig. S8) shows it is confined to lower altitudes unlike those from the west coast.



Deleted:

Formatted: Font:(Default) Arial, Bold

Formatted: Font:(Default) Arial, Bold

Formatted: Justified, Space Before: 6 pt, Line spacing: 1.5 lines, Tabs:Not at 7.75 cm

Deleted: hr

Deleted: S4

Deleted: .

Formatted: Font:(Default) Arial, Bold

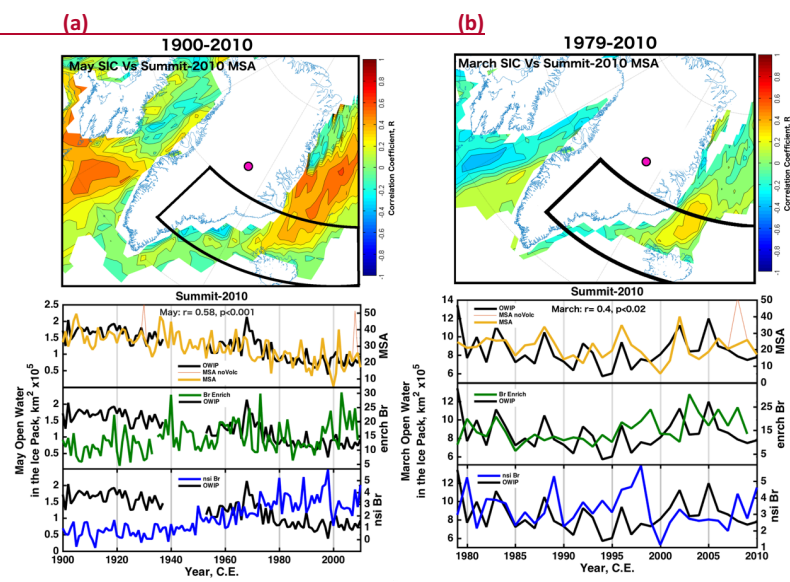


**Figure 6.** Upper plot: Correlation map of monthly sea ice concentration (SIC) derived from the Summit-2010 ice core. The SIC map displayed corresponds to the month which shows the highest OWIP correlation (lower plot) with the annual MSA. Other monthly maps are shown in Fig. S9. (a) HadISST1 ICE dataset from 1900-2010 C.E. correlated with annual records of MSA (with outlier removed). Only locations that showed a SIC variability greater than 10% and have a significant correlation (t-test,  $p < 0.05$ ) are displayed. The area of sea ice that is the likely source of MSA (as indicated by the air mass trajectories) are outlined in black [ $70^{\circ}$ – $63^{\circ}$ N,  $0^{\circ}$ – $45^{\circ}$ W]. (b) As for (a) but focused on the satellite period 1979-2010 C.E. Lower plots: The correlation between the area of Open Water within the Ice Pack (OWIP) calculated within the black outlined areas shown on the upper maps and the annual MSA records (red, outliers removed), orange, nM). Summit-2010 MSA shows a significant, positive correlation with the amount of OWIP during spring within the integrated regions over both time periods. The highest correlations were found for March over the 1979-2010 period and May for the 1900-2010 period. In (b) if the MSA source region is enlarged to [ $70^{\circ}$ – $63^{\circ}$ N,  $0^{\circ}$ – $60^{\circ}$ W] the March OWIP/MSA correlation increases slightly (from 0.38 to 0.4). The Summit-2010 enrBr(Na) (nM) and nsiBr (nM) records are also compared to the same OWIP records. Particularly over the longer time period there is little correlation between the series.

Formatted: Font: Theme Body (Calibri), 16 pt, Bold

Deleted: s

Formatted: Justified, Space Before: 0 pt, Tabs: 8.5 cm, Left

Deleted: 2

Deleted: . Outliers were

Deleted: from the MSA records before the correlations were performed. Month labels indicate the month of SIC compared with the annual MSA value.

Deleted: -

Deleted:

Deleted: 15

Deleted:

Deleted: Graphed is

Deleted: open water in the sea ice in this region

Deleted: ,

Deleted: ) overlaid on

Deleted: -

Deleted: ). (b) As for the upper panel but focused on the satellite period 1979-2012 C.E.

Deleted: region.

Page Break

... [3]

Formatted: Font: (Default) Arial, Bold



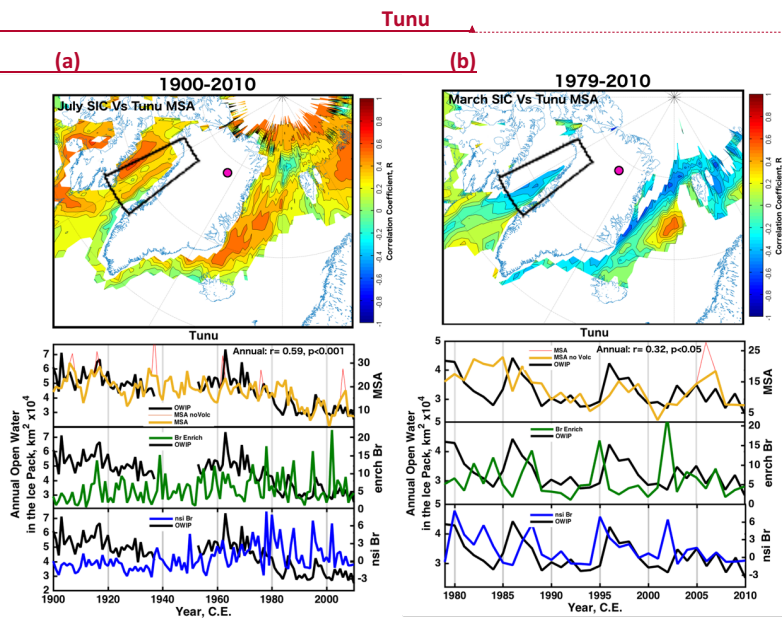


**Figure 7. Upper plots:** Correlation maps of monthly sea ice concentration (SIC) derived from the Tunu ice core. (a) HadISST1 ICE dataset from 1900–2012 C.E. correlated with annual records of MSA. The monthly SIC map displayed corresponds to the month which shows the highest OWIP correlation (lower plot) with the annual MSA. Other monthly maps are shown in Fig. S10. Only locations that showed a SIC variability greater than 10% and have a significant correlation (t-test,  $p < 0.05$ ) are displayed. The area of sea ice that is the likely source of MSA (as indicated by the air mass trajectories) are outlined in black [77°–67°N, 62°–50°W]. (b) As for (a) but focused on the satellite period 1979–2012 C.E. Lower plots: The correlation between the area of Open Water within the Ice Pack (OWIP) calculated within the black outlined areas shown on the upper maps and the annual MSA records (red, outliers removed - orange). The Tunu enrBr(Na) (nM) and nsiBr (nM) records are also compared to the same OWIP records and show poor correlation, particularly over the longer time period.

Formatted: Font:Times New Roman, Not Bold

Formatted: Font:+Theme Body (Calibri), 16 pt

Deleted: Outliers were removed from the MSA records before the correlations were performed. Month labels indicate

Deleted: of SIC compared

Deleted: value

Deleted: -

Deleted: 80°–73°

Deleted: 20°–0°

Deleted: Graphed is

Deleted: open water in the sea ice in this region

Deleted: ,

Deleted: overlaid

Deleted: Like in the Summit-20101 ice core,

Deleted: MSA

Deleted: shows a significant, positive correlation with the amount of

Deleted: during spring but the

Deleted: is highest when MSA is compared to the annual OWIP in

Deleted: source region. (b) As for the upper panel but focused on the satellite period 1979–2012 C.E. Again MSA shows a significant, positive correlation with the amount of OWIP during spring at both sites. During the satellite

Deleted: the correlation between OWIP and MSA concentrations at Tunu is greatly increased when a second, closer region is also included in the integration [80°–73° N, 20°–0° W].



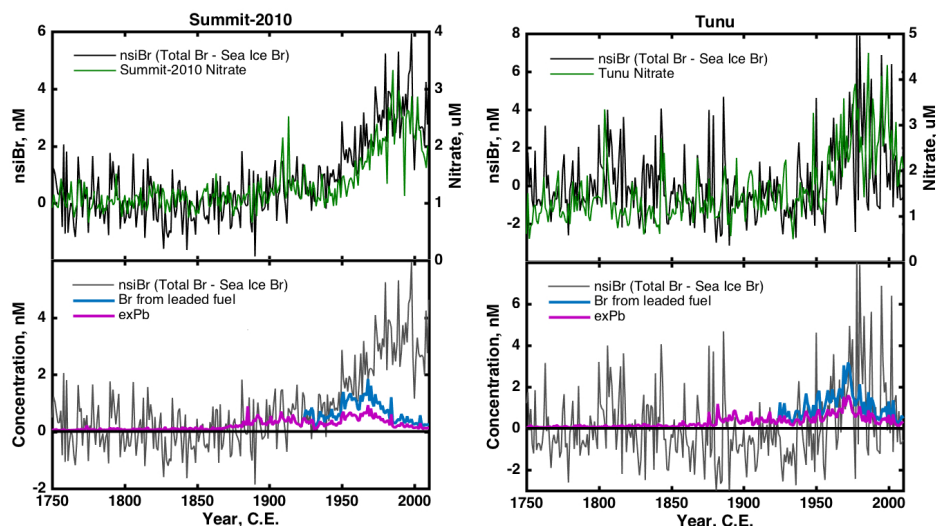


**Figure 8.** Upper panels: Comparison between bromine in excess of what is expected from a purely sea ice source (nsiBr, black) and nitrate. The temporal similarities between the nitrate and nsiBr records are high and indicate that nitrate is a likely driving force for the enhanced release of bromine species from sea ice sources. Lower panels: Comparison between the calculated nsiBr record and excess lead (exPb, purple) measured in the ice cores. The lower panels also show the upper limit to the amount of bromine that could be derived from leaded fuel combustion by assuming exPb:Br ratio of 1:2 after 1925 (blue). After 1970, when world consumption of leaded gasoline began to fall, nsiBr concentrations continued to rise at both ice core sites far above the concentrations that could be explained by leaded gasoline sources.

Deleted: ... [4]

Formatted: Font:(Default) Arial, Bold

Formatted: Font:(Default) Arial, Bold

Deleted: measurements of excess lead (exPb, purple shading) and

Deleted: the preindustrial (1750-1880) Br/MSA relationship (exBr

Deleted: ). Between 1925-1940 world-wide leaded gasoline sources contained a Pb:Br molar ratio of 1:2 (aviation fuel). After 1940 only Russia continued to use

Deleted: 1:2 ratio in their leaded fuel whilst the rest of the world changed to a 1:1 ratio. The green shading shows an estimate

Deleted: leaded fuel combustion over the 1925-1940 period (relative to the exPb concentrations).

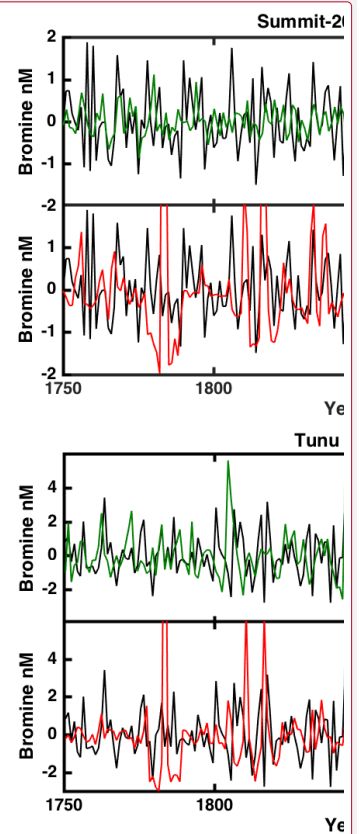
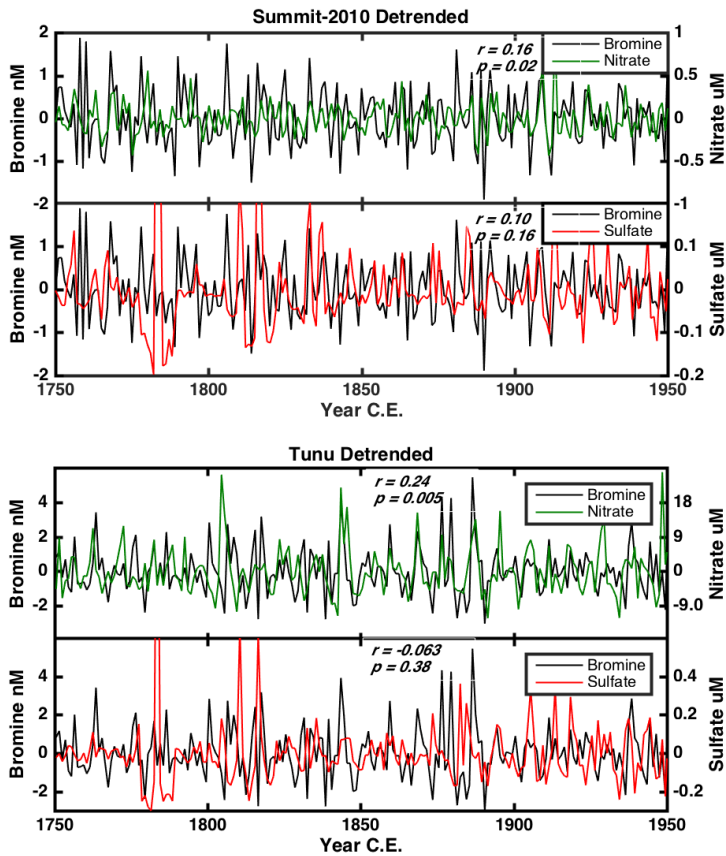
Deleted: blue shading shows

Deleted: (relative to exPb)

Deleted: 1940.

Deleted: exBr

Formatted: Font:Times New Roman, Not Bold



Deleted:

Formatted: Font:(Default) Arial, Bold

Formatted: Font:(Default) Arial, Bold

**Figure 9.** High frequency comparison between the annual bromine, nitrate and sulfate records measured in the ice cores. Each series has been detrended with an 11 year running average before comparison to remove the low frequency changes in each record. The correlation is highest between bromine and nitrate at both sites. The r-value for bromine versus nitrate at Summit increases in significance ( $r=0.24$ ,  $p=0.001$ ) when the entire period (1750-2010) is considered. At both sites there is a close relationship between the variability in the nitrate and bromine due to their intimate relationship during emission from the sea ice, transport and deposition onto the snow pack. The correlation between sulfate (or indeed bulk acidity) and bromine is not significant over any of the time periods shown at either site. Particularly

Deleted: significant

138 evident is the non-response of the bromine signal to the sulfur rich volcanic events as described in  
139 Sect.4.2.2.  
140

Formatted: Left, Space Before: 0 pt, Line spacing: single

Abbatt, J., Oldridge, N., Symington, a, Chukalovskiy, V., McWhinney, R. D., Sjostedt, S. and Cox, R. a: Release of gas-phase halogens by photolytic generation of OH in frozen halide-nitrate solutions: an active halogen formation mechanism?, *J. Phys. Chem. A*, 114(23), 6527–33, doi:10.1021/jp102072t, 2010.

Abbatt, J. P. D.: Interactions of HBr, HCl, and HOBr With Supercooled Sulfuric- Acid- Solutions of Stratospheric Composition, *J. Geophys. Res.*, 100(D7), 14009–14017, 1995.

Abbatt, J. P. D., Thomas, J. L., Abrahamsson, K., Boxe, C., Granfors, A., Jones, A. E., King, M. D., Saiz-Lopez, A., Shepson, P. B., Sodeau, J., Toohey, D. W., Toubin, C., von Glasow, R., Wren, S. N. and Yang, X.: Halogen activation via interactions with environmental ice and snow in the polar lower troposphere and other regions, *Atmos. Chem. Phys.*, 12(14), 6237–6271, doi:10.5194/acp-12-6237-2012, 2012.

Abram, N. J., Wolff, E. W. and Curran, M. A. J.: A review of sea ice proxy information from polar ice cores, *Quat. Sci. Rev.*, 79, 168–183, doi:10.1016/j.quascirev.2013.01.011, 2013.

Appenzeller, C., Schwander, J., Sommer, S. and Stocker, T. F.: The North Atlantic Oscillation and its imprint on precipitation and ice accumulation in Greenland, *Geophys. Res. Lett.*, 25(11), 1939, doi:10.1029/98GL01227, 1998.

Barrie, L. A., Hoff, R. M. and Daggupaty, S. M.: The influence of mid-latitudinal pollution sources on haze in the Canadian arctic, *Atmos. Environ.*, 15(8), 1407–1419, doi:10.1016/0004-6981(81)90347-4, 1981.

Bertram, F. J. and Kolowich, J. B.: A study of methyl bromide emissions from automobiles burning leaded gasoline using standardized vehicle testing procedures, *Geophys. Res. Lett.*, 27(9), 1423–1426, doi:10.1029/1999GL011008, 2000.

Bowen, H. J. M.: Environmental chemistry of the elements / H. J. M. Bowen, Academic Press, London ; New York., 1979.

Chen, Q. S., Bromwich, D. H. and Bai, L.: Precipitation over Greenland retrieved by a dynamic method and its relation to cyclonic activity, *J. Clim.*, 10(5), 839–870, 1997.

Chu, L. and Anastasio, C.: Formation of hydroxyl radical from the photolysis of frozen hydrogen peroxide, *J. Phys. Chem. A*, 109(28), 6264–6271, doi:10.1021/jp051415f, 2005.

Curran, M. A. J. and Jones, G. B.: Dimethyl sulfide in the Southern Ocean: Seasonality and flux, *J. Geophys. Res.*, 105(D16), 20451, doi:10.1029/2000JD900176, 2000.

Curran, M. A. J., van Ommen, T. D., Morgan, V. I., Phillips, K. L. and Palmer, A. S.: Ice core evidence for Antarctic sea ice decline since the 1950s., *Science*, 302(5648), 1203–1206, doi:10.1126/science.1087888, 2003.

Draxler, R. R. and Hess, G. D.: An Overview of the HYSPLIT\_4 Modelling System for Trajectories, Dispersion, and Deposition., *Aust. Meteorol. Mag.*, 47(June 1997), 295–308, 1998.

Fan, S.-M. and Jacob, D. J.: Surface ozone depletion in Arctic spring sustained by bromine reactions on aerosols, *Nature*, 359(6395), 522–524, doi:10.1038/359522a0, 1992.

Felix, J. D. and Elliott, E. M.: The agricultural history of human-nitrogen interactions as recorded in ice core  $\delta^{15}\text{N-NO}_3^-$ , *Geophys. Res. Lett.*, 40(8), 1642–1646, doi:10.1002/grl.50209, 2013.

Finlayson-Pitts, B. J.: The Tropospheric Chemistry of Sea Salt: A Molecular-Level View of the Chemistry of NaCl and NaBr, *Chem. Rev.*, 103(12), 4801–4822, doi:10.1021/cr020653t, 2003.

Fischer, H. and Wagenbach, D.: Large-scale spatial trends in recent firn chemistry along an east-west transect through central Greenland, *Atmos. Environ.*, 30(19), 3227–3238, doi:10.1016/1352-2310(96)00092-1, 1996.

Frinak, E. K. and Abbatt, J. P. D.: Br<sub>2</sub> production from the heterogeneous reaction of gas-phase OH with aqueous salt solutions: Impacts of acidity, halide concentration, and organic surfactants., *J. Phys. Chem. A*, 110(35), 10456–64, doi:10.1021/jp063165o, 2006.

George, I. J. and Anastasio, C.: Release of gaseous bromine from the photolysis of nitrate and hydrogen peroxide in simulated sea-salt solutions, *Atmos. Environ.*, 41(3), 543–553, doi:10.1016/j.atmosenv.2006.08.022, 2007.

Hunke, E. C., Notz, D., Turner, A. K. and Vancoppenolle, M.: The multiphase physics of sea ice: a review for model developers, *Cryosph.*, 5(4), 989–1009, doi:10.5194/tc-5-989-2011, 2011.

Jacobi, H. W., Kleffmann, J., Villena, G., Wiesen, P., King, M., France, J., Anastasio, C. and Staebler, R.: Role of nitrite in the photochemical formation of radicals in the snow, *Environ. Sci. Technol.*, 48(1), 165–172, doi:10.1021/es404002c, 2014.

Kahl, J. D. W., Martinez, D. A., Kuhns, H., Davidson, C. I., Jafferezo, J. L. and Harris, J. M.: Air mass trajectories to Summit, Greenland : A 44-year climatology and some episodic events, *J. Geophys. Res. Ocean.*, 102(C12), 26861–26875, 1997.

Kerkweg, A., Jöckel, P., Warwick, N., Gebhardt, S., Brenninkmeijer, C. a. M. and Lelieveld, J.: Consistent simulation of bromine chemistry from the marine boundary layer to the stratosphere – Part 2 : Bromocarbons, *Atmos. Chem. Phys. Discuss.*, 8(3), 9477–9530, doi:10.5194/acpd-8-9477-2008, 2008.

Kinnard, C., Zdanowicz, C. M., Koerner, R. M. and Fisher, D. A.: A changing Arctic seasonal ice zone: Observations from 1870-2003 and possible oceanographic consequences, *Geophys. Res. Lett.*, 35(2), 2–6, doi:10.1029/2007GL032507, 2008.

Lamarque, J.-F., Dentener, F., McConnell, J., Ro, C.-U., Shaw, M., Vet, R., Bergmann, D., Cameron-Smith, P., Dalsoren, S., Doherty, R., Faluvegi, G., Ghan, S. J., Josse, B., Lee, Y. H., MacKenzie, I. A., Plummer, D., Shindell, D. T., Skeie, R. B., Stevenson, D. S., Strode, S., Zeng, G., Curran, M., Dahl-Jensen, D., Das, S., Fritzsche, D. and Nolan, M.: Multi-model mean nitrogen and sulfur deposition from the Atmospheric Chemistry and Climate Model Intercomparison Project (ACCMIP): evaluation of historical and projected future changes, *Atmos. Chem. Phys.*, 13(16), 7997–8018, doi:10.5194/acp-13-7997-2013, 2013.

Langendörfer, U., Lehrer, E., Wagenbach, D. and Platt, U.: Observation of filterable bromine variabilities during Arctic tropospheric ozone depletion events in high (1 hour) time resolution, in *Journal of Atmospheric Chemistry*, vol. 34, pp. 39–54., 1999.

Legrand, M., Hammer, C., De Angelis, M., Savarino, J., Delmas, R., Clausen, H. and Johnsen, S. J.: Sulfur-containing species (methanesulfonate and SO<sub>4</sub>) over the last climatic cycle in the Greenland Ice Core Project (central Greenland) ice core, *J. Geophys. Res.*, 102(C12), 26663, doi:10.1029/97JC01436, 1997.

Lehrer, E., Wagenbach, D. and Platt, U.: Aerosol chemical composition during tropospheric ozone depletion at Ny Ålesund/Svalbard, *Tellus B*, 49(5), doi:10.3402/tellusb.v49i5.15987, 1997.

Li, S.-M. and Barrie, L. A.: Biogenic sulfur aerosol in the Arctic troposphere: 1. Contributions to total sulfate, *J. Geophys. Res.*, 98(D11), 20613, doi:10.1029/93JD02234, 1993.

Macias Fauria, M., Grinsted, A., Helama, S., Moore, J., Timonen, M., Martma, T., Isaksson, E. and Eronen, M.: Unprecedented low twentieth century winter sea ice extent in the Western

Nordic Seas since A.D. 1200, *Clim. Dyn.*, 34(6), 781–795, doi:10.1007/s00382-009-0610-z, 2010.

Mann, M. E., Bradley, R. S. and Hughes, M. K.: Global-scale temperature patterns and climate forcing over the past six centuries, *Nature*, 392(6678), 779–787, doi:10.1038/33859, 1998.

McConnell, J. R. and Edwards, R.: Coal burning leaves toxic heavy metal legacy in the Arctic., *Proc. Natl. Acad. Sci. U. S. A.*, 105(34), 12140–12144, doi:10.1073/pnas.0803564105, 2008.

McConnell, J. R., Lamorey, G. W., Lambert, S. W. and Taylor, K. C.: Continuous ice-core chemical analyses using inductively coupled plasma mass spectrometry., *Environ. Sci. Technol.*, 36(775), 7–11, doi:10.1021/es011088z, 2002.

McConnell, J. R., Edwards, R., Kok, G. L., Flanner, M. G., Zender, C. S., Saltzman, E. S., Banta, J. R., Pasteris, D. R., Carter, M. M. and Kahl, J. D. W.: 20th-Century Industrial Black Carbon Emissions Altered Arctic Climate Forcing, *Science* (80-. ), 317(5843), 1381–1384, doi:10.1126/science.1144856, 2007.

Millero, F. J.: The Physical Chemistry of Seawater, *Annu. Rev. Earth Planet. Sci.*, 2(1), 101–150, doi:10.1146/annurev.ea.02.050174.000533, 1974.

Moldanová, J. and Ljungström, E.: Sea-salt aerosol chemistry in coastal areas: A model study, *J. Geophys. Res.*, 106, 1271, doi:10.1029/2000JD900462, 2001.

Montzka, S. and Reimann, S.: Scientific Assessment of Ozone Depletion 2010: Scientific Summary Chapter 1 Ozone-Depleting Substances (ODSs) and Related Chemicals. [online] Available from: <http://www.esrl.noaa.gov/csd/assessments/ozone/2010/summary/ch1.html> (Accessed 23 December 2015), 2010.

Morin, S., Savarino, J., Frey, M. M., Yan, N., Bekki, S., Bottenheim, J. and Martins, J. M. F.: Tracing the origin and fate of NO<sub>x</sub> in the Arctic atmosphere using stable isotopes in nitrate., *Science*, 322(5902), 730–2, doi:10.1126/science.1161910, 2008.

Mulvaney, R., Pasteur, E. C., Peel, D. A., Saltzman, E. S. and Whung, P.-Y.: The ratio of MSA to non-sea-salt sulphate in Antarctic Peninsula ice cores, *Tellus B*, 44(4), doi:10.3402/tellusb.v44i4.15457, 1992.

Nghiem, S. V., Rigor, I. G., Richter, A., Burrows, J. P., Shepson, P. B., Bottenheim, J., Barber, D. G., Steffen, A., Latonas, J., Wang, F., Stern, G., Clemente-Colón, P., Martin, S., Hall, D. K., Kaleschke, L., Tackett, P., Neumann, G. and Asplin, M. G.: Field and satellite observations of the formation and distribution of Arctic atmospheric bromine above a rejuvenated sea ice

cover, *J. Geophys. Res. Atmos.*, 117(D17), n/a–n/a, doi:10.1029/2011JD016268, 2012.

O'Dwyer, J., Isaksson, E., Vinje, T., Jauhiainen, T., Moore, J., Pohjola, V., Vaikmaa, R. and van de Wal, R. S. W.: Methanesulfonic acid in a Svalbard ice core as an indicator of ocean climate, *Geophys. Res. Lett.*, 27(8), 1159–1162, doi:10.1029/1999GL011106, 2000.

Ordóñez, C., Lamarque, J.-F., Tilmes, S., Kinnison, D. E., Atlas, E. L., Blake, D. R., Sousa Santos, G., Brasseur, G. and Saiz-Lopez, A.: Bromine and iodine chemistry in a global chemistry-climate model: description and evaluation of very short-lived oceanic sources, *Atmos. Chem. Phys.*, 12(3), 1423–1447, doi:10.5194/acp-12-1423-2012, 2012.

Parrella, J. P., Jacob, D. J., Liang, Q., Zhang, Y., Mickley, L. J., Miller, B., Evans, M. J., Yang, X., Pyle, J. A., Theys, N. and Van Roozendaal, M.: Tropospheric bromine chemistry: implications for present and pre-industrial ozone and mercury, *Atmos. Chem. Phys.*, 12(15), 6723–6740, doi:10.5194/acp-12-6723-2012, 2012.

Pasteris, D. R., McConnell, J. R. and Edwards, R.: High-resolution, continuous method for measurement of acidity in ice cores, *Environ. Sci. Technol.*, 46, 1659–1666, doi:10.1021/es202668n, 2012.

Pratt, K. A., Custard, K. D., Shepson, P. B., Douglas, T. A., Pöhler, D., General, S., Zielcke, J., Simpson, W. R., Platt, U., Tanner, D. J., Gregory Huey, L., Carlsen, M. and Stirm, B. H.: Photochemical production of molecular bromine in Arctic surface snowpacks, *Nat. Geosci.*, 6(5), 351–356, doi:10.1038/ngeo1779, 2013.

Rankin, A. M., Wolff, E. W. and Martin, S.: Frost flowers: Implications for tropospheric chemistry and ice core interpretation, *J. Geophys. Res. Atmos.*, 107(D23), 4683, doi:10.1029/2002JD002492, 2002.

Rayner, N. A.: Global analyses of sea surface temperature, sea ice, and night marine air temperature since the late nineteenth century, *J. Geophys. Res.*, 108(D14), 4407, doi:10.1029/2002JD002670, 2003.

Röthlisberger, R., Bigler, M., Hutterli, M., Sommer, S., Stauffer, B., Junghans, H. G. and Wagenbach, D.: Technique for continuous high-resolution analysis of trace substances in firn and ice cores, *Environ. Sci. Technol.*, 34(2), 338–342, doi:10.1021/es9907055, 2000.

Röthlisberger, R., Mulvaney, R., Wolff, E. W., Hutterli, M. a., Bigler, M., Sommer, S. and Jouzel, J.: Dust and sea salt variability in central East Antarctica (Dome C) over the last 45 kyrs and its implications for southern high-latitude climate, *Geophys. Res. Lett.*, 29(20), 1–4,



doi:10.1029/2003GL016936, 2002.

Saltzman, E. S., Dioumaeva, I. and Finley, B. D.: Glacial/interglacial variations in methanesulfonate (MSA) in the Siple Dome ice core, West Antarctica, *Geophys. Res. Lett.*, 33(11), 1–4, doi:10.1029/2005GL025629, 2006.

Sander, R., Rudich, Y., von Glasow, R. and Crutzen, P. J.: The role of BrNO<sub>3</sub> in marine tropospheric chemistry: A model study, *Geophys. Res. Lett.*, 26(18), 2857–2860, doi:10.1029/1999GL900478, 1999.

Sander, R., Keene, W. C., Pszenny, a. a. P., Arimoto, R., Ayers, G. P., Baboukas, E., Cainey, J. M., Crutzen, P. J., Duce, R. a., Hönninger, G., Huebert, B. J., Maenhaut, W., Mihalopoulos, N., Turekian, V. C. and Van Dingenen, R.: Inorganic bromine in the marine boundary layer: a critical review, *Atmos. Chem. Phys. Discuss.*, 3, 1301–1336, doi:10.5194/acpd-3-2963-2003, 2003.

Schönhardt, A., Begoin, M., Richter, A., Wittrock, F., Kaleschke, L., Gómez Martín, J. C. and Burrows, J. P.: Simultaneous satellite observations of IO and BrO over Antarctica, *Atmos. Chem. Phys.*, 12(14), 6565–6580, doi:10.5194/acp-12-6565-2012, 2012.

Sharma, S., Chan, E., Ishizawa, M., Toom-Sauntry, D., Gong, S. L., Li, S. M., Tarasick, D. W., Leaitch, W. R., Norman, a., Quinn, P. K., Bates, T. S., Levasseur, M., Barrie, L. a. and Maenhaut, W.: Influence of transport and ocean ice extent on biogenic aerosol sulfur in the Arctic atmosphere, *J. Geophys. Res. Atmos.*, 117(12), n/a–n/a, doi:10.1029/2011JD017074, 2012.

Sigl, M., McConnell, J. R., Layman, L., Maselli, O. J., McGwire, K., Pasteris, D., Dahl-Jensen, D., Steffensen, J. P., Vinther, B., Edwards, R., Mulvaney, R. and Kipfstuhl, S.: A new bipolar ice core record of volcanism from WAIS Divide and NEEM and implications for climate forcing of the last 2000 years, *J. Geophys. Res. Atmos.*, 118(3), 1151–1169, doi:10.1029/2012JD018603, 2013.

Sigl, M., Winstrup, M., McConnell, J. R., Welten, K. C., Plunkett, G., Ludlow, F., Büntgen, U., Caffee, M., Chellman, N., Dahl-Jensen, D., Fischer, H., Kipfstuhl, S., Kostick, C., Maselli, O. J., Mekhaldi, F., Mulvaney, R., Muscheler, R., Pasteris, D. R., Pilcher, J. R., Salzer, M., Schüpbach, S., Steffensen, J. P., Vinther, B. M. and Woodruff, T. E.: Timing and climate forcing of volcanic eruptions for the past 2,500 years, *Nature*, 523(7562), 543–9, doi:10.1038/nature14565, 2015.

Simpson, W. R., von Glasow, R., Riedel, K., Anderson, P., Ariya, P., Bottenheim, J., Burrows, J., Carpenter, L. J., Friess, U., Goodsite, M. E., Heard, D., Hutterli, M., Jacobi, H.-W., Kaleschke, L., Neff, B., Plane, J., Platt, U., Richter, a., Roscoe, H., Sander, R., Shepson, P., Sodeau, J., Steffen, a., Wagner, T. and Wolff, E.: Halogens and their role in polar boundary-layer ozone depletion, , 4375–4418, doi:10.5194/acpd-7-4285-2007, 2007.

Sjostedt, S. J., Huey, L. G., Tanner, D. J., Peischl, J., Chen, G., Dibb, J. E., Lefer, B., Hutterli, M. a., Beyersdorf, a. J., Blake, N. J., Blake, D. R., Sueper, D., Ryerson, T., Burkhardt, J. and Stohl, a.: Observations of hydroxyl and the sum of peroxy radicals at Summit, Greenland during summer 2003, *Atmos. Environ.*, 41(24), 5122–5137, doi:10.1016/j.atmosenv.2006.06.065, 2007.

Smith, S. J., van Aardenne, J., Klimont, Z., Andres, R. J., Volke, A. and Delgado Arias, S.: Anthropogenic sulfur dioxide emissions: 1850–2005, *Atmos. Chem. Phys.*, 11(3), 1101–1116, doi:10.5194/acp-11-1101-2011, 2011.

Spolaor, A., Vallelonga, P., Plane, J. M. C., Kehrwald, N., Gabrieli, J., Varin, C., Turetta, C., Cozzi, G., Kumar, R., Boutron, C. and Barbante, C.: Halogen species record Antarctic sea ice extent over glacial-interglacial periods, *Atmos. Chem. Phys.*, 13, 6623–6635, doi:10.5194/acp-13-6623-2013, 2013a.

Spolaor, A., Gabrieli, J., Martma, T., Kohler, J., Björkman, M. B., Isaksson, E., Varin, C., Vallelonga, P., Plane, J. M. C. and Barbante, C.: Sea ice dynamics influence halogen deposition to Svalbard, *Cryosph.*, 7(5), 1645–1658, doi:10.5194/tc-7-1645-2013, 2013b.

Spolaor, A., Vallelonga, P., Gabrieli, J., Martma, T., Björkman, M. P., Isaksson, E., Cozzi, G., Turetta, C., Kjær, H. A., Curran, M. A. J., Moy, A. D., Schönhardt, A., Blechschmidt, A.-M., Burrows, J. P., Plane, J. M. C. and Barbante, C.: Seasonality of halogen deposition in polar snow and ice, *Atmos. Chem. Phys.*, 14(18), 9613–9622, doi:10.5194/acp-14-9613-2014, 2014.

Spolaor, A., Opel, T., McConnell, J. R., Maselli, O. J., Spreen, G., Varin, C., Kirchgeorg, T., Fritzsche, D., Saiz-Lopez, A. and Vallelonga, P.: Halogen-based reconstruction of Russian Arctic sea ice area from the Akademii Nauk ice core (Severnaya Zemlya), *Cryosph.*, 10, 245–256, doi:10.5194/tcd-9-4407-2015, 2016.

Sturges, W. T. and Harrison, R. M.: Bromine:Lead ratios in airborne particles from urban and rural sites, *Atmos. Environ.*, 20(3), 577–588, doi:10.1016/0004-6981(86)90101-0, 1986.

Thomas, V. M., Bedford, J. A. and Cicerone, R. J.: Bromine emissions from leaded gasoline,

Geophys. Res. Lett., 24(11), 1371–1374, doi:10.1029/97GL01243, 1997.

Vestreng, V., Ntziachristos, L., Semb, A., Reis, S., Isaksen, I. S. A. and Tarrasón, L.: Evolution of NO<sub>x</sub> emissions in Europe with focus on road transport control measures, Atmos. Chem. Phys., 9(4), 1503–1520, doi:10.5194/acp-9-1503-2009, 2009.

Wagner, T., Leue, C., Wenig, M., Pfeilsticker, K. and Platt, U.: Spatial and temporal distribution of enhanced boundary layer BrO concentrations measured by the GOME instrument aboard ERS-2, J. Geophys. Res., 106(D20), 24225, doi:10.1029/2000JD000201, 2001.

Walsh, J. E.: A data set on Northern Hemisphere sea ice extent, Natl. Snow Ice Data Cent., 49–51, 1978.

Weißbach, S., Wegner, A., Opel, T., Oerter, H., Vinther, B. M. and Kipfstuhl, S.: Spatial and temporal oxygen isotope variability in northern Greenland - implications for a new climate record over the past millennium, Clim. Past Discuss., 11(3), 2341–2388, doi:10.5194/cpd-11-2341-2015, 2015.

Weller, R.: Postdepositional losses of methane sulfonate, nitrate, and chloride at the European Project for Ice Coring in Antarctica deep-drilling site in Dronning Maud Land, Antarctica, J. Geophys. Res., 109(D7), 1–9, doi:10.1029/2003JD004189, 2004.

WMO: Scientific Assessment of Ozone Depletion: 1994. Chapter 10: Methyl Bromide, Geneva., 1995.

WMO: Scientific Assessment of Ozone Depletion: 2002. Chapter 1: Controlled Substances and Other Source Gases., 2002.

Wolff, E. W.: Ice sheets and nitrogen, Philos. Trans. R. Soc. Lond. B. Biol. Sci., 368, doi:10.1098/rstb.2013.0127, 2013.

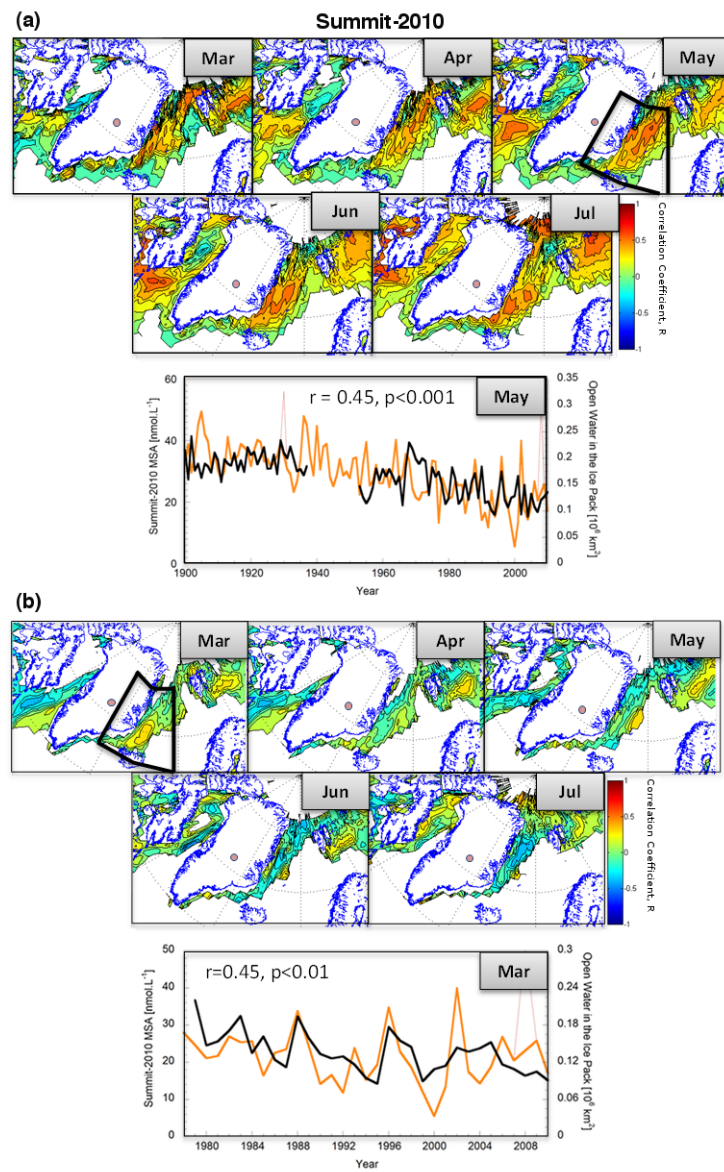
Wolff, E. W., Rankin, A. M. and Röthlisberger, R.: An ice core indicator of Antarctic sea ice production?, Geophys. Res. Lett., 30(22), 2–5, doi:10.1029/2003GL018454, 2003.

Xu, L., Russell, L. M., Somerville, R. C. J. and Quinn, P. K.: Frost flower aerosol effects on Arctic wintertime longwave cloud radiative forcing, J. Geophys. Res. Atmos., 118(23), 13282–13291, doi:10.1002/2013JD020554, 2013.

Yang, X., Pyle, J. A. and Cox, R. A.: Sea salt aerosol production and bromine release: Role of snow on sea ice, Geophys. Res. Lett., 35(16), 1–5, doi:10.1029/2008GL034536, 2008.

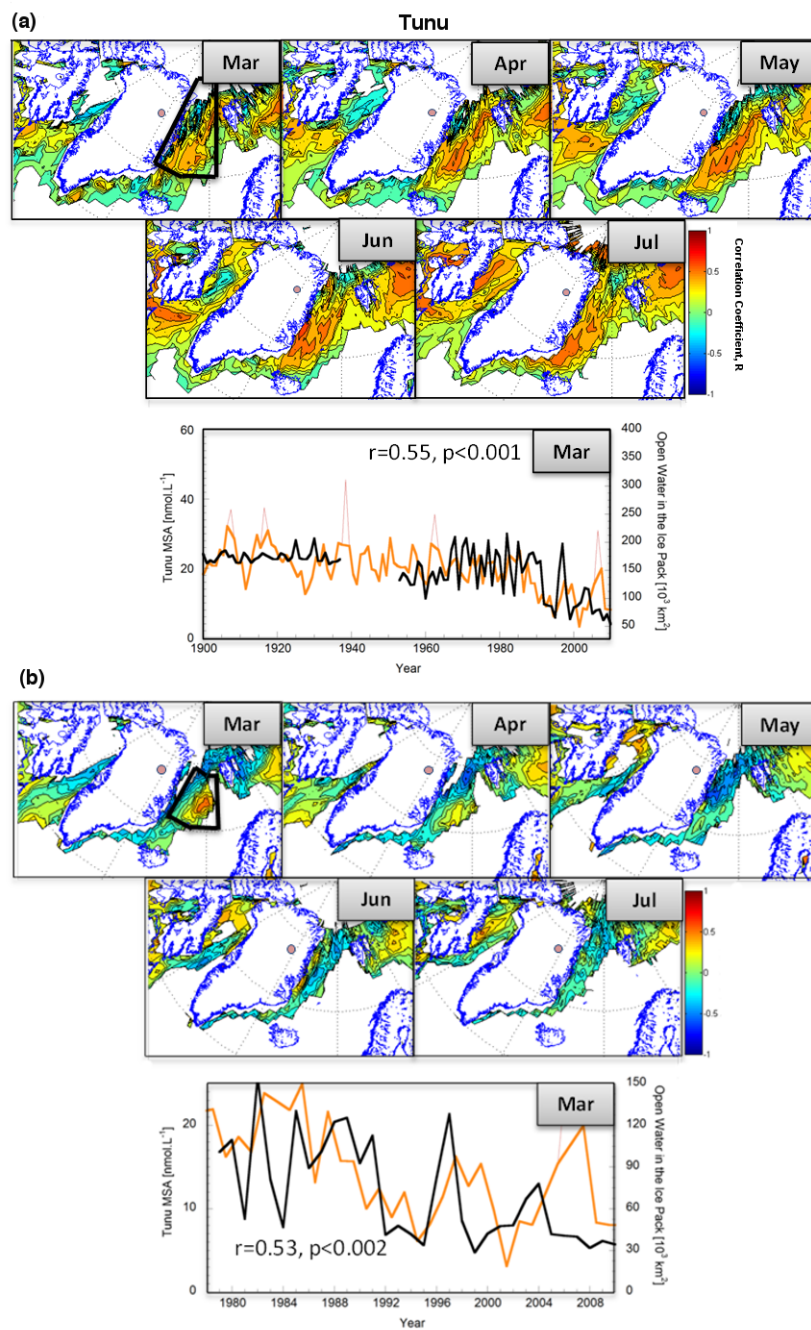
Yang, X., Pyle, J. A., Cox, R. A., Theys, N. and Van Roozendael, M.: Snow-sourced bromine and its implications for polar tropospheric ozone, *Atmos. Chem. Phys.*, 10(16), 7763–7773, doi:10.5194/acp-10-7763-2010, 2010.

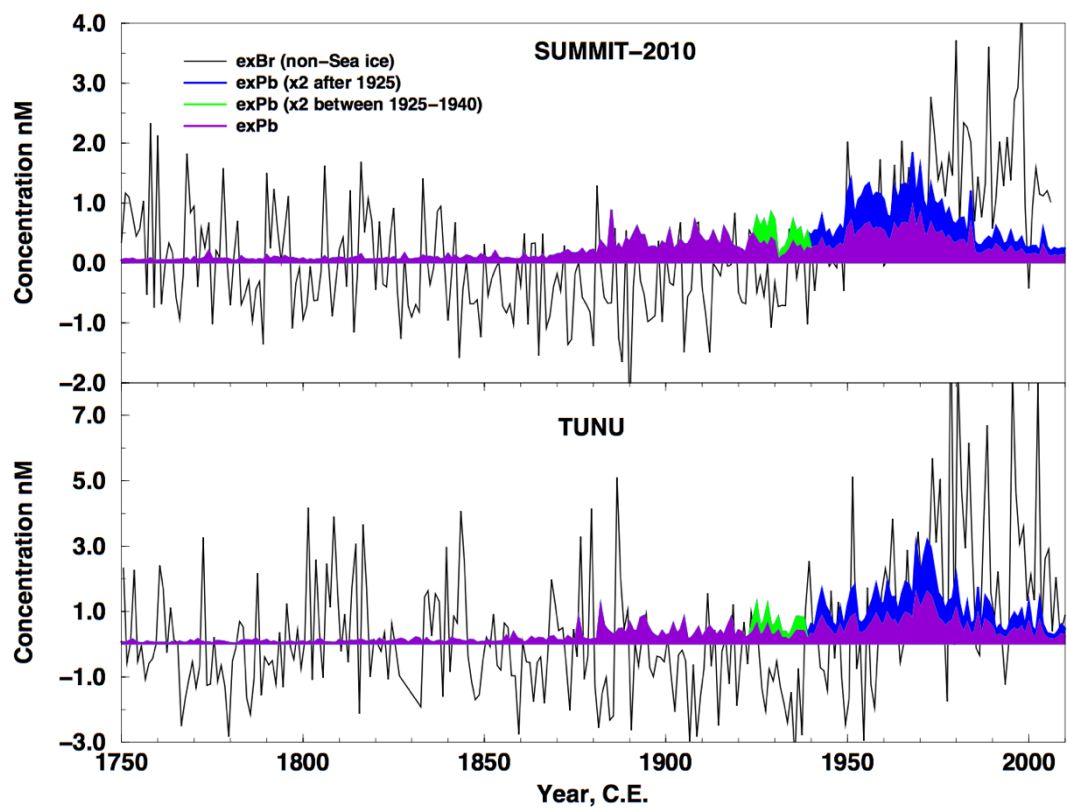
Yung, Y. L., Pinto, J. P., Watson, R. T. and Sander, S. P.: Atmospheric Bromine and Ozone Perturbations in the Lower Stratosphere, *J. Atmos. Sci.*, 37(2), 339–353, doi:10.1175/1520-0469(1980)037<0339:ABAOPI>2.0.CO;2, 1980.



region.

Page Break





## 1

**Table S1.** Summary of timings of each inflection in the 3-step linear regression of annual bromine and MSA at Summit and Tunu. Regression was performed on the data sets with outliers removed as described in Fig. 2. The signs indicate the direction of the inflection in the record, errors are  $2\sigma$ .

5

Timing of inflection (Year, C.E.)							
	Infl. 1		Infl. 2		Infl. 3		Infl. 4
	Br	MSA	Br	MSA	Br	MSA	Br
Summit-2010	(-)1819 ±22	(-)1854 ±12	(+)1879 ±22	(+)1878 ±12	(+)1932 ±10	(-)1930 ±16	(-)1974 ±20
Tunu	(-)1842 ±22	(-)1812 ±12	(+)1857 ±24	(+)1821 ±21	(+)1944 ±18	(-)1984 ±4	(+)1966 ±20

6

7

8



1 **Table S2.** Summary of the average aerosol concentrations as determined by the 3-step linear regression of  
2 annual bromine and MSA at Summit and Tunu displayed in Fig. 2. The duration of each step in concentration  
3 is bracketed by the inflection points summarized in Table S1. Concentrations are in units of nM. MSA did not  
4 show a stable period after the third infection in the series and so was not assigned a concentration value for  
5 ‘Step 3’. Errors represent  $2\sigma$  in the concentration value.  
6

	Concentration (nM)				
	Step 1		Step 2		Step 3
	Br	MSA	Br	MSA	Br
Summit-2010	5.4±0.2	48±1	4.2±0.2	36±2	5.5±0.3
Tunu	4.2±0.3	25±1	3.2±0.3	21.2±0.7	4.8±0.5

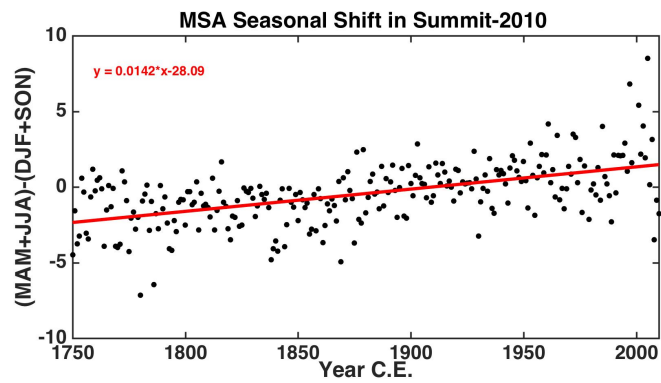


**Figure S1.** Illustration of the shift in the seasonal MSA peak along the length of the Summit-2010 ice core. The difference in amplitude between the spring/summer and winter/fall MSA signal each year was calculated ((MAM+JJA)-(DJF+SON)) and observed to shift linearly along the length of the ice core. At the shallowest, part of the ice core the positive values show the MSA peak appears in the spring/summer whilst in the deepest and oldest part of the ice core the signal has shifted to a winter/fall annual maximum. This phenomenon has previously been attributed to annual salt gradients within the ice core driving the migration of the MSA toward the higher salt location, winter (Mulvaney et al., 1992; Weller, 2004).

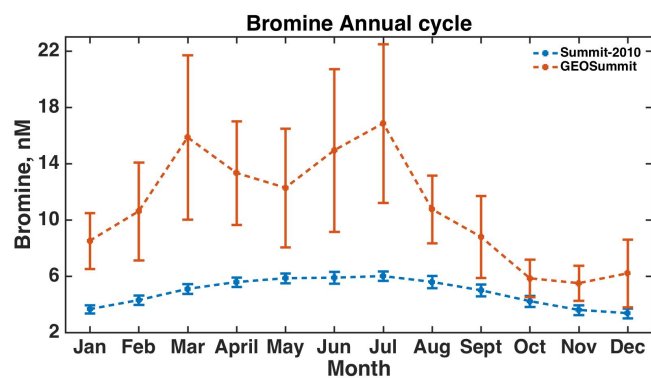


**Figure S2.** Comparison between the annual cycle in inorganic Br measured at Summit from snow samples taken as part of the GEOSummit project (2007-2013) and in the Summit-2010 ice core (1900-2010). The snow samples were analysed for inorganic Br on the same system used to measure the ice core records. The results of the snow samples support the observation from the ice cores that the maximum flux of Br is in summer with a possible secondary peak in spring. The error bars represent  $1\sigma$ .

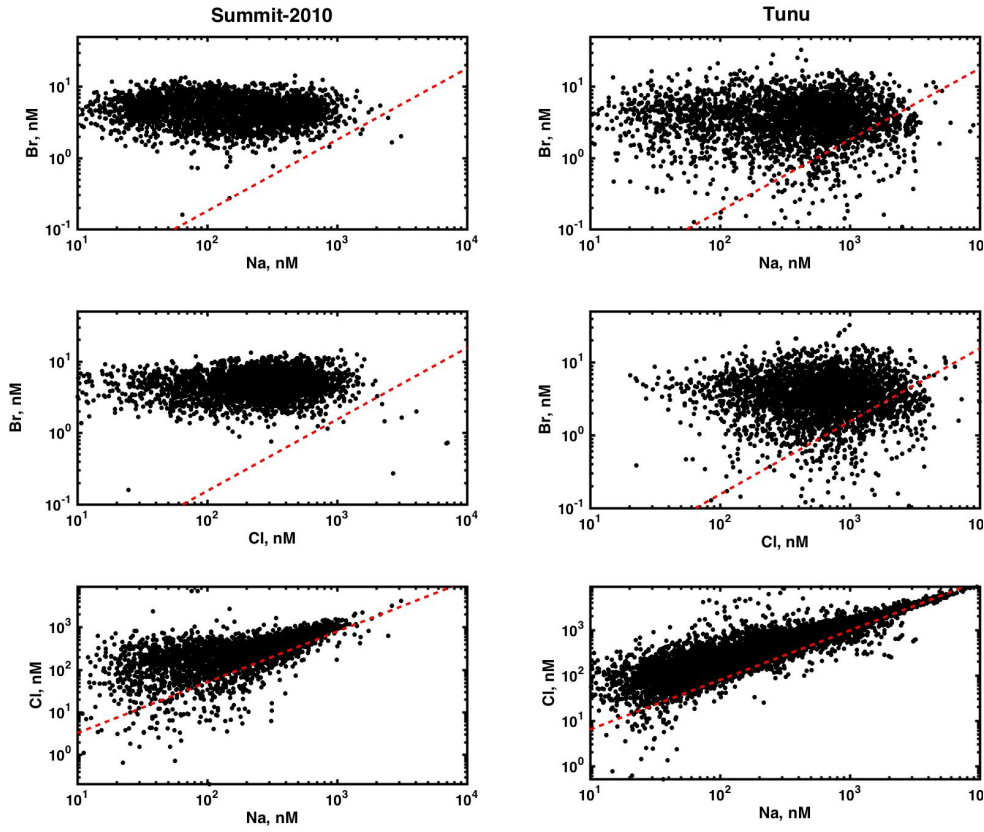


**Figure S3.** Monthly values of bromine, sodium and chlorine compared with their sea water ratio (red). At both sites, both the Br/Na and Br/Cl lie predominantly above the sea water ratio, whilst Cl/Na shows only a small Cl enrichment which increases at small sodium concentrations. At Tunu, 11% and 12% of the points show bromine depletion relative to Na and Cl, respectively.  $([Br]/[Na])_{\text{seawater}} = 1.793 \times 10^{-3}$ ,  $([Br]/[Cl])_{\text{seawater}} = 1.539 \times 10^{-3}$ .  $([Cl]/[Na])_{\text{seawater}} = 1.165$

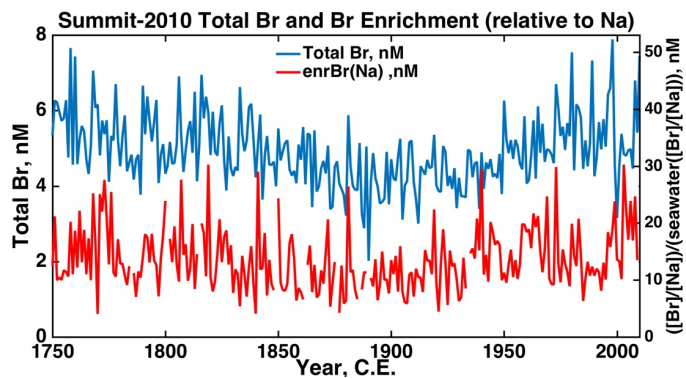


**Figure S4.** Total bromine and bromine enrichment (relative to sodium) from the Summit-2010 ice core.

**Deleted:** The time-series have been plotted to match the signal variability in the preindustrial era (1750-1850 C.E.).

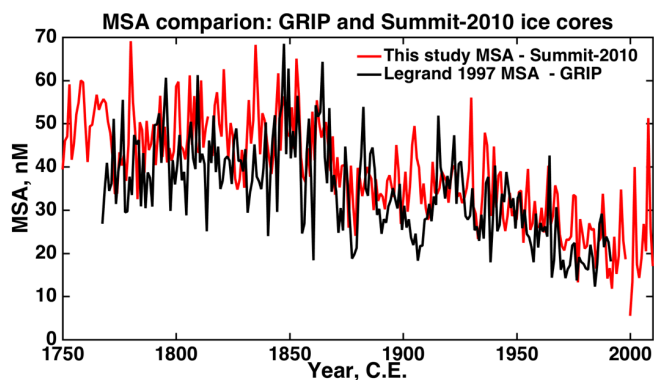


**Figure S5.** Comparison between the MSA record obtained from the GRIP ice core (Legrand et al., 1997) in 1993 and the Summit-2010 ice core from this study. The Summit-2010 ice core drill-site (72°20'N 38°17'24"W) is located 35 km SW of the GRIP ice core drill-site (72°34'N, 37°38'W). The GRIP MSA was measured in discrete samples using ion chromatography compared with the Summit-2010 ice core which was measured using the new technique of continuous melting of the ice core combined with continuous analysis by electrospray triple-quad mass spectrometry (as described in the text). The tight overlap between low frequency trend of the two series demonstrates that the new, continuous measurement technique is able to achieve a comparable accuracy in MSA concentration measurements to the discrete technique. It also demonstrates that negligible amounts of MSA are being lost during the continuous melt method. Discrepancies between the high frequency features of the two records is expected as the measurement resolution of the continuous method is much higher than the discrete method and the two records are from different ice core sites.

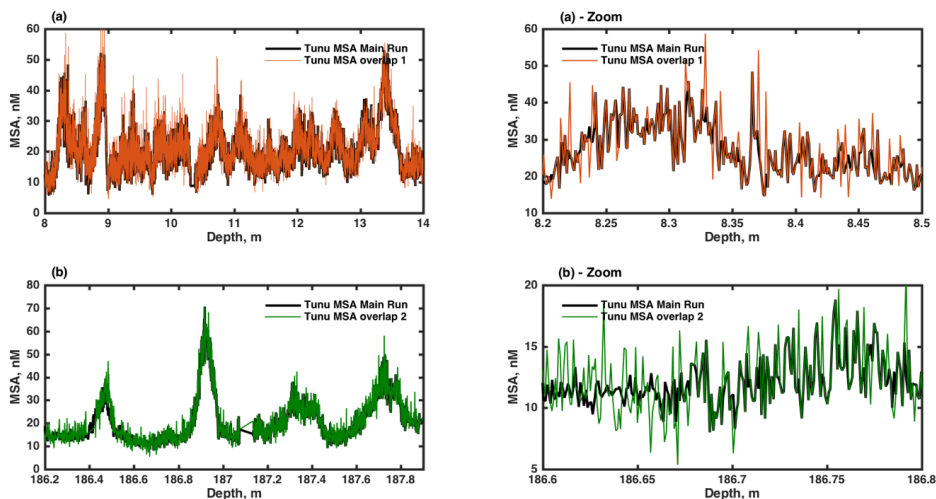


**Figure S6.** Demonstration of the reproducibility of the MSA online, continuous measurements performed on the Tunu ice core. Two different depths of the Tunu ice core are shown where the replicate analysis was performed by melting a secondary stick of ice cut from the same ice core and overlapping in depth (**‘overlap’ ice sticks**): (a) Six ‘overlap’ ice sticks were melted sequentially to replicate the MSA record over the depth 8-14 m. (b) Two ‘overlap’ ice sticks were melted sequentially over the depth 186.2-187.9 m. Zooming in on a small section of the record at each depth demonstrates that the high frequency signal is real (not noise) and well replicated by the continuous MSA technique.

Deleted: cores

Deleted: cores

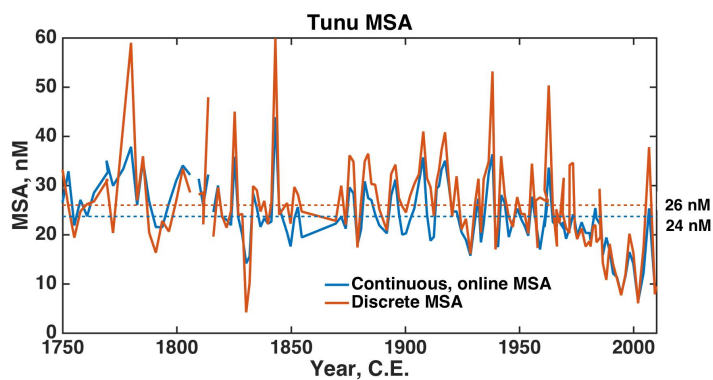


**Figure S7.** Comparison between discrete and continuous, online measurements of MSA measurements from the Tunu ice core samples. The discrete samples were collected as the continuous measurements were performed by directing part of the sample stream into an auto-sampler collection system just before they entered the analyzer. The samples were then frozen and later measured using ion chromatographic separation and the ESI/MS/MS detection. In this plot the continuous data have been averaged over the same depth range covered by each discrete sample and then both series plotted as the average age over that depth range. Over the 1750-2012 period the Tunu discrete measurements were, on average, 7% higher than the online measurements (dashed lines indicate average values over the 1750-2012 period). Both the discrete and continuous samples experienced identical conditions from ice melt to collection so the reason for offset in measured concentration is likely due to differences in post-processing of the data.



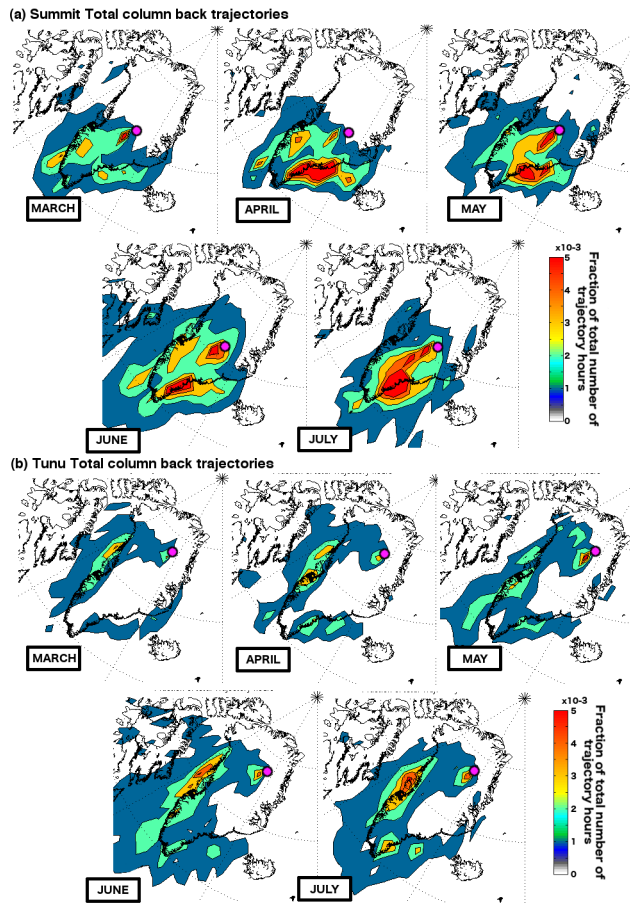
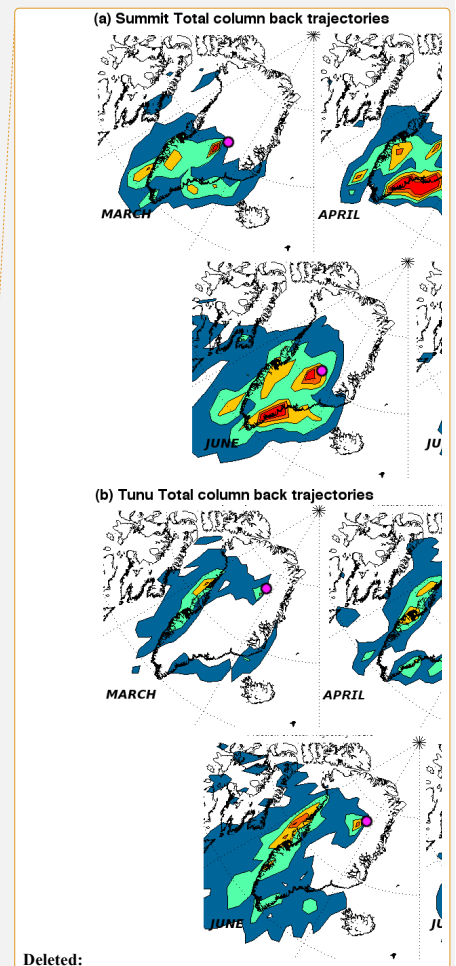


**Figure S8.** Total column air mass back trajectories from the (a) Summit-2010 and (b) Tunu ice core sites over the period 2005-2013 C.E. Maps display the fraction of the total number of trajectory hours ( $\sim 100000$  hrs month<sup>-1</sup>) spent within the total vertical column (under 10000 m). Back trajectories were allowed to travel for 10 days. New trajectories were started every 12 hours. Map grid resolution is 2°x2°. Ice core locations are shown by a pink circle. Maps show that air masses consistently arrive at Summit from the SE Greenland coast with a smaller contribution from the SW coast, consistent with the trajectories seen in the boundary layer (Fig. 5). Air masses consistently arrive at Tunu from the western Greenland coast with a smaller contribution from the SE.



Deleted:

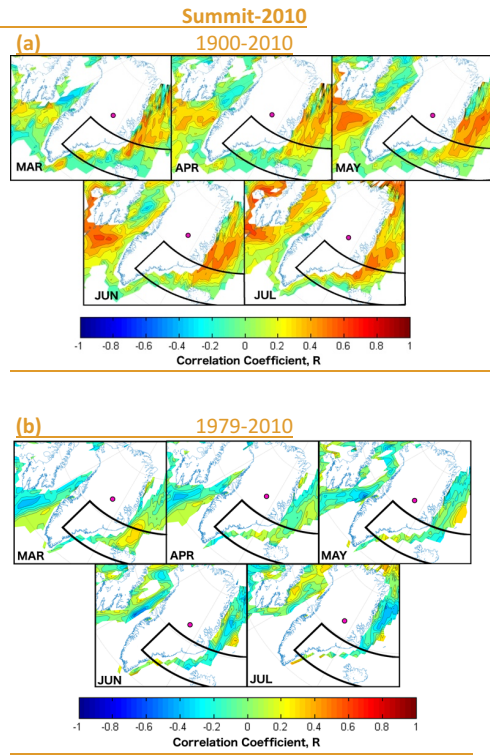


**Figure S9.** Correlation maps of monthly sea ice concentration (SIC) derived from the Summit-2010 ice core. (a) HadISST1 ICE dataset from 1900-2010 C.E. correlated with annual records of MSA. Outliers were removed from the MSA records before the correlations were performed to prevent distortion of the correlations. Month labels indicate the month of SIC compared with the annual MSA value. Only locations that showed a SIC variability greater than 10% and have a significant correlation (t-test,  $p < 0.05$ ) are displayed. The area of sea ice that is the likely source of MSA (as indicated by the air mass trajectories) are outlined in black [70°– 63°N, 0°– 45°W]. (b) As for (a) but focused on the satellite period 1979-2010 C.E. and the outlined area covers [70°–63°N, 0°–60°W].

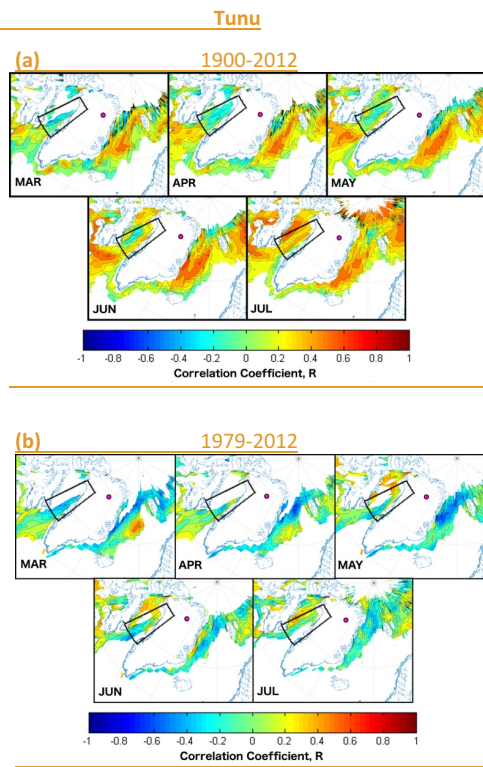


**Figure S10.** Correlation maps of monthly sea ice concentration (SIC) derived from the Tunu ice core. (a) HadISST1 ICE dataset from 1900-2012 C.E. correlated with annual records of MSA. Outliers were removed from the MSA records before the correlations were performed to prevent distortion of the correlations. Month labels indicate the month of SIC compared with the annual MSA value. Only locations that showed a SIC variability greater than 10% and have a significant correlation (t-test,  $p < 0.05$ ) are displayed. The area of sea ice that is the likely source of MSA (as indicated by the air mass trajectories) are outlined in black [77°–67°N, 62°–50°W]. (b) As for (a) but focused on the satellite period 1979-2012 C.E.

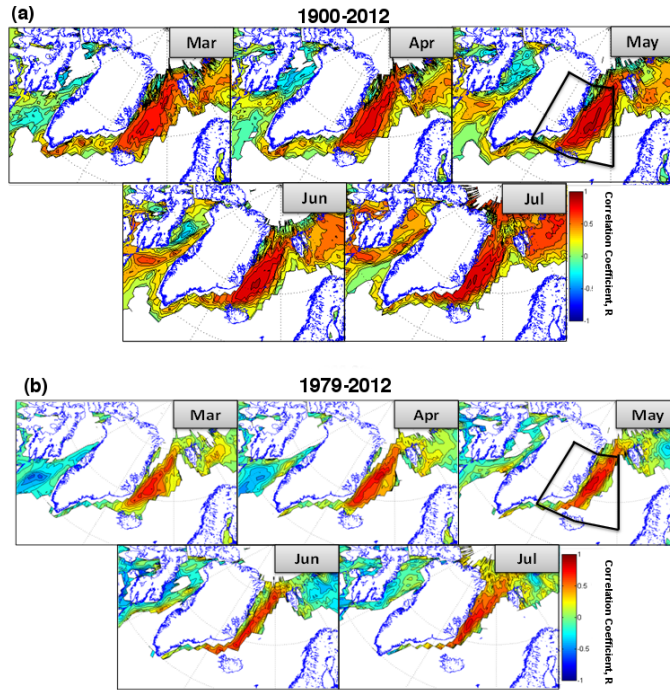


**Figure S11.** Autocorrelation maps of SIC during (a) the extended era (1900–2012 C.E.) and (b) satellite era (1979–2012 C.E.). Monthly SIC values were compared with the average SIC record from the area which shows the high positive correlation to the Summit-2010 MSA record (outlined in black in Figs. 6a, 6b). There is clearly a negative correlation between sea ice on the east and west coast which is seen over both era from March through to May, but the relationship turns positive in June and July over the extended time period (1900–2012 C.E.)

Deleted: S9

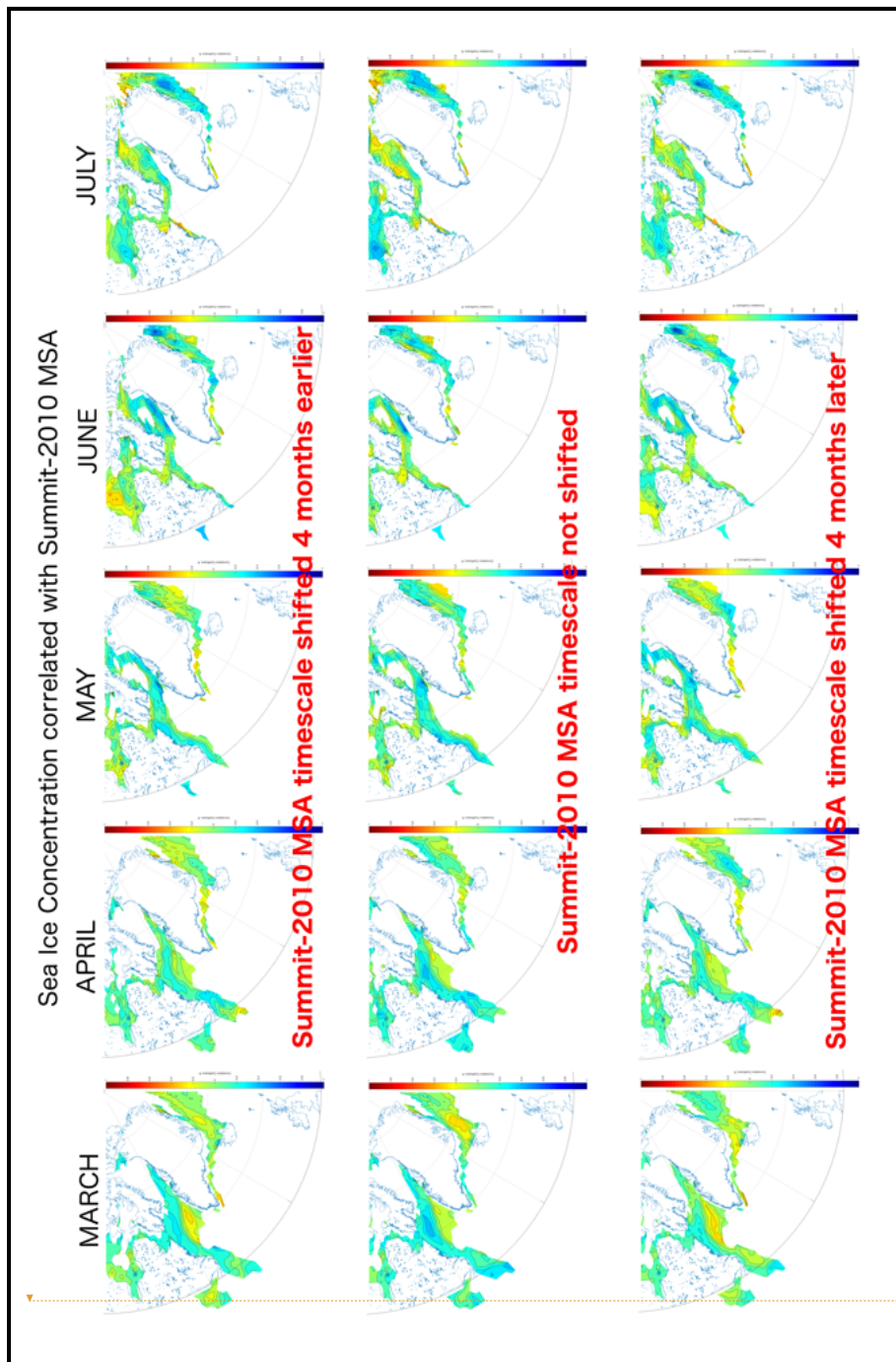


Figure S12



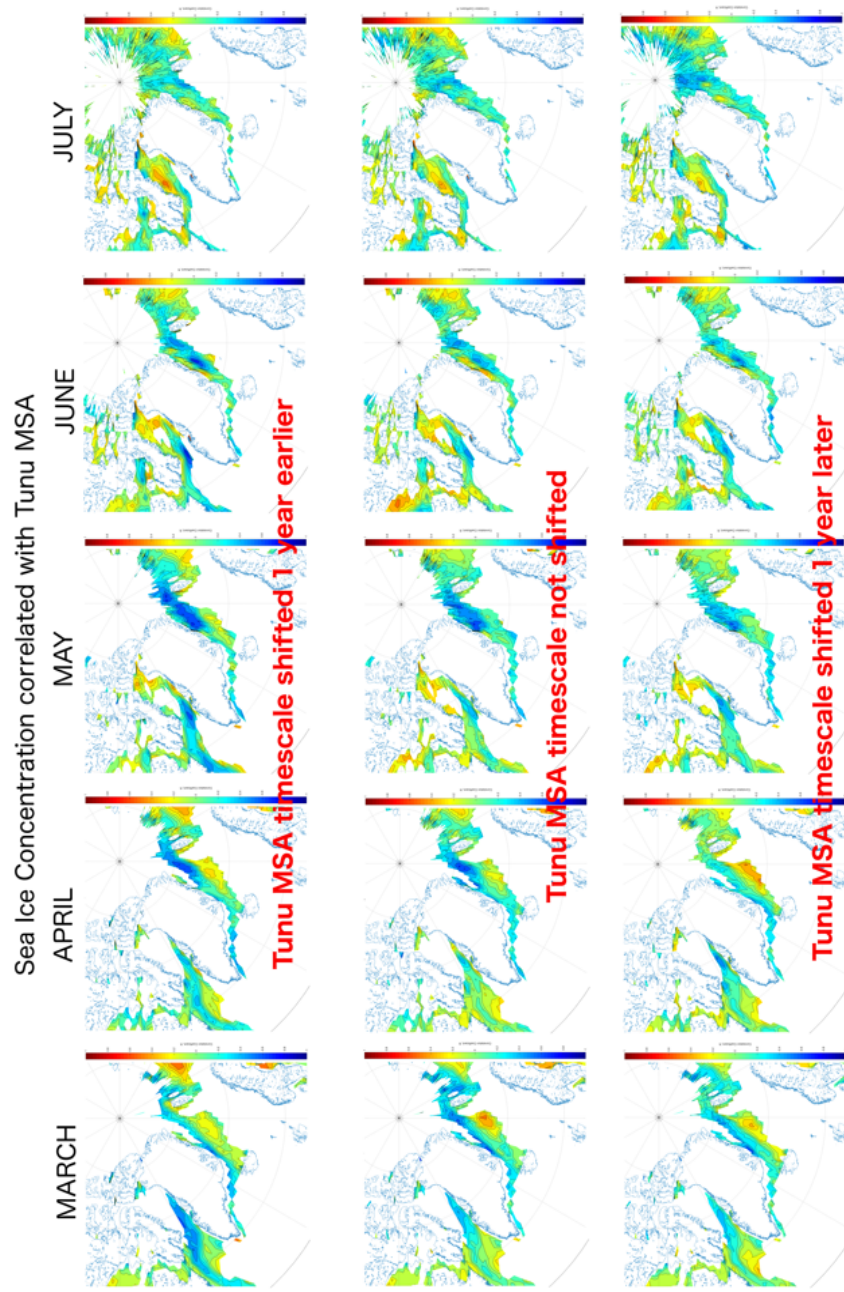
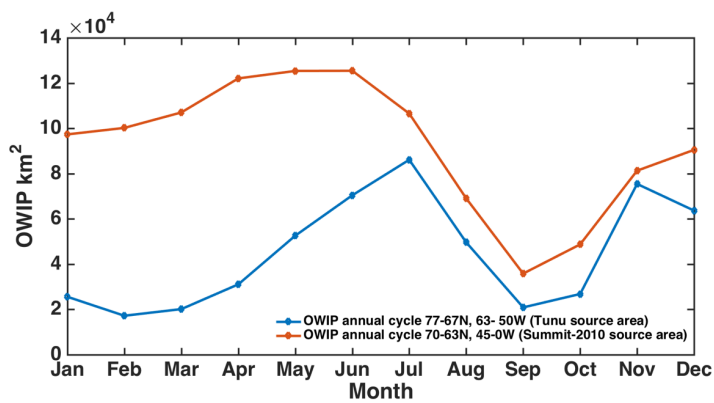


Figure S12 continued

**Figure S12.** Analysis of the effect of errors in the ice core timescales on the correlation between the site MSA record and the local sea ice concentrations (SIC). By shifting the dating of the MSA records to either extreme of the dating error estimate and replotting the SIC correlation plots (Figs. 6 and 7) it is clear the error in the dating of the MSA records does not affect the sign of the correlations displayed on the maps but can have an affect on the magnitude of the correlation found in different locations. This is likely a result of the peaks in the MSA record being shifted in or out of temporal coherence with peaks in SIC at the different locations.

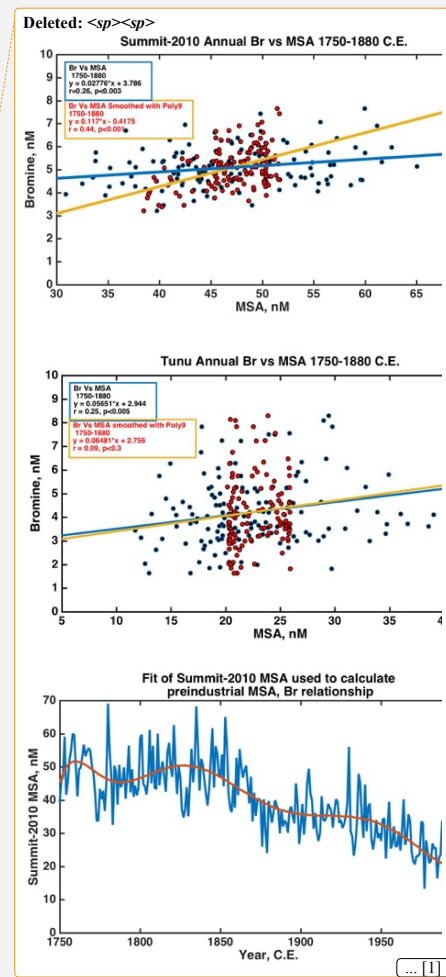
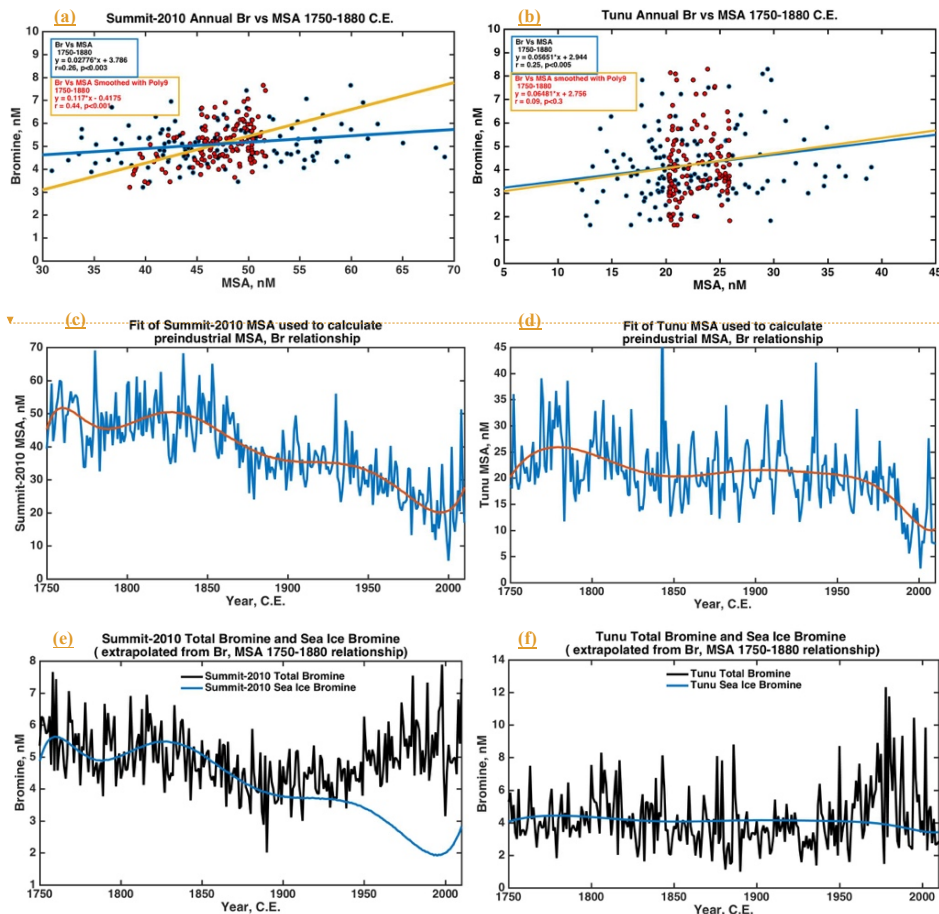
Deleted: 0



**Figure S13:** Annual cycle of open water in the ice pack (OWIP) within the aerosol source regions designated in Figs. 6 and 7. The annual cycle has been averaged over the period 1900-2012. The satellite period 1979-2012 shows the same temporal variability in OWIP at both sites but at reduced OWIP values.

Deleted: 1





1 e and f is the amount of bromine in excess of what is expected from a purely sea ice source (nsiBr; see Fig.  
2 8).

§

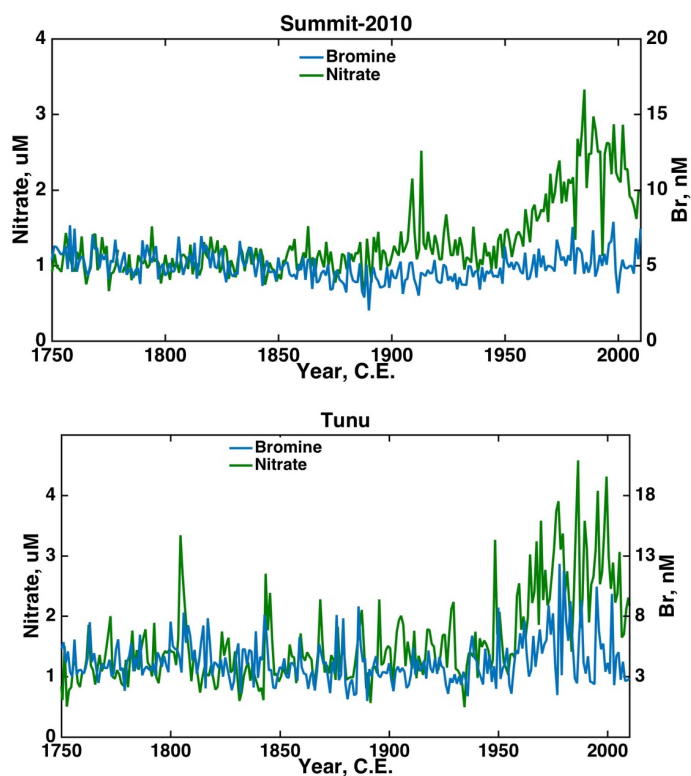


**Figure S15:** Comparison between nitrate and bromine records at both ice core sites. The difference between the two time-series is most dramatic at the Summit-2010 site because the sea ice record changes most dramatically at this site – and sea ice is the underlying driver of the bromine record.

**Deleted: 3**

**Deleted:** The time-series have been plotted to match the signal variability in the preindustrial era (1750-1850 C.E.).

## References

- Legrand, M., Hammer, C., De Angelis, M., Savarino, J., Delmas, R., Clausen, H. and Johnsen, S. J.: Sulfur-containing species (methanesulfonate and SO<sub>4</sub>) over the last climatic cycle in the Greenland Ice Core Project (central Greenland) ice core, *J. Geophys. Res.*, 102(C12), 26663, doi:10.1029/97JC01436, 1997.
- Mulvaney, R., Pasteur, E. C., Peel, D. A., Saltzman, E. S. and Whung, P.-Y.: The ratio of MSA to non-sea-salt sulphate in Antarctic Peninsula ice cores, *Tellus B*, 44(4), doi:10.3402/tellusb.v44i4.15457, 1992.
- Weller, R.: Postdepositional losses of methane sulfonate, nitrate, and chloride at the European Project for Ice Coring in Antarctica deep-drilling site in Dronning Maud Land, Antarctica, *J. Geophys. Res.*, 109(D7), 1–9, doi:10.1029/2003JD004189, 2004.

(a)

(b) (d)

(c)

